Aus dem Institut für Medizinische Psychologie

Institut der Universität München

Vorstand: Prof. Martha Merrow, Ph.D.

Changes in Dynamic Functional Connectivity of Default Mode Network in Two Different Mental States: Episodic Memory Retrieval and Resting State

Dissertation

zum Erwerb des Doktorgrades der Humanbiologie

an der Medizinischen Fakultät der

Ludwig-Maximilians-Universität zu München

vorgelegt von

Garam Jeong

aus

Daejeon

Jahr

2022

Mit Genehmigung der Medizinischen Fakultät
der Universität München

Berichterstatter:	Prof. Dr. Dr. h.c. Ernst Pöppel
Mitberichterstatter:	Dr. Daniel Keeser Prof. Dr. Leonhard Schilbach
Mitbetreuung durch den promovierten Mitarbeiter:	Prof. Dr. Yan Bao
Dekan:	Prof. Dr. med. Thomas Gudermann
Tag der mündlichen Prüfung:	08.12.2022

Table of content

Zusammenfassung (Deutsch):

fMRT-Studien haben gezeigt, dass die Hirnregionen, die mit dem Ruhezustand und dem episodischen Gedächtnisabrufzustand des Menschen verbunden sind, große Überlappungen aufweisen. Diese Regionen werden als default mode network bezeichnet. Die Gemeinsamkeit zwischen den beiden mentalen Zuständen wurde anhand des default mode network umfassend untersucht. Dahingegen wurden die Unterschiede der beiden mentalen Zustände in fMRT-Studien bisher nicht untersucht. Da die beiden mentalen Zustände die räumliche Charakteristik teilen, sollten ihre Unterschiede im zeitlichen Bereich liegen. Diese Studie untersucht, wie ihre Unterschiede durch dynamische funktionale Konnektivität (DFC) analysiert werden können. In diesem Zusammenhang wird DFC als die zeitliche Varianz funktioneller Korrelationen zwischen Hirnregionen definiert. In dieser Studie wird eine neue Analysemethode namens One-ROI-centered DFC vorgeschlagen, um zu zeigen, dass sich die DFC des default mode network in Abhängigkeit vom mentalen Zustand ändert. Ein fMRI-Einzelexperiment und ein fMRI-Gruppenexperiment wurden durchgeführt, um die neue Analysemethode zu testen. In beiden Experimenten wurden die Probanden gebeten, ihre Morgenroutine dreimal für den episodischen Gedächtnisabrufzustand abzurufen und einmal im Ruhezustand zu sein. Die Ergebnisse der One-ROI-centered DFC-Analyse zeigen die Ähnlichkeit der DFC in den drei Durchläufen des episodischen Gedächtnisabrufzustands. Darüber hinaus wird auch ihr Unterschied zum Ruhezustand durch die Analyse aufgedeckt. Damit erweist sich die neue Analysemethode als geeignet, um den Ruhezustand und den episodischen Gedächtnisabrufzustand im zeitlichen Bereich zu unterscheiden. Die Ergebnisse legen nahe, dass die neue Methode es ermöglicht, in fMRT-Studien die Unterschiede aufzudecken von zwei beliebigen mentalen Zuständen, die ein räumliches Gehirnaktivierungsmuster teilen.

Abstract (English):

The brain regions associated with the resting state and the episodic memory retrieval state of humans have been established to have large overlaps by fMRI studies. These regions are called the default mode network. The commonality between the two mental states has been studied widely based on the default mode network. On the other hand, the differences between the two mental states have not been investigated thus far in fMRI studies. Since the two mental states share a spatial characteristic, their differences should reside in the temporal domain. This study examines how their differences can be analyzed through dynamic functional connectivity (DFC). In this context, DFC is defined as the temporal variance of functional correlations between brain regions. In this study, a new analysis method called one-ROI-centered DFC is proposed to show that the DFC of the default mode network changes depending on the mental state. A single case fMRI experiment and a group fMRI experiment were conducted to test the new analysis method. In both experiments, subjects were asked to retrieve their morning routine three times for the episodic memory retrieval condition and to be in the resting state once. The results of one-ROI-centered DFC analysis show the similarity of DFC in the three runs of the episodic memory retrieval state. Furthermore, their difference from the resting state is also revealed by the analysis. The new method of analysis is thus shown to be suitable for distinguishing the resting state and the episodic memory retrieval state in the temporal domain. The results suggest that the new method enables to reveal in fMRI studies the differences of any two mental states that share a spatial brain activation pattern.

List of figures

List of tables

List of abbreviations

AEMR = Autobiographical Episodic Memory Retrieval

AG = Angular Gyrus

BA = Brodmann Area

BOLD = Blood Oxygenated Level Dependent

DFC = Dynamic Functional Connectivity

DMN = Default Mode Network

DTI = Diffusion Tensor Imaging

EEG = Electroencephalography

fMRI = Functional Magnetic Resonance Imaging

ICA = Independent Component Analysis

LFP = Local Field Potential

MEG = Magnetoencephalography

PCA = Principal Component Analysis

PCC = Posterior Cingulate Cortex

PET = Positron Emission Tomography

PHC = Parahippocampal Cortex

PRC = Precuneus

ROI = Region of Interest

RSC = Restrosplenial Cortex

1. Introduction

Humans actively interact with the given environment as a part of it. The environment of the earth is a large set of diverse organisms and non-organic materials. To survive and thrive in this diversity, humans and animals have developed a center of information processing called the brain (Allman, 1999). One of the extraordinary features of the human brain is that it could rebuild the external world internally based on its abundant memory (Tulving, 2002). This feature has been studied under different names including episodic memory retrieval and imagery, theory of mind, and a resting state (Buckner & Carroll, 2007; Hassabis & Maguire, 2007). In this thesis, I define them with the term 'the construction of the internal world'. The brain regions processing the construction of the internal world show high correlations in fMRI studies of functional connectivity when humans are in a resting state, so it was defined as the default mode network (Raichle, 2015). Since they share the default mode network as a common spatial activity pattern, their temporal realization should be different to realize differences in their functions. For example, when we retrieve a particular episodic memory, the brain should realize the context of consecutive episodes from memory (Tulving, 1972). On the other hand, when we are in a resting state, there is no predefined context for it. The question is how functional connectivity could measure their innate differences existing in their temporal characteristics. DFC has been studied to reveal temporal characteristics of brain networks for the last decade (Allen, et al., 2014; Hutchison, et al., 2013). However, the changes in DFC of default mode network in different mental states has not been studied. The reason could be found from the complex structure and mechanisms of the brain that makes neuronal signals measured by fMRI technology stochastic. In this thesis, how the stochastic dynamics of the neuronal signals measured with fMRI can be described as nearly deterministic dynamics was discussed in terms of the self-organizing system (Ashby, 2017). Following the discussion, a new analysis method called one-ROI-centered dynamical functional connectivity (DFC) was suggested. One-ROI-centered DFC analysis reduces the dimension of DFC by looking into the connectivity of the centered ROI only. After this dimensionality reduction, its orthogonal directions of variance for a given time course were calculated by principal component analysis. By comparing the principal components, its directional preference to encode variance depending on the mental state could be shown. The episodic memory retrieval state of a blind subject and normal subjects were analyzed by one-ROI-centered dynamical connectivity analysis. Subjects were asked to retrieve their morning routine three times in an fMRI machine. By comparing how similar the directional preferences of one-ROI-centered DFC of three trials within an individual, one could test whether it is possible to abstract brain activities measured with fMRI to approximate to deterministic one or not. After that, two different mental states, the result of one-ROI-centered DFC analysis of episodic memory retrieval state and the resting state were compared to know whether their difference could be revealed by temporal characteristics abstracted with the analysis.

This thesis was written in the following order. In chapter 2, literature about the physical foundation of fMRI technique, analysis methods of fMRI data, and functional connectivity analysis were reviewed. In chapter 3, the dynamics of the brain functions were reviewed with known examples. Also, a hypothesis about how dynamics of functional connectivity of the brain could be abstracted was suggested based on a concept of the self-organizing system (Ashby, 2017). In chapter 4, examples of memory systems were reviewed. The commonality found by fMRI studies between the episodic memory retrieval state and the resting state of humans was reviewed in the same chapter. Also, known functions of brain regions in the default mode network were briefly summarized. The experimental setups and processes to explore DFC of the default mode network in the two different mental states were introduced in chapter 5. In chapter 6, a new analysis method

called one-ROI-centered DFC analysis was described. The results of the analysis were reported in chapter 7, and their implications and limits were discussed in chapter 8.

2. fMRI and Functional Connectivity Analysis

The functional magnetic resonance imaging (fMRI) technique offers non-invasive methods to measure the neuronal activities of humans and animals (Ogawa, Lee, Nayak, & Glynn, 1990). It has been widely used to study human brain activities related to the function of specific brain regions concerning the behaviors (Kwong, et al., 1992; Ogawa, et al., 1992; Hall, et al., 1999; Kourtzi & Kanwisher, 2001). Imaging of neuronal activities of the brain which are the substrate of behaviors of humans and animals is called functional MRI (Ogawa, Menon, KimS, Ugurbil, 1998). It has an ability to measure the entire brain with the millimeter resolution. It shows which part of the brain is most active while a person performs given tasks in an MRI machine. fMRI technique opened the door to investigate activities of the brains without using the postmortem brains. Now, we know there is a brain region that almost exclusively reacts to human faces, the fusiform face area (Kanwisher, McDermott, & Chun, 1997), and taxi drivers in London have a larger hippocampus than average people (Maguire et al., 2000) with the help of fMRI. The fast development of high-end technology gives researchers more abundant and detailed measurements of the brain, and our understanding of the function of the brain has increased with it. At the same time, analyzing a large amount of information in a proper way to extract the interesting property is critical to having a better understanding of the function of the brain. In this chapter, the physical definition of the fMRI technique and its biochemical mechanism were reviewed. In addition, analysis methods to interpret the measures of fMRI were briefly revised. Specifically, the concept of functional connectivity and brain networks with known literature were discussed.

2.1.1 Physical and Biological Foundation of fMRI

fMRI is using a magnetic field to take images of the brain. A simple way to understand the fMRI technique is that it measures the changes in magnetic fields surrounding a subject caused by physiological changes in the brain (Ogawa, Lee, Kay, & Tank, 1990). A neuron requires oxygen to produce an action potential which is the result of ion flows crossing its membrane. The action potential of neurons from such biochemical activities changes the oxygen level of blood flows because they consume energy. Hemoglobin molecules in red blood cells carry oxygen which is necessary for the cells to produce energy. A hemoglobin molecule becomes oxygenated when it is saturated with oxygen and deoxygenated when it is not saturated with oxygen (Pauling & Coryell, 1936). An oxygenated hemoglobin molecule is diamagnetic, and a deoxygenated hemoglobin molecule is paramagnetic (Logothetis, 2008). The change of the amount of oxygenated and deoxygenated hemoglobin molecules in red blood cells within the blood flows of the brain is measurable when it is exposed to an enough strong magnetic field (Ogawa, Lee, Nayak, & Glynn, 1990). Paramagnetic deoxygenated hemoglobin molecules distort the external magnetic field due to their magnetic field. This distortion affects the relaxation time of nearby cells' hydrogen nuclei (Logothetis, 2008). The relaxation time of the hydrogen nucleus refers to the time that it takes for the hydrogen nucleus to turn back to its ground state after it got excited due to the external magnetic field. The constant that is related to the relaxation time in the distorted magnetic field is called T2* (Ogawa, et al., 1992). In short, T2* is changed following the oxygenation level of hemoglobin of the nearby blood flow of cells. It is called the blood oxygenation level dependent signal (BOLD signal) (Ogawa, et al., 1993). The T2* is proportional to the strength of the external magnetic field. Nowadays the 1.5T and 3T strength of magnetic fields are most widely used for fMRI scanning (Logothetis & Wandell, 2004).

The physiological mechanism connecting BOLD signals to neuronal activities has been under inspection by many researchers. Logothetis and colleagues (2001) measured BOLD signals via fMRI, the local field potentials (LFP), and the single- and multi-unit activities from the primary visual cortex (V1) of anesthetized monkeys (Logothetis, Pauls, Augath, Trinath, & Oeltermann, 2001). They showed that evoked BOLD signals by visual stimuli in V1 are linearly correlated with the LFP measured in the same brain area. Simultaneous measurement of fMRI and the LFP, and the multi-unit activities from V1 of awakening monkeys also showed that the BOLD signal has a high correlation with the LFP (Goense & Logothetis, 2008). According to the experiment presented in this paper, the amplitude of BOLD signals was lower in anesthetized monkeys, but still showed a high linear correlation with the LFP. They suspected that the source of LFP is the synchronized dendro-somatic inputs. Therefore, they concluded that the BOLD signals represent the input signals of neuronal activities. Similarly, Nir and colleagues (2007) measured the linear correlation of BOLD signals with single neuron activities and the LFP from the auditory cortex of humans (Nir et al., 2007). They measured around 50 single neurons activity while subjects are watching a video clip with audio. The collected neuronal signals were summed up and convolved with the hemodynamic response function (HRF) to design a spike predictor. BOLD signals predicted by the spike predictor and the real BOLD signals from the auditory cortex measured by fMRI were linearly correlated. They also measured the LFP and used it as the predictor of the BOLD signals and showed the same result.

Recently, the optogenetic fMRI (ofMRI) was introduced by Lee and colleagues to measure direct BOLD signals driven by neurons (Lee, et al., 2010). Lee and colleagues drove channelrhodopsin-2(ChR2) expression in the principal cells of the primary motor cortex of rats. With this gene expression in the principal cells, they are activated to respond to optic stimuli like lasers delivered by optical fibers. They could measure the optic stimuli-induced BOLD signals in the primary motor cortex of anesthetized rats. In a related manner, Desai and colleagues tested the ofMRI with awake mice (Desai, et al., 2011). In their experiment, the pyramidal cells in the primary somatosensory cortex were prepared to have ChR2 expression. With optic stimuli, they observed induced BOLD activities in other brain regions, mainly in the secondary somatosensory cortex, the primary motor cortex, the caudoputaman, and the contralateral primary somatosensory cortex. These experiments proved that the BOLD signals are directly induced from the neuronal activities of the cortex.

2.1.2 Experimental Design and Data Analysis of a fMRI Study

As reviewed above, several lines of evidence tell us that BOLD signals offer a good chance to measure neuronal activities of the brain. However, due to its high dependence on physiological and biological interaction apart from pure neuronal activities, to have a clear experimental design and analysis are necessary to get a proper result of an experiment. Two experimental designs, the block design, and the event related design have been most widely used for fMRI experiments to study human brain functions (Dale, 1999; Smith, 2004; Worsley & Friston, 1995). Both aim to measure the stimuli evoked responses of the brain. An experiment following the block design presents prepared stimuli and control conditions for 20 secs to 60 secs for the balanced time and frequency (Logothetis, 2008). Each stimulus and control-related period are called the task block and the control block respectively. The block design determines the cognitive functions caused by the prepared stimuli by subtracting the measured BOLD signals of control blocks from those of the task blocks and vice versa. The most critical property of the block design is the assumption that it is possible to see the task-specific response by subtracting effects of control condition, i.e.,

brain functions can be expressed in terms of their linear relations (Smith, 2004). Therefore, when the BOLD is a measure of group activities of intermingled neurons, this assumption is not strongly supported (Logothetis, 2008).

The block design requires a long presentation of stimuli and performance of the prepared tasks for each block, so it is not suitable to measure instant transitions happening in the brain. To measure such instant reactions of the brains, the event related design is more proper (Josephs, Turner, Friston, 1997). In this experimental design, stimuli are presented one by one at the beginning of the interstimulus interval (ISI) for the designed time interval. Consequently, it measures the HRF arising as a response to each stimulus (Amaro Jr & Barker, 2006). Because of its sensitivity to the presence of each stimulus, the event related design can measure the stimulus-specific brain activity. For the same reason, the temporal setups of the experimental design and its analysis are vital to get statistically significant results from the event related designed experiments (Josephs & Henson, 1999). Statistically significant results of the event related design can be achieved by using the randomized ISI (Dale, 1999). When the ISI is fixed but not randomized, it is recommended to set it longer than 20 secs. Dale (1999) showed the statistical power of results from event related designed experiments is reliably large in a short time, like a few seconds, with the randomized ISI.

After collecting fMRI data sets from a nicely designed experiment, an analysis method and statistical inference of the data should be organized to get reliable results eventually. There are several methods for that. The following review is mainly from the statistical parametric maps which have been widely used in fMRI studies (Friston, et al., 1994). The most widely used method to analyze the collected fMRI data with tasks is the general linear model (GLM) (Smith, 2004). In fMRI studies, the GLM aims to estimate the size of the effects of given tasks on each voxel. The estimated size of the effect of each voxel should go through the right statistical inference, to eventually conclude what is the effect of given stimuli or tasks on the brain. At the first level analysis, the size of the effect from every single subject is tested in general with a t-test (Friston, et al., 1995). The null hypothesis of a t-test, in this case, is that there is no effect of the given stimuli. Therefore, only the voxels showing the statistically significant response to the stimuli are selected by the first level analysis (the single subject analysis). The effect in the selected population is estimated at the second level analysis (the group level analysis) (Ashburner, et al., 2016). The type of statistics should be chosen to correspond to the experimental design. To see the effect of one variable, one sample t-test or two sample t-test (more than one group) are used (Flandin & Friston, 2008). If an experiment is designed to measure more than one effect of a single or many independent variables, the analysis of variance (ANOVA) is a common choice. ANOVA interprets the statistical distribution of the group, which is the representative sample of the population, as the sum of the effect of each variable having different means with the same variance (St & Wold, 1989). One can estimate statistically significant effects in different combinations of each variable with ANOVA (Kim, 2014). For that, setting the right experimental design is helpful to reduce the potential uncertainty of the statistical inference. It can be done by questioning what the independent variables should be to prove the hypothesis of an experiment and what the possible dependency between these variables is. Finally, the most crucial factor for the high statistical power of the analyzed result of an fMRI experiment is enough amount of data from carefully selected subjects representing the target population (Desmond & Glover, 2002).

To sum up, fMRI is a good method to measure the functioning human brain if a proper experimental design, a clear statistical inference, and an analysis method are accompanied. The common purpose of experimental designs is to measure stimuli evoked responses of the brain under

the control of experimenters. A clear experimental design controls random variables that can affect a result of an experiment. On the other hand, experimental design with a small number of independent variables is mainly to measure simple reactions of the brain to simple stimuli. Therefore, it is not proper to observe high-level perception and cognition of humans with a simple experimental design. To remedy the limit of fMRI studies, new types of experimental design with self-control or without exogenous controls from experimental designs have been tested since the end of the 1990s (Biswal, Zerrin Yetkin, Haughton, & Hyde, 1995; Kucyi & Davis, 2014; Raichle, et al., 2001; Shirer, Ryali, Rykhlevskaia, Menon, & Greicius, 2012).

2.2 Functional Connectivity of Brain

2.2.1 Connectionist Model

The number of neurons in the human brain is around 86 billion, and the number of their synaptic connection is easily larger than 10^{14} when each neuron has around a few thousand synaptic connections with other neurons (Herculano-Houzel, 2009). Since various variables are involved simultaneously to construct unified scenes of perception and cognition, neurons form networks via their synaptic connections to create high-level perception and cognition (Sporns & Zwi, 2004). Presuming perception and cognition are emergent phenomena of the neuronal networks could be compared with the connectionist model (Feldman & Ballard, 1982). By the connectionist model, a single neuron does not carry entire information about an object or a phenomenon but carries only partial information. Synaptic connections between neurons form a network while inducing behaviors or cognition by carrying and processing distributed information among neurons in parallel (Gluck & Rumelhart, 1990). Feldman and Ballard (1982) summarized that the connectionist sees the brain as a parallel computer. According to the definition of the connectionist model by Feldman and Ballard (1982), perception and cognition are represented via the parallel connections between single neurons containing partial distributed information. This connectionist point of view has been a driving force of the rapid development of artificial intelligence using artificial neural networks. The predominant advantage of the connectionist model is that it is very flexible by learning new connections among the local memories representing general properties of experiences, but not an individual thing or an event (Feldman & Ballard, 1982; Hinton, 1990; McClelland, Rumelhart, & PDP Research Group, 1986). Whereas this advantage accelerated the development of artificial intelligence, the massive connections between several neurons in biological networks are hard to be clearly explained as artificial neural networks are. The synaptic connections between neurons are very leaky, and the number of synaptic connections per neuron is around a few thousand, so how a neuronal network can be established with the connection of thousands of leaky inputs per neuron with the functional coherence is unclear (Gerstner, Kistler, Naud, & Paninski, 2014). Although there is a gap between the connectionist model and the real biological brain, many neurons in the brain are active simultaneously when it processes perception and cognition (Douglas & Martin, 2004) (Markram, et al., 2004) (Sporns & Zwi, 2004). Therefore, to assume the existence of connections between them is reasonable to explain the functions of the brain.

Technically, it is hard to delineate what is corresponding to the connectionist model and what is not by fMRI studies of the brain. The reason the connectionist model is introduced here is to show that the interest of this study is the brain as a global network via local units and their parallel connections. Similarly, many studies have focused on the network structures of the brain for the

last few decades (Bassett & Bullmore, 2006; Buckner, Andrews-Hanna, & Schacter, 2008; Bullmore & Sporns, 2009). It is known that there exist groups of neurons that respond to only a specific feature of the sensory input. Many different such neuronal groups are required to represent full aspects of the sensory inputs (Averbeck, Latham, & Pouget, 2006; Hochstein & Ahissar, 2002; Merzenich, Knight, & Roth, 1975). For example, in the visual cortex, simple cells respond to the orientation and spatial frequency of lines, and the complex cells respond not only to those but also to the movement of lines (Hubel & Wiesel, 1965). The existence of functionally modulated neuronal units in the sensory cortices requires a network of functional units to connect a possible spectrum of sensory inputs (Szentágothai, 1975). To form a network means that the members of the structure are connected to form perception and cognition, and the configuration of the network embodies perception and cognition. Therefore, most neuroscience researchers studying the formation of perception and cognition are relying on connections between functionally coherent units.

Generally speaking, one can classify most neurosciences as being in the realm of the connectionist model. However, the inclusion of simultaneous parallel processes is where the connectionist model establishes itself. Research about the representation of sensory inputs in the sensory cortices mainly has relied on a functional hierarchical structure. The hierarchical model assumes information is processed step by step consecutively through a conveyor belt to reach the full form of the sensory perception. A well-studied example is the hierarchical structure of the visual cortex (Van Essen & Maunsell, 1983). In the hierarchical model without a simultaneous parallel process of information, the connections between functional units have the role of paths leading to the next working station. On the other hand, the connectionist model with the simultaneous parallel process considers connections critical to forming perception and cognition. The brain regions processing high- or low-level stimuli have parallel connections to process stimuli simultaneously in both directions (Baumann & Stiller, 2005). Connections between functional units are critical to organizing the constellation of its network (Feldman & Ballard, 1982). Following this connectionist model, the changes of connections mean the changes in perception and cognition.

It is expected that the extent of networks existing in the brain could vary largely. The brain has evolved through the history of animals including humans. If the evolution of the brain mainly has improvised to adjust itself to survive and thrive, there is a high chance that many different mechanisms have coexisted in the brain. To investigate the potential coexisting mechanisms, it would be useful to describe the brain on a different physical scale. Conventionally, neuroscience is described at three scales, namely the microscopic, the mesoscopic, and the macroscopic scale. At the microscopic level, the cellular level of neuroscience is studied by neurobiology and neurochemistry. The main interests of studies at the microscopic scale are the activities of single neurons, and the formation of small units of neighboring neurons via synaptic connections. The connectionist model at the microscopic scale may not be useful since the studies at the microscopic scale focus on the local interaction of single neurons. The mesoscopic scale in neuroscience is concerned with neural circuits. Neural circuits are defined as the structural units of neurons that are connected via synaptic connections (Hopfield & Tank, 1986). There are global neural circuits like the cortico-basal ganglia-thalamo-cortical circuit connecting the cortex, the basal ganglia, the thalamus by forming a loop (Parent & Hazrati, 1995), and local circuits like the trisynaptic circuit within the hippocampal formation (Knierim, 2015). These neural circuits form closed loops between a few types of neurons, therefore it is classified as a global and local (‘glocal’) property of the brain. Their interaction with other remote brain regions including various types of neurons has been studied to discover its role in the global brain function (Halassa & Haydon, 2010; Tau & Peterson, 2010; Tye & Deisseroth, 2012).

The connectionist model may be useful to understand the formation of high-level brain functions, which are described at the macroscopic scale. The high-level brain functions are found from, for example, abstractions of different types of sensory inputs, their application to new environments, and multi-tasking. When one takes the connectionist point of view, the high-level brain functions are represented via networks of many lower-level brain networks. It may be possible to explain the neuronal substrate of a shift of attention as the changes in the functional network of the brain (Rosenberg, et al., 2016). Overall, following the connectionist model's point of view, many brain regions should be simultaneously active to form high-level perception and cognition while processing various types of information in parallel. The measured BOLD signals from the whole brain contain the quasi-simultaneous activity of the brain called spontaneous BOLD signals (Lewis, Baldassarre, Committeri, Romani, & Corbetta, 2009). When the connectionist model is applied to measurements by fMRI, one could interpret coherent activities between brain regions measured by spontaneous BOLD signals as the functional connectivity of a brain network manifesting high-level perception and cognition (Van Den Heuvel & Pol, 2010).

2.2.2 Functional Connectivity and Default Mode Network

Functional connectivity is defined with correlations of neuronal activities found on time series signals collected from remote brain regions (Friston, Frith, Liddle, & Frackowiak, 1993). It was defined in PET and fMRI studies to study coherent activity between remote brain regions. The Pearson correlation coefficient, which ranges between [-1,1], is the standard method used in statistics to measure the linear bivariate correlation between two variables (Pearson, 1896). If the Pearson correlation coefficient is close to –1, then the given variables are said anti-correlated or negatively correlated and said positively correlated if their Pearson correlation coefficient is close to 1 (see Appendix A for details). The Pearson correlation coefficients should be interpreted carefully since it only shows the correlation between two variables in a linear manner. In the case that two variables are correlated nonlinearly, Pearson correlation coefficients are not a proper way to measure it. However, it is often used when there is no explicitly known information on the structure of the given variables to measure correlations between variables (Kendall & Stuart, 1973).

One of the first works on functional connectivity was about the intrinsic connectivity of the motor cortex. Biswal and colleagues (1995) calculated Pearson correlation coefficients of spontaneous BOLD signals collected from the motor cortex area reflecting hand movements to define inherent connectivity within the bilateral motor cortex (Biswal, 1995). In this paper, they reported significantly high correlations of low frequency (< 0.08Hz) BOLD signals within the motor cortex of resting human subjects. Further research on the functional correlation using fMRI data revealed inherent correlation within the bilateral visual cortex when subjects were in complete darkness (Nir, Hasson, Levy, Yeshurun, & Malach, 2006). The two studies of the motor cortex and the visual cortex confirmed the intrinsic connectivity within a functionally coherent area without the presence of corresponding stimuli.

Both studies chose the regions of interest (ROI) based on prior studies and computed the correlation between selected ROIs (Poldrack, 2007). This method is called ROI to ROI analysis (Nieto-Castanon, 2020). In addition to ROI-to-ROI analysis, there are two most widely used methods to calculate functional connectivity of the whole brain. For the seed to voxel-based connectivity analysis, a seed region is chosen and Pearson correlation coefficients between BOLD signals outside of the seed region and the seed region are calculated (Fox & Raichle, 2007). Accordingly, the result of the seed to voxel analysis depends on the choice of the seed region. Quigley and colleagues (2003) used the seed to voxel analysis to observe the interhemispheric connectivity of

the sensorimotor cortex and the auditory cortex in corpus callosum agenesis patients (Quigley, et al., 2003). They defined the seed voxels of each subject as significantly active voxels which have strong responses to sensorimotor stimuli and auditory stimuli in their BOLD signals. Then the whole brain connectivity of the resting state was analyzed by calculating the correlation between seed voxels and other voxels in the whole brain. In this paper, they showed that the effect of the corpus callosum is to connect each hemisphere by comparing the results of the seed to voxel analysis of a patient group and a normal control group. The ROI to ROI and seed to voxel analysis are computationally simple, but it is necessary to know functionally well-defined isolated brain regions in advance, since their results show the connectivity concerning the functional regions.

Another popular method is independent component analysis (ICA). It is an analysis method to identify independent sources of observed multi-variable signals under the assumption of the statistical independence of the source signals (Bell & Sejnowski, 1995; Calhoun, Adali, & Pekar, 2001; McKeown, 1998). The independence of the sources that it computes is measured via the kurtosis and the skewness of their signal distribution compared to the normal distribution of signals (Hyvärinen & Oja, 2000). When it is applied to resting state fMRI data, BOLD signals collected from the whole brain can be accounted for as mixtures of signals from independent sources (Calhoun, Adali, & Pekar, 2001) (see Appendix A for details). Such independent sources of BOLD signals are called the independent intrinsic brain networks (Allen, et al., 2014). ICA does not need any prior knowledge about sources, like where the functionally coherent brain regions regarding a specific function are, but it derives brain networks from collected data. Allen and colleagues (2014) analyzed resting state images of 405 young adults using group ICA (Allen, et al., 2014). Based on their analysis, they could classify seven independent brain networks called intrinsic connectivity networks. These seven independent brain networks were well matched with the functionally coherent regions like the bilateral visual cortex, the auditory cortex, the sensory-motor cortex. A similar study was done by Shirer and colleagues (2012) (Shirer, Ryali, Rykhlevskaia, Menon, & Greicius, 2012). They analyzed subject-driven cognitive brain states with ICA. In their study, 14 independent brain networks covering the whole brain were defined. They compared functional connectivity patterns of the 14 brain networks of four different tasks, the rest task (to be in resting state), the memory task (to retrieve events in the morning), the music task (to hum the favorite song in mind) and the subtraction task (to perform simple subtractions). Their results showed that the corresponding functional connectivity patterns of independent brain networks regarding different cognitive tasks could well be distinguished.

The most intensively studied topic of functional connectivity is the resting state functional connectivity (Allen, et al., 2014) (Andrews-Hanna, Smallwood, & Spreng, 2014; Buckner, Andrews-Hanna, & Schacter, 2008; Buckner & Carroll, 2007; Chang & Glover, 2010; Fox & Raichle, 2007; Gusnard & Raichle, 2001; Raichle, 2015; Vanhaudenhuyse, et al., 2010; Öngür, et al., 2010). A resting state means the state of mind in the absence of any stimuli, tasks, and focus on certain thoughts (Raichle, 2015). The highly correlated brain regions in the resting state are called the default mode network (DMN) (Raichle, et al., 2001). The regions forming the DMN are varied by different studies. The most often reported areas of the DMN are composed of the medial prefrontal cortex (mPFC), the posterior cingulate cortex (PCC), the precuneus (PRC), the posterior lateral parietal region, and the medial temporal lobe mainly including the angular gyrus (AG) and the parahippocampal cortex (PHC) (Raichle, 2015) (Figure a). They are located remote from each other in the human cortex and were not classified into a set of functionally coherent areas before the functional connectivity studies identified it. The role of the DMN was first suggested as the default mode of the human brain by Raichle and colleagues (2001) (Gusnard & Raichle, 2001;

Raichle, et al., 2001). In these papers, the reduced brain activity was reported in the PCC, the PRC, the mPFC, and some regions from the posterior lateral cortex when the subjects performed goal-directed or attention-demanding tasks. Similarly, the anti-correlation between the task-positive brain network which is the brain regions activated when subjects performed given tasks, and the task-negative brain network which are the brain regions deactivated during the performance of tasks were reported by functional connectivity study of BOLD signals (Fox, et al., 2005; Fransson, 2006).

Figure a: Brain regions reported as the default mode network from 777 studies.

The image file (.nii) was downloaded from neurosynth.org, meta-analyses, with the term 'default mode', then modified.

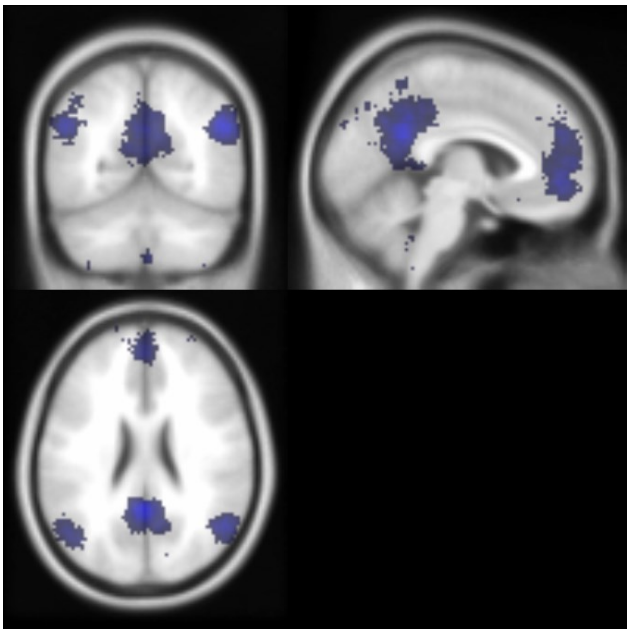

The exact functional role of the DMN is not yet fully understood. A clear functional difference of the DMN compared to other brain regions is that they are highly correlated when no cognitive activities are focusing on the physical interaction with the external world as mentioned above. Many researchers speculated that its functional role is deeply related to the internal world. Researchers have agreed that the internal world is the reference of 'self', so it makes this possible to process the self-toward tasks, to retrieve autobiographical memory, to imagine the own future (self-projection), and to conceive others' minds (Theory of Mind) (Andrews-Hanna, Smallwood, & Spreng, 2014; Buckner & Carroll, 2007; Buckner, Andrews-Hanna, & Schacter, 2008; Raichle, 2015). A meta-analysis done by Spreng and colleagues (2008) reported a great overlap between the activation map of each self-toward task and the DMN (Spreng, Mar, & Kim, 2008). It was discussed in more detail in chapter 3.

The discovery of the DMN accelerated the development of functional connectivity research toward medical purposes. If it is the default mode of the human brain representing our internal world, it should also give insights into the state of mental disorder and neurological degenerative diseases of the brain. Greicius and colleagues (2004) found the abnormality of DMN in mild Alzheimer's disease (AD) patients (Greicius, Srivastava, Reiss, & Menon, 2004). They compared the DMN of AD patients and the similarly aged control subjects to the predefined DMN template of young adults. The DMN of the AD patient was matched significantly less than that of the control group.

In further research of the DMN of AD patients combined with PET study reported the high beta-amyloid deposition in the PCC, lateral parietal lobule, and the mPFC (Buckner, et al., 2009). The abnormality of the DMN in bipolar disorder (BD) patients and schizophrenia patients was also reported (Öngür, et al., 2010). In both patient groups, the correlation of mPFC within the DMN was reduced compared with that of the normal control group. BD patients showed abnormally high correlations of the parietal cortex regions to the DMN. In schizophrenia patients, the same abnormality was observed in the basal ganglia. Furthermore, it turned out that the DMN is not well defined in the group of patients being minimally conscious, vegetative, and in coma (Vanhaudenhuyse, et al., 2010). More studies are ongoing to apply the functional connectivity study to medical purposes to help diagnose the mental disorder in its early stage and to find the physiological implications of abnormalities in the brain connectivity.

2.2.3 Graph Theory and Hubs of Brain

As mentioned above, it is possible to divide brain regions into a few intrinsic connectivity networks with ICA. The organization within and between the intrinsic brain networks also have been studied to understand their functions in the brain. Graph theory offers a very useful method to abstract a complex system with many entities and their connections as a simple network system of graphs (Pavlopoulos, et al., 2011). Graphs are formed by nodes and edges. A node represents a point and edges represent connections between nodes (Brandes & Erlebach, 2005). Using graphs, to describe the existing networks in a complex system and their connection is possible. In fMRI functional connectivity study, the graph theory is applied in the following manner (Bullmore & Sporns, 2009): first, the correlation coefficients between the whole brain regions are compared, then highly connected neighboring regions form a group or a cluster (node). Then it is possible to calculate correlations between nodes indicating a connection between them (edge). Some nodes are connected to many other nodes through only a few edges, i.e., their connection distance is short, and some are connected with other nodes through many connecting edges (Figure b, (d)). There are brain nodes with many short and direct connections to other nodes, called functional hubs. Non-hub nodes are connected via the functional hubs (Bullmore & Sporns, 2009). Each node is a functionally coherent unit of the brain network, and edges indicate the functional correlation between them. The functional hubs of the brain network facilitate fast and efficient communication in brain networks.

A small world network is a network having a short average minimum distance and a high average clustering coefficient (Watts & Strogatz, 1998). It has properties that make it a preferable network of the brain. The clustering coefficient measures how many nodes are connected by comparing the number of nodes and the number of edges in the network defined with graphs (Figure b). When the clustering coefficient is close to 1, then most nodes are connected directly. In this case, the communication between nodes is fast because of their direct connections but the amount of energy for the maintenance of the system and the complexity of the system is increased (Bullmore & Sporns, 2009). On the other hand, when nodes of a network are connected randomly to each other, their connections are not optimal in terms of function since some nodes are too far from each other and other nodes are unnecessarily close, i.e., there exists no subnetwork that might enhance the efficiency and the speed of communication (Baumann & Stiller, 2005). A small world network has rather large clustering coefficients compared with a random network and a relatively short mean distance between nodes. It implies that the network is efficient in terms of energy consumption and communication (Bassett, Meyer-Lindenberg, Achard, Duke, & Bullmore, 2006). Researchers could find out that the network of the anatomical structure of the cerebral cortex of

macaques and cats matches characteristics of the small world network (Hilgetag, Burns, O'Neill, Scannell, & Young, 2000; Latora & Marchiori, 2001). fMRI and MEG data from human subjects in a resting state and a task performing state also found that the functional network of the human brain is close to a small world network (Achard, Salvador, Whitcher, Suckling, & Bullmore, 2006; Bassett, Meyer-Lindenberg, Achard, Duke, & Bullmore, 2006; Eguiluz, Chialvo, Cecchi, Baliki, & Apkarian, 2005; Salvador, et al., 2005)

Figure b: Examples of Graphs

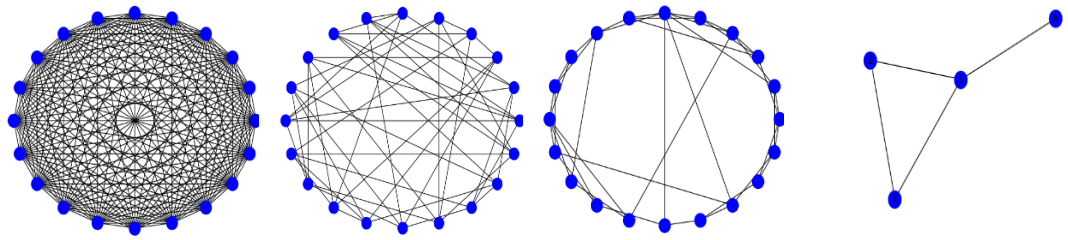

(a) Regular graph (b) Random graph (c) Small world graph (d) Graph with 4 nodes and 4 edges

In a small world network, a node is called as a hub, when it has a relatively large number of edges than other nodes have. It implies that a cluster is formed around a hub. Remote brain regions communicate with each other via connections between hubs. The network analysis of the brain revealed that the structural hubs of the human brain are well matched to the functional hubs (van den Heuvel & Sporns, 2013). The brain regions included in the DMN have been reported most often as functional hubs of the brain (Buckner, Andrews-Hanna, & Schacter, 2008; Buckner, et al., 2009; Hagmann, et al., 2008; Tomasi & Volkow, 2011). Especially, the PCC has been repeatedly reported as one of the main structural and functional hubs of the human brain (Leech & Sharp, 2014). The network analysis of the brain connectivity revealed that the average network changes along with the development of the human brain (Fair, et al., 2007). Fair and colleagues (2007) analyzed the resting state fMRI data from children (average aged 8.6), adolescents (average aged 11.9), and young adults (average aged 24.1) using graph analysis. It was reported in their paper that the interconnectivity between the frontoparietal and the cingulo-opecular network, which are the cognitive control function relevant networks, is inversely proportional to age. Also, the long-range connectivity within each network tends to increase along with age, and some hubs of each network develop their functional connectivity to the cerebellum and the DMN. Later, it was also confirmed by Biswal and colleagues (2010) that age is a factor that indicates changes in functional connectivity. They proved this by comparing functional connectivity maps from over one thousand human subjects with ages ranging or from 13 to 85 (Biswal, et al., 2010). Integration and segregation between the structural and functional networks of the human brain may enhance our understanding of its functional development.

It is possible to see a property of a network in the brain structure by using diffusion tensor imaging. The diffusion tensor imaging (DTI) technique measures the diffusion of water molecules along with axonal bundles or white matter (Mori & Zhang, 2006). The diffusion of water molecules along axons is mainly determined by the structure of axons regardless of physiological effects so that the DTI data give insights into the structural connectivity of the brain (Alexander, Lee, Lazar, & Field, 2007). Hagmann and colleagues (2008) analyzed the DTI data with graph analysis and defined structural hubs (Hagmann, et al., 2008). They reported that the DMN except the mPFC is included in the structural hub. Furthermore, the functional connectivity of the same subjects in a resting state was highly correlated to the structural connectivity measured by DTI. Also, they found

that the PCC is one of the nodes having a relatively large number of edges in the brain network. To understand the structural connectivity of the DMN better, Greicius and colleagues (2009) analyzed the structural connectivity between the mPFC, the PCC, the retrosplenial cortex (RSC), and the medial temporal lobe (Greicius, Supekar, Menon, & Dougherty, 2009). They reported that the mPFC is connected to the PCC and the medial temporal lobe including the PHC, which has anatomical connections to the RSC. These studies indicate that there is corresponding structural connectivity to the functional connectivity of the DMN.

One can see also the possible connection between the structural connectivity and the functional connectivity with simulated data. Honey and colleagues used simulated neuronal activity on the structural hubs of macaques to study this topic (Honey, Kötter, Breakspear, & Sporns, 2007). First, they defined a structural network with structural hubs of macaques using graph theory analysis. Then they measured the transfer entropy of simulated neuronal activities of the structural network to define functional connectivity between the structural hubs. The transfer entropy shows how much information exchanges happen between two nodes (Schreiber, 2000). High transfer entropy means two brain regions exchange a lot of information; therefore, they are functionally connected. Honey and colleagues (2007) found out that the structural connectivity calculated with graph analysis and the functional connectivity of the simulated data overlapped with around 80%.

Due to the short history of connectivity research on the brain, there are a limited number of studies about the correspondence between structural connectivity and functional connectivity. Hence, it is critical to study the relation more thoroughly between these two concepts for further development of connectivity research.

2.2.4 Dynamic Functional Connectivity

The functional connectivity relies on Pearson correlation coefficients averaged over the whole-time course of an experiment session (Biswal, 1995; Fox, et al., 2005). Conventionally, a period of a session is around 8 to 10 minutes for a resting state fMRI. As a result, calculated correlation coefficients have little information about the dynamics of functional connectivity in the brain (Hutchison, et al., 2013). In the case of an fMRI experiment with the external performance of tasks, it is expected to detect dynamics of brain activity by the dynamics of the tasks. On the other hand, an fMRI experiment without any external performance of a task, like a resting state, has no specific time points where one can expect to see changes in brain activity. Dynamic functional connectivity is a theory suggested to solve this problem. Chang and Glover (2010) used the sliding-window correlation analysis to see the dynamics of connectivity of the resting state fMRI data (Chang & Glover, 2010). The sliding window correlation analysis measures a set of consecutive correlations for a time window between two brain regions. The analysis is usually used to process time series data in terms of consecutive changes in the short time series data. Change and Glover (2010) reported that temporal variation of functional connectivity between the PCC and other brain regions calculated via the sliding window correlation analysis is relatively high in a resting state. Similarly, Allen and colleagues (2014) combined sliding window correlation with the so-called k-mean clustering to check whether there are temporary stable states in a resting state (Allen, et al., 2014). The k-mean clustering is an algorithm classifying a data set into k different clusters, such that the sum of the total variance of each data point is minimized for the mean, called the centroid, of each cluster to which they belong (Hartigan & Wong, 1979). They classified the dynamic functional connectivity of brain networks into seven centroids. They labeled the DFC maps with the seven different states and identified the resting state fMRI data with these seven states

to check changes of those states in time. They could not find a regular pattern of rising and falling of the states but reported that transition between them does not happen frequently.

The DFC can also be combined with the behavioral observations of subjects. Bassett and colleagues (2011) analyzed the dynamics of modules of the whole brain network, while the subjects were performing motor learning tasks (Bassett, et al., 2011). Using graph theory, they grouped local networks of the whole brain network which have relatively dense connectivity around hubs and called them modules of the network. Furthermore, they analyzed changes of modules in brain networks at the scales of days, hours, and minutes. For that, they measured the modularity of brain networks at each time scale. Modularity shows how dense connections are between nodes in the same module (Fortunato, 2010). They could observe high modularity at all time scales and smooth changes of modules, i.e., flexible reorganizations of hubs and nodes at all time scales. The flexibility of modules appeared more clearly when the time scale was small. Also, the modularity increased first, then decreased at the day scale. They suggested it as an implication of the correlation between learning and modularity. Interestingly, they did not report a correlation between behavioral results and changes of modules in brain networks on the paper.

In cognitive neuroscience and neuropsychology, it is important to see the correspondence between the behavioral and neuronal measures to estimate functions of functional connectivity. To see the behavioral relevance of DFC, Kucyi and Davis (2014) compared the 'daydreaming frequency (DDF)' indicating how often the subject daydream, which is collected via questionnaires, to the variability of the functional connectivity of the DMN using the sliding window correlation analysis the of resting state fMRI data (Kucyi & Davis, 2014). They found subjects who reported a high frequency of daydreaming showed high variability of PCC-MTL connectivity in the DMN. In clinical research on schizophrenia patients done by Damaraju and colleagues (2014), it was reported that the patient group showed a tendency to stay longer in a weakly correlated connectivity state of intrinsic brain networks than the healthy control group by comparing their functional connectivity and DFC (Damaraju, et al., 2014). In this study, they also confirmed the hyperconnectivity between the thalamus and sensory networks including visual, auditory, and sensorymotor networks by the functional connectivity and DFC in brain networks of schizophrenia patients. Similar results have been reported by other functional connectivity studies (Anticevic, et al., 2014; Woodward, Karbasforoushan, & Heckers, 2012). Taken together, these studies support the idea that DFC has the potential of becoming a tool to study dynamics of perception and cognition corresponding to observable behaviors.

Many interesting new methods also have been suggested to explore the mechanism of structural and functional connectivity, and DFC (Preti, Bolton, Van De Ville, 2017). To explain the foundation of the emergence of functional connectivity and DFC in the brain, Deco and colleagues (2017) suggested a dynamical model of local nodes in the brain (Deco, Kringelbach, Jirsa, & Ritter, 2017). They suggested the Hopf bifurcation as a local dynamical model of nodes producing BOLD signals. Bifurcation describes the dynamic evolution of the state of a system for equilibrium along with changes in the parameters of the system (Seydel, 2009). Using Hopf bifurcation, they produced noisy oscillatory signals in each brain node, then simulated interaction between them by changing the coupling parameter between nodes. The coupling parameter was estimated by average functional connectivity and DFC of collected resting state fMRI data. They could find similar brain networks from their simulated data including the DMN. Sizemore and colleagues (2018) applied algebraic topology to study the formation of the structural connectivity observed by DTI (Sizemore, et al., 2018). In their study, they could simulate the formation of the brain network defined via structural connectivity by investigating a combination of all to all connectivity between

nodes, which are called cliques. Because of its combinatorial approach to building a structure using small building blocks (cliques), they could simulate the entire structural connectivity of the brain without bias towards the local connectivity.

It is also possible to observe DFC without averaging correlation coefficients within a short time interval. Saggar and colleagues (2018) suggested a topological data analysis method to apply to fMRI data, while they avoided averaging the data into a time interval (Saggar, et al., 2018). In this paper, they analyzed fMRI data collected from four different tasks performance states within a scanning session. They clustered the activity patterns of voxels, i.e., functional segregation of data, over each time point. Then they connected clusters defined at a time point if the clusters are close in time. By doing so, they suggested a way of tracking DFC at a short time scale around 4-9 secs. However, they did not compare directly how their topologically organized graph could be connected to the known functional brain networks.

As mentioned earlier, several DFC studies have been done for the last decade. They have agreed that there are intrinsic dynamics of functional connectivity. However, some concerns about DFC have been raised at the same time. Hindriks and colleagues (2016) showed the importance of the right statistical test to confirm the DFC of the real dynamics of functional connectivity, but not of the noise or random effects (Hindriks, et al., 2016). They systematically analyzed how to estimate the power of statistical inference in measured DFC. Then they applied their suggestions on a simulated fMRI data set and a real data set from macaques and human subjects using the sliding window correlation analysis. In this paper, they showed the length of a measured session and the chance of detecting significant DFC is proportional. They concluded that it is insufficient to apply the sliding correlation window analysis to a short single run of fMRI data to detect DFC.

Even the right statistical test is applied to define DFC, still there are several remaining concerns about DFC. Hutchison and colleagues (2013) pointed out the following (Hutchison, et al., 2013). If functional connectivity itself is not static, i.e., the functional connectivity constantly in a long-time span, the changes should be included in the calculation of DFC. They also pointed out that its small number of data points for the calculation of correlations in general. In the case of sliding window analysis, it is very sensitive to physiological noises, like head motion and respiratory movement. Laumann and colleagues (2017) expressed their concern, especially on resting state DFC, that it may not be a real functional characteristic of the brain, but an artifact mainly originated from physiological noises (Laumann, et al., 2017). Overall, these concerns about DFC suggest that the current understanding of DFC is not sufficient to conclude that DFC shows the real sign of functional changes in brain networks. Hutchison and colleagues (2013) suggested that fMRI combined with other measurement methods like electroencephalography, LFP, and behavioral response from subjects may enhance the understanding of DFC.

2.2.5 Self-driven tasks

To identify the causality of a phenomenon objectively, the scientific description of a cause (stimuli) and its corresponding results (observed brain activities) should agree with each other. For that, experimenters prepare independent stimuli which are spatial-temporally well-defined, like a pure tone or a Gabor patch. The physiological reactions of the brain to the prepared stimuli are collected using a relevant technique. Then the collected data sets are analyzed by a linear regression model with a design matrix containing information of the time points of presentation of stimuli (Smith, 2004). Most neuropsychology experiments have followed this conventional experimental

setup to evoke specific functions of the brain corresponding to the stimuli. This guarantees the objectivity of the measured brain activities with minimal influences from unknown variables.

A type of task, which allows more freedom to subject, for example, to retrieve memory without cues or to hum a favorite song in their mind (Shirer, Ryali, Rykhlevskaia, Menon, & Greicius, 2012), has not been a preferable experimental design, since it is not possible to have an explicit prediction for a moment to observe reactions of the brain concerning a stimulus. In the real world, most perception and cognition do not rely on well-defined spatial-temporally independent stimuli but rather rely on a continuous rush of multisensory inputs and internal motivations to act on an environment. Therefore, studying the brain activities during the performances of realistic tasks with less control from the experimental designs should be accepted as a relevant method, too. I will refer to such a task as a self-driven task. Connectivity studies require the measure of spontaneous brain activity without an explicit temporal control from outside. The DMN defined while a human subject is in a resting state without specific tasks to perform is a good example. It is also proper to consider the multimodality of the brain. Multisensory inputs are processed by the cooperation between many brain regions which are functionally separated. In contrast to the conventional fMRI studies with experimental designs to measure the causality between independent stimuli and responses of the brain to them, functional connectivity measures the correlations of brain activities from different brain regions, which is a relative feature. Therefore, functional connectivity is a suitable parameter to highlight the parallel characteristics of many brain regions.

The network analysis of functional connectivity and DFC tells us the dynamics of interaction between and within brain networks, which might be functional units for high-level cognition and perception. Studying functional connectivity and DFC is an intriguing journey to establish a comprehensive understanding of the function of the brain as a whole system. However, many questions need to be asked and answered. It can tell us only about the observable phenomena of the brain at the macroscopic scale spatiotemporally. We do not know how this macroscopic picture is related to the microscopic picture of single neurons, and the mesoscopic picture of neural circuits. The current topics of neuroscience are scattered independently at the different spatiotemporal scales. To have a complete understanding of the brain mechanism, the integration of the current knowledge crossing all scales is necessary. However, a better understanding of brain networks and their dynamics should be acquired before we move to the next step.

It is in general recommended to employ various methods with different perspectives to observe a complex phenomenon to compensate for the innate shortages of each method. In the case of the studies concerning the human brain, particularly behavioral responses from subjects may offer useful insights in combination with measured neuronal activities. A self-driven task is a highly relevant experimental design to study high-level perception and cognition. When it is analyzed with DFC, which is a proper analysis method to show spontaneous changes of brain networks, it will give insights into the formation of high-level perception and cognition. Because of this reason, the focus of this thesis is on DFC of the brain networks which is measured while subjects perform self-driven tasks. I explored a new analytic method to extract changes in DFC of the DMN while human subjects performed different self-driven tasks, which are being in a resting state and an episodic memory retrieval state. The analysis was accompanied by behavioral observations to understand the meaning of the analysis results in connection with perception and cognition. Before moving there, I discussed relevant topics and literature in the next two chapters to my research interest.

3. Brain as Dynamical System

The systematic analysis of an object of study requires a proper understanding of the spectrum of its physical scale. In neuropsychology, its spectrum starts from neuronal excitation and inhibition, which are responses to stimuli, and ends at the group activities of neuronal populations, which are considered relevant to explain the behaviors of humans. Data collected with fMRI, PET, EEG, and MEG are interpreted as neural markers of behavioral observations (Heeger & Ress, 2002). So far there has been no explicit understanding of how BOLD signals and neuronal activities are connected. To understand their relationship is critical to specify the meaning of experimental results from the fMRI study. At the same time, studying the fundamental building block of fMRI through their connection to behavioral observation is also necessary. It enhances our understanding of the high-level perception and cognition which could be observed from behavioral measurements of subjects.

We know by our experiences in everyday life, that our perceptive and cognitive activities shift from time to time while we are awake. If BOLD signals reflect certain parts of neuronal activities, then such perceptive and cognitive shifts should be projected on them. Time-dependent changes of a system can be described with a dynamical system. A dynamical system has its states, and their changes are described with the flow of time. Let's imagine a ball rolling along on a hillside. All possible positions of the ball are states of the ball's dynamical system. The position of the ball changes through time and it can be calculated based on Newton's laws of motion. In other words, Newton's law describes the time evolution of the position of the ball. The change of its position or the path of the rolling ball can be calculated based on Newton's laws with a given initial position of the ball and its initial velocity. Newton's laws of motion were established based on observations and measurements of the movement of objects. Observations and measurements were formulated with mathematical language, called the equation of motion, to describe the dynamic changes of a state of an object. Could we find such dynamics from measured BOLD signals to describe changes in their state? If it is possible, the identified state and dynamics of BOLD signals might have certain correspondence to behavioral measurements. To investigate it, I reviewed what the known examples of the brain as a dynamical system in various perspectives are, especially related to the measured oscillatory signals by EEG and LFP. Furthermore, interesting theoretical dynamic models based on basic structural and functional properties of the brain were briefly reviewed. After the review, a proposal on how it might be possible to describe the brain as a dynamical system using BOLD signals was stated.

3.1 Approximately Deterministic Dynamical System

There are two types of dynamical systems, a deterministic dynamical system, and a stochastic dynamical system, depending on how the time evolution of the state of the system could be predicted explicitly (Honerkamp, 1993). When a dynamical system is mentioned in the context of classical mechanics, it means a deterministic dynamical system. Also in this thesis, a dynamical system means a deterministic dynamical system. To describe a system as a dynamical system, one needs to define a measurable set, a measure, and a measure-preserving transformation of the set (Brin & Stuck, 2002). Here a measurable set means a group of measurable states of a dynamical system. A measure means a method to assign a certain number or value to states. A measure-preserving transformation of the set guarantees that the state of a system stays in a measurable set after iteration of time evolution (Meiss, 2007). In the previous example of a rolling ball on a hillside, the position of the ball changes on the hillside because of the gravity applying

to the ball. When we define a dynamical system with the position of the ball on the hillside and gravity as the driving force of rolling, a flying ball over the hillside accelerating itself upward does not belong to the measurable set of the defined dynamical system. If the ball starts flying at a point of time, then from that time point the system should be redefined with a new measurable set and a new measure-preserving transformation. Dynamical systems could be defined in a fully deterministic way when there is no or negligible random noise. When the initial condition is given, then its state after a certain time could be predicted surely based on the equation of motion describing changes of the state. Under the assumption of no fraction between the rolling ball and the surface of the hillside, one can solve the equation of motion of the ball. Hence it is possible to predict the ball's position at a given time point exactly. On the other hand, there are cases that such random noises have effects on the evolution of the dynamic system severely. In the rolling ball example again, if an earthquake happens on the hillside so the ball hops randomly while it is rolling, the effect from the earthquake should be counted to describe the changes of the ball's state. Dynamical systems with random noises are described with stochastic dynamical systems. Stochastic dynamical systems evolve under the effects of random noise (Turelli, 1997). Consequently, the evolution of the system only could be described in probabilistic ways when one knows about the statistical distribution of the noise.

The complexity of a brain as a biochemical machine is believed very high. It consists of billions of neurons and non-neuronal cells working at the molecular scale of chemical reactions. Individual dynamical systems like the action potentials of a neuron with specific inputs and coupling between two neurons might be close to a deterministic system. On the other hand, when they couple with each other, its massive connections between neurons through wide synaptic networks in different physical scales might be close to a stochastic dynamical system. The high degrees of freedom of a system is the other name of the randomness of the system. Each degree of freedom is supposed to be independent, therefore each of them has the freedom to have any value regardless of other independent variables. Consequently, it makes the system random or non-deterministic at the macroscopic scale (Honerkamp, 1993). Thus, it is hard to imagine defining a brain as a deterministic dynamical system due to its high structural complexity. To assume that it is a stochastic dynamical system sounds more reasonable when the structural complexity of the brain is considered.

At the same time, the mental state of humans without severe mental disorders or neuronal degenerative diseases shifts from one to the others with certain predictability, when they are in a familiar environment. A stochastic dynamical system could be decomposed into the deterministic dynamical system and additional stochastic terms. When the stochastic terms do not strongly contribute to the evolution of the dynamical system, then it is considered an almost deterministic system. This might be the most proper situation to describe systems in real. In physics, the degree of freedom of dynamic systems could be reduced by taking a limit to an extreme number of particles, temperature, or time and so on (Hill, 1986). For example, in a thermodynamic system, the ideal gas has a reduced number of degrees of freedom by assuming negligible interaction between atoms and describing the system in terms of macroscopic variables like pressure, volume, temperature, and the number of atoms. Through the reduction of the degree of freedom, it could be described as a deterministic dynamical system. Is it reasonable to expect to find a similar way in the brain to approximate the random microscopic system to the deterministic macroscopic system?

At the first look, it seems quite difficult to find a corresponding way in the case of the brain. The problem is that the complexity of the brain itself plays an important role in its function. The law of

evolution has enforced animals to be adaptive to many unexpected environments. Therefore, to keep a certain level of the structural complexity of the system to adjust itself to the various environments might have been beneficial to survive and thrive. At the same time, biochemical machines have a physical limit to expand their structural complexity due to their energy efficiency and performance efficiency (functional efficiency). The functional complexity could be measured by the result of animals' interaction with a system or their performance on the system. It may offer the threshold to structural complexity. As time goes by, it is reasonable to assume that redundant tools of the system and rarely used ones are dismissed when the structural complexity of a system has reached its threshold given by the functional efficiency. As the result, the only structures that cannot be abstracted together are left. Thus, the brain evolves an ensemble of various tools that have been designed for its functional purpose with a certain amount of efficiency. Nevertheless, its complexity reflects the amount of the complexity of the environment. This picture may be able to explain the observed functional and structural complexity of the brain with its approximately deterministic property. To sum up, to account for the complexity of the brain coming from the simultaneous activation of the diverse units and regions of the brain, it is reasonable to explain the brain as an approximately deterministic dynamical system. Hence, to ask how such approximately deterministic property is realized in the brain is an intriguing question.

3.1.1 Example of Dynamical Brain Model: Oscillation

Many interesting models of dynamics of the brain describing its approximately deterministic property have been suggested. The most well-known dynamical property of the measured brain signal is oscillation. Oscillation is repetitive activity within a specific range of the variance of a state. The repetitive property is described with its wavelength or frequency, phase, and amplitude. It is repetitive along the time, so one could predict how the system evolves for the given period when its initial conditions are known. Since the first oscillatory signals were measured from humans by German psychiatrist Hans Berger (Berger, 1929) using EEG, it has been one of the main branches of neuroscience to measure changes of oscillatory signals on the scalp with respect to tasks and stimuli. Also, using intracranial electrodes researchers have found out the broad oscillatory activities from single neurons to the population of neurons, and the entire brain (Buzsáki & Draguhn, 2004). Its exact role in the brain function and its generation mechanism have been discussed with several human and animal experiments.

One of its possible functions is the binding. The repetitive appearance of the oscillatory signals within and between populations of neurons offers a good tool to bind neural activities spatially and temporally. Pöppel (1997) suggested that the temporal binding of inputs to the brain happened by oscillation (Pöppel, 1997). He showed that the order of events is not recognizable when they fall into a too short time duration, which is shorter than the possible wavelength (~30 milliseconds) of the binding oscillation. Not only at the microscopic time scale, but it could also be expanded into a larger time scale around 3 seconds which is relevant for perception and cognition. The events bound in short time or high frequency oscillation are bound again in low frequency oscillations, and it offers the basic unit of perception and cognition that could be recognized with observable meanings. On a more expanded time scale, theta wave from hippocampal formation has been thought to be related with binding of the events in long term memory (Gray, König, Engel, & Singer, 1989). Not only the temporal binding, but also the spatial binding between remote brain regions may rely on the oscillation. In a paper on the large-scale phase synchronization in the brain, Varela and colleagues reviewed various experimental measurements showing the phase synchrony in the brain (Varela, Lachaux, Rodriguez, & Martinerie, 2001). They pointed out

that synchrony patterns were measured from spatially remote brain regions, crossing the microscopic (up to 2 mm) to the macroscopic scale (larger than 2 cm), when subjects performed multimodal tasks. Despite the existing experimental measurements, its embodiment in the cellular level has not been known yet. An interesting model regarding it was suggested by Buzsáki and colleagues (Buzsáki, Geisler, Henze, & Wang, 2004). In this paper, they proposed that dense local connections and sparse long-range connections are the key to spatial and functional integration of neural activities by neural oscillations. They hypothesized that the diverse interneurons are functionally discriminated against. According to their proposal, the function of interneurons is producing dense local oscillation and long-range oscillation. The local neurons get connected densely via interneurons producing dense local oscillations and form hubs and the hubs are connected via long range oscillation of sparse interneurons to form a small world network. Together, the oscillatory activities of the brain explain spatiotemporal binding of neuronal activities via dynamical changes in the coherence of simultaneous neuronal activities of multiple neuronal units.

3.1.2 Example of Dynamical Brain Model: Predictive Coding

The oscillatory activities of the brain are induced from experimental observations. On the other hand, few theoretical works have also been done to explain how perception and cognition could be interpreted with the dynamics of the brain. Predictive coding has been under the spotlight of the neuroscientist community for the last few decades. According to predictive coding, perception and cognition follow the unconscious inference introduced by Hermann von Helmholtz (von Helmholtz, 1925). Helmholtz regards visual perception as a process of recognition, not a direct representation of external stimuli. It means that the brain actively infers which environment it belongs to, and the external stimuli are used to confirm its inference. The external stimuli are delivered through the thalamocortical connection to the cortex. Then they are processed in different layers simultaneously so that inference and confirmation processes happen in parallel (Mumford, 1992). To understand how predictive coding works, the generative model needs to be introduced. The generative model is for the classification of the hidden variables (latent variables) of the given data, or observations. In other words, it aims to classify the hidden causes of their observations (Ng & Jordan, 2001). When we apply this to predictive coding, the brain infers what causes the input signals, i.e., what are the hidden variables of the observed world represented by the inputs to the brain. The produced prediction over the hidden variables is updated by its prediction error, which is the difference between the prediction and the delivered input (Friston, 2010).

The structural and functional hierarchy in the cortex and its relationship to predictive coding was suggested by Mumford (Mumford, 1992). In this paper, predictive coding was defined following. A functionally higher cortex, where processes of abstract information from wide receptive fields, produces cognitive templates or predictions. It is realized with deep pyramidal cells located at the infragranular layer (layer 5 and 6). The predictions are delivered to its supragranular layer (layer 2 and 3) and the infragranular layer of a functionally lower cortex via its granular layer (layer 4) where it processes fine information in small receptive fields. The prediction errors (residuals) are processed in the supragranular layer then delivered to the infragranular layer of the higher cortex again to update the prediction. The connection from the functionally higher cortex to the lower cortex is a descending pathway/ top-down processing, and the connection in the other way around is an ascending pathway/ bottom-up processing (Mumford, 1992).

The predictive coding with the hierarchical generative model has been extended to explain the structure and function of the brain. Particularly, it has been actively discussed how the hierarchical generative model could be implanted in the laminar structure of the cortex. Barrett and colleagues

(2015) suggested how the laminar cytoarchitecture of the cortex can be applied to predictive coding (Barrett & Simmons, 2015). They explained that the agranular cortex area, which has no granular layer (layer 4) but has abundant pyramidal cells in its layer 5/6, generates predictions from neurons in layer 5/6 and descends it to the granular cortex, which has well-developed layer 4. Granular neurons in layer 4 of the granular cortex area distribute amplified thalamocortical projections to all layers, and prediction errors are calculated in supragranular layers. These prediction errors are projected via cortico-cortical connection to layer 5/6 of the agranular cortex. Due to the lack of layer 4 in the agranular cortex, its delivered thalamocortical projections and prediction errors are not amplified and distributed. As a result, the pyramidal neurons in layer 5/6 update their prediction slowly. Furthermore, they applied their model to the insula cortex to explain the interoception in terms of predictive coding relying on its dorsally granular structure and ventrally agranular structure. Similarly, an interpretation of the motor cortex using predictive coding was suggested by Adams and colleagues (Adams, Shipp, & Friston, 2013). The motor cortex has an agranular laminar structure. In their model, its role is to produce proprioceptive predictions, not to drive movements by descending neural signals of planned movements to motor neurons. According to this model, prediction errors are calculated by alpha motor neurons and fed forwarded to the somatosensory cortex. The picture of reciprocal connection of the predictive coding is extended also to the microcircuit within cortical columns. Bastos and colleagues (2012) presented a possible structural mechanism of predictive coding using inhibitory and excitatory neuronal units within layers in cortical columns (Bastos, et al., 2012). In this paper, they summarized that the role of inhibitory neurons is for feedback processing, but the excitatory neurons might have roles in both the feedback and feed-forward processing.

In addition to the explanation about predictive coding with the laminar structure of the brain, computational models for predictive coding have been suggested (Dayan, Hinton, Neal, & Zemel, 1995; Friston, 2010; Rao & Ballard, 1999). Dayan and colleagues (1995) proposed a possible mathematical model for predictive coding called the Helmholtz machine (Dayan, Hinton, Neal, & Zemel, 1995). In this paper, the Helmholtz machine is composed of artificial neurons of layers having a hierarchy structure. Following the definitions in the paper, its top-down processing is represented with the generative model, and the bottom-up processing is represented with the recognition model. The generative model of this machine might have numerous explanations on the relationship between an observation and the cause that is generated through layers connected nonlinearly. Therefore, extracting an exact explanation of a cause and an observation takes a lot of energy and time. Dayan and colleagues suggested a recognition model, which is a rough guess about the generative model with an assumption of independence of explanation at each layer of the computation process. The recognition model can compute an explicit explanation of a cause and observation, but it may or may not be close to the true explanation of the generative model. The generative model produces predictions on the causes of observations, and the recognition model infers the prediction with its simplified model of prediction. They adapt to each other to minimize the Helmholtz free energy expressing the difference between them. In terms of predictive coding, the Helmholtz free energy is the prediction error (Dayan, Hinton, Neal, & Zemel, 1995). It is not equal to the Helmholtz free energy of a thermodynamic system. The Helmholtz machine was rephrased and adapted as the free energy principle for the brain by Friston and colleagues (Friston, Kilner, & Harrison, 2006; Friston, Trujillo-Barreto, & Daunizeau, 2008; Friston, 2010). In the series of papers, the free energy principle for the brain is a specialized Helmholtz machine to explain the principle of the brain mechanism (Friston, 2010). According to this idea, an agent interacts with the environment where it belongs by acting on the environment and perceiving the changes of the environment. The agent aims to minimize the Helmholtz free

energy. By doing so, the agent gets optimized to survive. Following their idea, this happens in two directions, one is the action done by agents exploring the environment to fit the external stimuli to its generative model, so prediction error gets reduced. Another way is to update its recognition model to fit the input stimuli coming from the external world (Friston, Kilner, & Harrison, 2006; Friston, Trujillo-Barreto, & Daunizeau, 2008; Friston, 2010). To describe it simply is the following. The physical inputs from the environment and predictions on them from the generative model should be compared to know the precision of its predictions. For that, physical inputs are reconstructed by the recognition model which is an inference of the generative model. The difference between them is called free energy (the prediction error), and the brain changes the environment or its recognition model to minimize it (Friston, 2010).

Apart from the advanced theoretical model of predictive coding, its computational model with simulation was done by Rao and Ballard (1999) with two layers of artificial neurons. Their computational model which learned the distribution of visual stimuli from natural images could mimic the end-stopping effect of the visual cortex (Rao & Ballard, 1999). In V1, there is a type of neuron that is highly active when a line in its receptive field does not reach both ends of its receptive field, and its activities are suppressed when the line reaches both ends of its receptive field. Such an activity pattern is called the end-stopping effect (Hubel & Wiesel, 1965). Rao and Ballard set a computational model with two-level hierarchies containing prediction coding neurons, and prediction error coding neurons. The receptive field of neurons in the upper layer is formed by combining the receptive fields of lower layer neurons with partial overlaps between them. The prediction neurons learned the prior probability distribution of natural images. By doing so, they could reproduce the end-stopping effect with their two-level artificial neurons. As one can see clearly through this computational model, predictive coding requires neuronal subunits to process prediction errors and forward them to the functionally higher area to update its prediction. The big question of predictive coding with the hierarchical generative model is coming from it. How does the brain process the prediction error and in which types of neuronal subunits do this?

The predictive coding schemes introduced above have been established on the hierarchical structure of the brain with parallel connections between hierarchical units. Engel and colleagues (2001) suggested a model of predictive coding without hierarchy (Engel, Fries, & Singer, 2001). In this paper, they proposed that top-down processing of the predictive coding is presented in oscillatory activities via synchrony of distributed neuronal assemblies or populations. This large-scale interaction is a self-generated pattern based on prior experiences that could produce prediction and expectation on the external world. Furthermore, they suggested that stimuli-evoked neuronal activities sharing the self-generated pattern could join in these oscillatory activities. Also, it can modulate neuronal activities of small neuronal assemblies so that it joins on the large-scale interaction (Engel, Fries, & Singer, 2001). An advantage of this model compared to the predictive coding with the hierarchical generative model is that they do not need separated neuronal units to code predictions and prediction errors. However, it is also questionable how the self-generated pattern is initiated between distributed neuronal assemblies and how the brain remembers the large-scale patterns.

3.1.3 Example of Dynamical Brain Model: Hopfield Model

The predictive coding and oscillation are discussing the general mechanism of the brain. There is also an intriguing dynamical model of a specific function of the brain called the Hopfield model (Hopfield, 1982; 1984). This model explains how associative memory could be realized via synaptic connections of neurons. Associative memory explains how the partial initial information, or

the memory cue could lead the brain to retrieve the right full memory associated with the cue. Hopfield (1982) designed memory as a pattern in a high-dimensional vector space. The patterns of memory are learned from a set of binary artificial neurons described with synaptic connections between them. Each memory is expressed with a different pattern in the high dimensional memory vector space. When a memory cue is suggested, the pattern triggered by the cue is compared with the stored memory patterns. The similarity between one of the memory patterns and the current pattern decides the activity of neurons at the next moment following the Hebbian learning rule (Hebb, 2005). In this way, the pattern of the memory cue is updated dynamically till it converges to the most similar memory pattern (Hopfield, 1982). Furthermore, Hopfield (1984) expressed it with an energy function so that this neuronal network can be explained in terms of a dynamical system evolving to the nearest stable energy states (Hopfield, 1984). To build a more realistic and plausible Hopfield model, the binary neurons are replaced with more relevant models of neurons (Gerstner, Kistler, Naud, & Paninski, 2014). The Hopfield model has been used for the optimization of a system in machine learning since it describes the general emergent property of a network that its members are defined with similar computational units of the neurons in the model (Hopfield, 2007). Even if it currently stays in the theoretical model for the brain, it could describe the dynamical evolution of a simple neural network explicitly (Hopfiled, 1982; Hopfield, 1984).

When we compare the top-down processing of predictive coding suggested by Engel and colleagues (2001) and the Hopfield model, it seems there is a commonality between them. Both models assume memory patterns that are saved in many neurons and the pattern is realized in a high-dimensional space. Notably, the modulatory role of the large-scale interaction of the model by Egel and Collegues (2001) is comparable with the memory pattern of the Hopfield model that modulates the activity of neuronal assemblies. However, the Hopfield model relies on the direct synaptic connections between neurons, so it is hard to apply to large-scale interaction. Also, explaining how oscillatory behaviors could appear in the Hopfield model should be carefully considered. The evidence reviewed here tells us that it would be interesting to test the compatibility between these two models.

3.2 Dynamics of BOLD Signals

The above examples described the brain as an approximately deterministic dynamical system holding its structural and functional complexity. Is it possible to understand BOLD signals in terms of an approximately deterministic dynamical system too? Does BOLD reflect reliably not only spatial compositions of neuronal activities but also its temporal characteristics? If it is possible to define changes of BOLD signals in terms of a deterministic dynamical system, it might help us to find a driving force of BOLD signals. However, BOLD signals contain random noises. Here, noises mean signals other than pure BOLD signals produced by neuronal activities. There are standard methods to remove known noises like the movement of a subject and physiological noises (Caballero-Gaudes & Reynolds, 2017). Even after known denoising processes, it is hard to say BOLD signals are purely produced from neuronal activities, till the explicit mechanism of generation of BOLD signals from neuronal activities is found. Therefore, there is still a chance that BOLD signals get affected by unknown random noises other than the true neuronal activities. All speculations that I would present from now on are with the acknowledgment of the limit of BOLD signals.

3.2.1 Self-Organizing System

The first step to formalize measured BOLD signals in terms of a dynamical system is to define measurable states. I will define states of BOLD signals as a set of representations of mental states generated by neuronal activities accompanied by observable behaviors to experimenters. The definition of observable behaviors to experimenters includes the case that they are reported by human subjects via oral statements or questionnaires. A state is a member of a state space which is a set of all possible states. The evolution of a dynamical system means the time dependent changes of a state of the system. Following the definition, the BOLD signal describes the time evolution of the mental state generated with neuronal activities accompanied by observable behaviors. In other words, the BOLD signal describes the dynamics of a mental state. It is unknown whether the neuronal activity of the brain is governed by deterministic dynamics or by stochastic dynamics. However, in the case of a BOLD signal, to assume that it follows stochastic dynamics sounds reasonable. There are a few reasons for that. First, the technical limits of fMRI are considerable. For example, the uneven magnetic field inside of an MRI machine, movement of a subject, and physiological noises, all these noises are removed as much as possible in the preprocessing stage. However, still, the signal-to-noise ratio of the fMRI data varies widely up to the task types and MRI machines (Welvaert & Rosseel, 2013). So, it is a generous choice to assume that the BOLD signals contain random noises.

Apart from these technical limits, the nature of the neuronal activities contains randomness. It is believed that neurons do not respond to the same stimulus always in the same way (Softky & Koch, 1993). Due to this reason, studies of direct measurement of single neurons are statistical measurements, like peri-stimulus time and post-stimulus time histogram. Furthermore, measuring the activities of a population of neurons is also a method to identify rather a deterministic relation between a stimulus and reaction (Gerstner W., Kistler, Naud, & Paninski, 2014; Zohary, Shadlen, & Newsome, 1994). However, the BOLD signals are not generated directly from neuronal activities, but as mentioned in the second chapter, generated via hemodynamics. Even though the exact relationship between the BOLD signals and neuronal activity is unknown yet, as previously mentioned, Nir and colleagues (2007) showed that it is possible to predict BOLD signals of the primary auditory cortex by using LFP of single neurons in the primary auditory cortex (Nir, et al., 2007). Not only this, other studies that I reviewed in the previous chapter also measured the correlation between BOLD signals and stimuli evoked LFPs from the primary visual cortex (Goense & Logothetis, 2008; Logothetis, Pauls, Augath, Trinath, & Oeltermann, 2001). Hence it seems good enough to assume BOLD signals are described with deterministic dynamics.

When one takes a close look at the listed examples showing the correlation between BOLD signals and LFPs, they measured the sensory stimuli evoked responses of neurons. It does not guarantee that the spontaneous neuronal activities without external stimuli also have the reliable deterministic dynamics of the BOLD signals. Jointly, to assume that BOLD signals are approximately deterministic might describe BOLD signals close to their real dynamics. However, it is unknown that whether it is the case also for the BOLD signals measuring spontaneous activities of the brain. The question is following. How one can assume that the BOLD signals of spontaneous brain activities follow deterministic dynamics?

Using the example of a rolling ball on the hill again, if earthquakes or whirlwinds hit the ball then its trajectory should be recomputed, but the ball is still rolling toward the lowest point of the hill because of gravity. In physics, such systems could be described in terms of chaotic complex systems (Jaeger & Haas, 2004). When the time evolution of a highly nonlinear dynamic system is sensitive to its initial condition, it is a chaotic complex system (Boccaletti, Grebogi, Lai, Mancini,

& Maza, 2000). Chaotic complex systems look unorganized and random due to their high complexity. There might be a hidden regulation governing the system, but it is unseen due to the complexity of the system. How can we access such a regulation of the chaotic complex system then? A self-organizing system is one way to understand a chaotic complex system (Ashby, 2017). Ashby (2017) suggested changing the point of view to describe a complex chaotic system to find a hidden regulation in it. Most of the time, a self-organizing system means the formation of the structure via connections between subsystems like cell assemblies. It could be applied more flexibly and generally than this. Following the definition of the self-organizing system by Ashby (2017), to self-organize means to adjust the system in good ways to the hidden regulation that the law governs the system. Good means that the system evolves to adjust itself toward stable states given by the law. The law itself can evolve, and its evolution is decided by only the external environments of the system to prevent the circular evolution of the law. Together, Ashby suggested that a self-organizing system is a system adjusting itself to its new environment.

To apply the concept of the self-organizing system to the rolling ball on a hillside, let us say the hillside is turned out to be a wall enveloping a pit, and the ball is rolling toward the bottom of the pit. In the beginning, gravity is the only law causing changes in the position of the ball. The equilibrium of the rolling ball is the bottom of the pit. The ball rolls on the wall toward the equilibrium. Now there have been few earthquakes and whirlwinds which hit the ball, so the ball had hopped from here to there on the wall whenever it was hit. The trajectory of the ball has been changed, but still the ball rolls toward the bottom of the pit. The one-ball system can be analyzed with phase transition of the system at that moment of each hit as like a low dimensional chaotic system. To expand it to a complex chaotic system, imagine that there are millions of balls on the wall of the pit and the slope of the wall is very shallow and the area of the wall is extremely large. If we observe this many balls system affected by earthquakes or whirlwinds and numerous collisions between balls additionally, the system will look randomly defined with many balls without regularity. To figure out whether there is any hidden regulation, using the observable state of many balls is more useful than trying to understand the system in terms of each ball and its explicit dynamics. To divide the wall into a few huge districts and monitor the changes of the ball density of each district would be a recommendable way to find a hidden regularity of the system. The density of the ball stays higher for the districts near the bottom of the pit than other districts. After hits of earthquakes and whirlwinds, the ball density of these districts may be reduced for some time but would be increased soon again. Since the number of balls is preserved on the wall, the high density of a few districts means a low density of the other districts. Therefore, when one observes only one district located far away from the bottom of the pit, the ball density of the district would reduce most of the time so that one could see there should be other districts of the wall having a higher density than it. Consequently, one could find a hidden regularity that attracts balls near an area of the wall. This analogy may apply to the spontaneous activities of a single neuron (a ball) and spontaneous neuronal activities of populations of neurons (many balls).

3.2.2 Deterministic Dynamics of Self-Driven State

How could the concept of self-organization be connected to the brain then? Neurons form a recurrent network with reciprocal and nonlinear connections comparable to a complex chaotic system. As mentioned already, the activities of cortical neurons without external stimuli look random, but when it is evoked by stimuli, their activity is statistically predictable. Rbinovich and Abarbanel (1998) proposed that the chaotic structure of the brain is due to its high complexity giving functional flexibility. Further, the ability of self-organization makes it possible to process structured

information despite its complexity (Rabinovich & Abarbanel, 1998). It has been actively studied how regularity could be raised from chaotic systems (Boccaletti, Kurths, Osipov, Valladares, Zhou, 2002). Pecora and colleagues (1990) showed that two chaotic circuits could be synchronized by a common external signal (Pecora & Carroll, 1990). Similar synchronization in neuronal activities was observed also on neocortical slices of a rat in vitro (Mainen & Sejnowski, 1995). In this paper, the temporally synchronized neuronal activity could be observed by inserting weak noisy signals besides constant stimuli. Several lines of evidence suggest that the stimuli evoked neuronal activities could be in order, possibly by adjusting the system to the external inputs.

When there are no specific external stimuli inputs, then what do neuronal activities look like? Some cognitive activities like daydreaming, spontaneous memory retrieval, and contemplation require no external inputs. Thus, it relies on the spontaneous activity of neurons and strong recurrent connections between them. Only recently, it has been revealed that there is a spatial pattern in the human brain in a resting state at the macroscopic scale via fMRI. However, is it possible to be in a state having no external inputs at all? Strictly speaking, it is impossible to realize an environment presenting no inputs from it. Therefore, it might be feasible to see that the passively collected external inputs drive the self-organization of the brain. Now, let us imagine that we are purely isolated from any type of external inputs to our body somehow. Can we still be in self-driven states? There is still interoception from the body. Also, one can move, think and still, memory is left regardless of the presence of external sensory stimuli to evoke it. It is hard to imagine that the self-driven states turned off at the moment of zero input from the external world.

Self-driven states always fluctuate rather easily most of the time. For example, on one hand, often the endless tides of thoughts occupy the mind. On the other hand, when one contemplates a painting, the static visual stimuli are presented. One can visually recognize the painting as the same painting whenever it is there. Therefore, the instability of self-driven states might come from the lack of static external stimuli which drive the synchronization of neuronal activities. How is the memory? Some memory can be retrieved consistently without structured external stimuli. When it is assumed that a memory system is composed of relevant neuronal assemblies, one of the probable laws to make it a self-organizing system is to keep a balance of recurrent connections between neuronal assemblies. In this system, the balance is described by correlations between neuronal assemblies. A simple example is the correlation coefficients between spike trains of neuronal assemblies. A set of possible balances is defined regardless of the current state of neuronal assemblies, but it is defined by other conditions in the brain to keep the definition of a self-organizing system proposed by Ashby (2017). For example, in the case of the Hopfield model of associative memory, the saved memory patterns are the law, and the presented initial memory pattern evolves to the most similar pattern among the saved memory patterns which is the stable state defined by the Hopfield model (Hopfield, 1984). The time evolution of the system could be different when a specific memory in the memory system is retrieved if its initial conditions are different. The two slightly different initial patterns of memory evolve to the same memory pattern via different time courses or paths of pattern changes in the Hopfield model (Hopfield, 2007). It might be possible to interpret the self-driven state similarly. If the brain is a self-organizing system, it evolves toward the stable states given by the law of the system which is assumed as a balance between correlations of neuronal assemblies here. In this way, the brain could be described as a deterministic dynamic system by taking the approach of a self-organizing system.

3.2.3 Episodic Memory and Self-Organizing System

The above descriptions are not enough to explain the memory with the causality of successive episodes, called episodic memory. In the next section, I will review the episodic memory introduced in neuropsychology. Before that, I will describe how episodic memory can be included in the perspective of a self-organizing system. Episodic memory contains more than one episode or event, so the memory system should evolve for the course of time from an episode to the next one successively. An episode is a unit containing a coherent structure of contents, as a scene (Hassabis & Maguire, 2007). When few events share a coherent structure, they can be abstracted within an episode. For example, [I went to a Café to meet a friend of mine by subway] could be an episode containing abstracted events that had happened for the time since I left home, walked to a subway station, entered in a subway, and stayed in the subway till arrived at the nearest subway station of Café and so on. These events (sub-episodes) share a coherent structure, a way to meet the friend. A sub-episode could be divided into smaller episodes, like [I left home] divided into [I took my bag, opened the door, walked down to the ground floor, then opened the gate]. In many cases, the sub-episodes and sub-sub-episodes do not need a specific time tag to reconstruct their temporal order due to their logical causality learned from repetition and experience (my flat is on the 4th floor then I should go down to the ground floor to leave my flat, and only after that I walk to the subway station). However, a higher level of abstract memory needs specific time order or context to retrieve them in a consistent order, like what I did after I met a friend.

For that, the law of the self-organizing system should describe the temporal structure of episodic memory. I will not discuss memory encoding with a self-organizing system, because encoding is more related to external inputs. I will discuss retrieval of episodic memory requiring the representation of existing information. Let say somehow, memory retrieval was triggered. First, one reaches a point of episodic memory, containing an episode for some time. Then also, let assume that the neuronal assemblies of episodic memory have two categories when they retrieve a memory. One category is to process the contents of an event or an episode and another is to process the temporal order of episodes. The balance of the self-organizing system could be applied to this system with two functionally discriminated subsystems. One more assumption is that the subsystem for the order of episodes is inversely coupled with the subsystem for episodes. When neuronal assemblies of episodes reach a stable state, then the coupled neuronal assemblies of orders become unstable, so it starts evolving to its stable state. If the law of the entire system is that the sum of balance between two subsystems β should be constant, then an increase of the balance of one subsystem causes the decrease of the balance of another system. For each subsystem, their stable state is when the balance is minimized (Figure c). Let assume there are many such stable states and each of them represents a specific episode or a specific time tag (order). Once one subsystem reaches its nearest stable state, then another one reaches a maximally unstable state, so that the unstable system starts evolving to its one of near stable states. The retrieval of episodic memory could be described with a system evolving to keep the sum of balance β consistent. When the two subsystems evolve to their stable states, episodic memory retrieval can happen through the system's various trajectories of time evolution. In short, it is possible to retrieve the same episodic memory through consecutive time evolution of neuronal activities in terms of a self-organizing system.

Figure c: Example of coupled time tag system and episode system

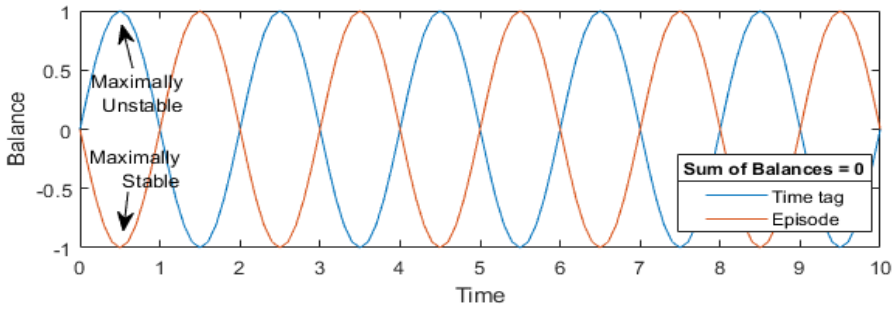

It is also feasible to assume that the brain is a complex system having a law to its neuronal activity of subsystems to synchronize each other so that their activity forms oscillation instead of random time evolution for self-driven states. For that, the law should have a temporal structure within it and be powerful enough to derive consistent synchronization for the entire time evolution of the brain against its complexity. Even if this is the case, the chance to observe such coherent oscillatory activity of neuronal assemblies in BOLD signals might be not too high. BOLD signals are averaged spatiotemporally to represent macroscopic observations on the highly complex nonlinear system composed of neurons and their synaptic connections (Logothetis, 2008). Also, highly nonlinear biochemical dynamic mechanisms generate BOLD signals. Therefore, it seems hard to expect to find linear temporal regularity from their time courses collected from self-driven states. When we assume that the suggested argument of a self-organizing system is appropriate to describe the self-driven state of the brain, then what is the proper perspective to find a hidden law of self-driven states from BOLD signals? To answer this question, I will present two fMRI studies of the DMN analyzed with dynamic functional connectivity. In the studies, I suggested a new analysis method measuring a consistent temporal feature of the mental state. The new analysis method may show how one can explain the brain as an approximately deterministic dynamic system. Before moving the experiment and analysis, I will briefly review neuropsychology literature about episodic memory in the next section.

4. Memory System of Human

The memory of humans and animals has been intensively studied due to its importance in everyday life to learn and to solve problems for survival (Klein, Cosmides, Tooby, & Chance, 2002; Sherry & Schacter, 1987; Sweller, 2003; Tulving, 2002). According to these studies, the memory of physically experienced events by oneself has been considered as one of the main prerequisites to define an individual. Since the functional and structural complexity of the brain to process perception and cognition is high, there are no clear borderlines to delineate the entire memory system into independent sub-memory systems. Here, I will review declarative memory which offers us the basis of many high cognitive activities (Squire & Zola, 1996). Specifically, episodic memory which is a declarative memory with consecutive episodes will be reviewed (Tulving, 1972). Also, its functional and structural commonality with the DMN is described. The function of each brain region in the DMN is summarized to understand the existing commonality in the brain when it processes episodic memory or the resting state. After reviewing the literature, I will propose the dynamics of the episodic memory system in terms of the self-organizing system.

4.1 Memory

The memory could be classified into two types of declarative memory concerning its accessible time, so-called short-term memory and long-term memory (Cowan, 2008). Following the definition of Cowan (2008), short-term memory is accessible only for a limited time around a few seconds and the amount of information is also limited. Long-term memory remains for non-limited time as far as it is retrieved from time to time. It contains an amount of information larger than that of short-term memory (Craik & Lockhart, 1972). Thus, it has been thought that long-term memory is pivotal for the successful evolution of humans and animals looking for the optimal environment for their thriving actively. Humans have a particularly flexible and fast learning ability to adjust themselves to any random environment. Long-term memory is one of the critical factors making it possible by offering a wide basis of learning. In the category of long-term memory, there are again two subcategories called explicit/declarative memory and implicit/non-declarative memory (Graf & Schacter, 1985). Non-declarative (implicit) memory system consists of procedural learning that one can successfully perform without cognitive processing, like skills, habitual behaviors, priming effect, and perceptual learning, and so on (Schacter, 1987). They are not processed at the cognitive level but influence the behaviors of humans and animals under the cognitive processes without being noticed explicitly. Explicit or declarative memory is conventionally classified into two types of memory, semantic memory and episodic memory (Tulving, 1972). Tulving (1972) proposed first the term episodic memory to contrast it to semantic memory. Following the definition of memory by Tulving (1972), semantic memory is a collection of facts indicating explicit knowledge or information on a topic or an object. On the other hand, episodic memory is a collection of experienced episodes containing spatial and temporal information. An important characteristic of episodic memory is that it contains spatial and temporal details of experiences of an episode. Semantic memory is also extracted from experiences in one's life. However, in this case the experiences are generalized then remain without its spatial and temporal information (Eichenbaum, 2001). At the same time, retrieving an episodic memory requires semantic memory to fill the experienced spatial and temporal structure of episodic memory (Conway & Pleydell-Pearce, 2000). Thus, the two types of declarative memory are mutually dependent.

4.1.1 Episodic Memory and Semantic Memory

The hippocampal complex has been known for its critical role in encoding and retrieval of both types of declarative memory (Eichenbaum, 2001). Here, the hippocampal complex includes hippocampal formation (CA fields, the dentate gyrus, and the subiculum), the entorhinal cortex, the perirhinal cortex, and the parahippocampal cortex. The lesion studies by Squire (1992) which were done on the hippocampal complex of humans, monkeys, and rats have proved that intact non-declarative memory and impairment in declarative memory could coexist (Squire, 1992). In this paper, Squire (1992) proved that semantic memory was relatively intact even with lesions on the hippocampal formation. Lesion studies of the hippocampus of monkeys reported in the same study showed that monkeys with lesions in their hippocampal formation were not able to perform inferential problem-solving tasks based on what they learned previously. The monkeys could solve simple pair tasks in a static environment through repetition, but they were unable to apply this memory to solve problems asking to infer the relationship between objects they learned previously (Squire, 1992). There is a lesion study of human patients reporting a similar result. Early hippocampal pathology does not cause severe impairment in semantic memory, but still, patients have severe impairment in episodic memory (Vargha-Khadem, et al., 1997). The emergence of semantic memory from episodic memory had been explained as the form of consolidation of memory in the neocortex as time passes (McClelland, McNaughton, & O'Reilly, 1995; Squire & Zola-Morgan, 1991; Squire, 1992; Squire & Alvarez, 1995). According to these studies, memory could be retrieved by neocortical activity solely after its consolidation in the neocortex. Following this point of view, it is common to both types of declarative memory. Therefore, the consolidated episodic memory is retrieved by neocortical activity too.

McClelland and colleagues (1995) proposed a model of learning and memory system concerning the complementarity of the hippocampal complex and the neocortex (McClelland, McNaughton, O'Reilly, 1995). In their ‘complementary learning system model’, the two memory systems explain the efficiency of associative learning. One system is the hippocampal complex encoding compressed memory rapidly and sparsely, and another system is the neocortex encoding memory slowly and distributed redundantly. Once they are exposed to new experiences, fast learning happens in the hippocampal complex and slow learning happens in the neocortex. A new concept enters the neocortex, then it does not cause any rapid changes in synaptic connections to build an exact structure of the concept. Rather, it is interleaved with existing similar concepts. When the neocortex gets repetitive inputs of the concept over time, the full structure of the concept is learned and consolidated. At the same time, the new concept enters the hippocampal complex with a highly compressed form containing the full structure of the concept decayed fast. The two systems have bidirectional connections so that it makes it possible to reinstate memory in both systems. As time goes by, the memory is consolidated then it can be retrieved without the help of the hippocampal cortex. In contrast to the complimentary learning model, a model of declarative memory by Moscovitch, Nadel and their colleagues (1997; 2000; 2005) proposed that the role of the hippocampal cortex is crucial for episodic memory regardless of its consolidation (Moscovitch, et al., 2005; Nadel & Moscovitch, 1997; Nadel, Samsonovich, Ryan, & Moscovitch, 2000). They named their model ‘multiple trace theory (MTT)’. MTT shares the idea about the role of the hippocampal complex that it encodes the structure of memory. In their theory, a trace is identified with basic units forming a memory system consisting of neuronal assemblies. Traces in the hippocampal complex contain a spatial structure of a specific memory and in the neocortex contain features of the memory. By MTT, semantic memory loses its part of a trace in the hippocampal

complex, after traces are abstracted and independently stored in the neocortex. However, episodic memory needs to be dependent on both the hippocampal cortex and the neocortex whenever it is retrieved.

These two views are differentiated from their opinion on the role of the hippocampal complex in the retrieval of episodic memory. Nevertheless, both agree with the role of the hippocampal complex to encode the spatial and temporal structure of memory to form episodic memory and semantic memory. Similarly, Eichenbaum (2001) summarized the role of the hippocampal complex related to episodic memory in three steps (Eichenbaum, 2001). First, it encodes episodic memory, then finds commonality between encoded memories to link them, and finally applies such memory networks to new inputs to infer them. In summary of these three models (Eichenbaum, 2001; McClelland, McNaughton, & O'Reilly, 1995; Moscovitch, et al., 2005; Nadel & Moscovitch, 1997; Nadel, Samsonovich, Ryan, & Moscovitch, 2000), the hippocampal complex draws a memory map having marks on spatial and temporal relationships between episodes and this map is used to navigate memory. Relying on this map, semantic memory could be encoded.

4.1.2 Episodic Memory and Default Mode Network

The previous models of memory systems classify the role of the hippocampal complex and the neocortex in the maintenance of context and contents respectively. Ranganath and Ritchey (2012) suggested functionally and structurally discriminated two memory systems including the hippocampal complex and the neocortex (Ranganath & Ritchey, 2012). In this paper, they classified them into the anterior temporal and posterior medial systems. The anterior temporal system processes the contents of memory. It includes the perirhinal cortex, which is the connection with the hippocampal complex, the lateral orbitofrontal cortex, the amygdala, and the ventral temporopolar cortex. They reported that the members of the anterior temporal system are known to be related to familiarity (recognition of known objects), emotional and social cognition, and semantic knowledge. Another system is the posterior medial system, which is composed of the DMN and the ventromedial prefrontal cortex. The posterior medial system processes contextual information of memory. They argued that the PHC is responsible to search for contextual similarity between external inputs and existing memory contexts, and the RSC transforms the external input into the allocentric frame so that the contextual information is represented in the DMN. Integration of contents and contexts happens in the hippocampal formation. The perirhinal cortex and the parahippocampal cortex are connected intensely with the lateral and medial entorhinal cortex respectively. The authors proposed that the connection of contents and context is facilitated by their reciprocal connection to the hippocampal formation (Ranganath & Ritchey, 2012).

Interestingly, the two functional roles of the cortex in respect of the memory system could be connected to an interesting result of a fMRI study founding functional correlation between the DMN and the hippocampal complex. In a study done by Vincent and colleagues (2006), they analyze the brain regions having functional connectivity to the hippocampal complex with seed-based functional connectivity analysis of resting state fMRI (Vincent, et al., 2006). Intrinsic functional connectivity to the hippocampal complex seed region (the dentate gyrus, the subiculum, the posterior entorhinal cortex, the PHC) was found on the bilateral inferior parietal lobules (including the AG), the left PCC, the PRC, and the RSC. As one can easily see, the listed brain regions are members of the DMN.

A potential functional role of the DMN is the construction of the internal world following their meta-analysis of the brain imaging studies of the resting state, episodic memory retrieval, episodic

imagery, theory of mind, and navigation (Andrews-Hanna, Smallwood, & Spreng, 2014; Buckner, Andrews-Hanna, & Schacter, 2008; Raichle, 2015; Spreng, Mar, & Kim, 2008). Two slightly different meanings coexist in ‘the construction of the internal world’. One of them is 'self-projection' (Buckner & Carroll, 2007). Buckner and Carroll (2007) proposed that the core brain network composed of the mPFC, the medial temporal lobe, and posterior-parietal regions including the PCC, the RSC, the PRC, and the AG overlapped with the DMN. They pointed out that the studies on resting state, episodic memory retrieval, episodic future imaginary, theory of mind, and navigation are not distinct tasks, but each of them is done by changes of perspective called self-projection. Following their definition, self-projection means to change one’s perspective from the present to different times and spaces. So, one could understand episodic memory retrieval as the self-projection into the past, the episodic future imaginary into the future. Correspondingly, the resting state is the default mode of self-projection. They concluded that the core brain network including the DMN is a multifunctional network of self-projection (Buckner & Carroll, 2007). Contrastingly, Hassabis and Maguire (2007) proposed that 'scene construction' is the fundamental role of the DMN (Hassabis & Maguire, 2007). In their paper, they reported that self-related high activation of the brain was only found in the PCC, the PRC, and the anterior mPFC by conjunction analysis of fMRI experiments. Other regions in the DMN showed high activations in episodic memory retrieval, episodic future imagery, and retrieval of previously learned fictitious memory tasks. They summarized that the functional commonality of those tasks including navigation and theory of mind is to construct coherent scenes. In this paper, they implied that the concept of self is unnecessary to understand the construction of the internal world (Hassabis & Maguire, 2007). These two studies have different views on what is more fundamental among the ‘internal world (self-projection)’ and ‘construction’. Nonetheless, both agreed that the DMN is a multifunctional network that forms the core network to construct the internal world. The role of the hippocampal complex and its connection to the DMN needs to be discussed to understand how the internal world is constructed by the DMN.

4.1.3 Cognitive Map

The hippocampal complex is one of the most intensively studied brain regions in memory and navigation research. Place cells are the neurons activated only when an animal visited a specific place in an environment and is located in the hippocampal formation (O'Keefe & Nadel, 1978). Following the finding, it has been proposed that the spatial map of a given environment is represented in the brain to navigate the environment. Another intriguing finding related to the hippocampal complex was made by Hafting and colleagues (2005) related to the spatial navigation task experiments of rats (Hafting, Fyhn, Molden, Moser, & Moser, 2005). They found that neurons in the medial entorhinal cortex fired when rats arrived at certain points, and the 2D mapping of firing patterns of neurons on the trace of rats formed the hexagonal grid structure. They named these neurons grid cells. Place cells and grid cells have been considered the clear sign of the cognitive map representing physical space in the brain. The relation between grid cells in the entorhinal cortex and place cells in the hippocampal formation has been very actively studied (Moser, Kropff, & Moser, 2008; O'keefe & Burgess, 2005; Schapiro, Turk-Browne, Botvinick, & Norman, 2017). Grid cell-like activity was measured in the human brain too (Doeller, Barry, & Burgess, 2010). Using fMRI data collected from human subjects navigating a virtual arena wearing virtual reality glasses, Doeller and colleagues (2010) found the modulated activity of BOLD signals in every 60 degrees, like a hexagonal activity pattern of grid cells. They found this pattern of BOLD signals in the entorhinal cortex, the mPFC, and the lateral temporal cortex. Furthermore, an interesting proposal related to place cells and grid cells of the human brain concerning the cognitive map was

made by Constantinescu and colleagues (Constantinescu, O'Reilly, & Behrens, 2016). They suggested that navigation in abstract cognitive space also might be supported by grid cells and place cells. They trained human subjects to learn arbitrary relations between visual stimuli and a bird painting. From the collected fMRI data while subjects were navigating the abstract cognitive map of visual stimuli and a bird painting, they found out collected BOLD signals were modulated every 60 degrees in the mPFC and the entorhinal cortex. They also reported the 60 degrees modulated BOLD signal changes in many other DMN components, like the PCC, the RSC, and the inferior parietal cortex (including the AG) (Constantinescu, O'Reilly, & Behrens, 2016). Aronov and colleagues (2017) speculated that place cell-like activity of the brain could be observed whenever tasks require an understanding of the structure of a given environment (Aronov, Nevers, & Tank, 2017). They designed a rat experiment with different frequency auditory stimuli. They showed that neurons in rats' CA1 and entorhinal cortex respond distinctively to the auditory stimuli of different frequencies. Following such experimental results, speculation about the general cognitive map has been studied intensively with the application of algorithms from machine learning. Stachenfeld and colleagues (2017) proposed that the role of place cells is not to envisage the current cognitive map spatially but predict the chance of transition from the current state to the other possible states at the next moment (Stachenfeld, Botvinick, & Gershman, 2017). The prediction is encoded by learning from previous experiences statistically while grid cells subserve the encoding of predictions. Behrens and colleagues (2018) extended this idea into the flexible learning ability in general (Behrens, et al., 2018). They speculated the actual role of place cells and grid cells is to abstract relations between the current state and the given environment. The learned general relations are then applied to different environments to optimize the survival of the agent (Behrens, et al., 2018).

In summary, the speculation on the cognitive map can explain a pivotal role of the hippocampal complex in episodic memory encoding and retrieval and spatial navigation. Additionally, this might also tell how the similar brain activity patterns of the episodic memory retrieval, episodic future imagery, theory of mind, and navigation observed by brain imaging studies could be explained as the construction of the internal world. The neocortex and the hippocampal complex communicate via the entorhinal cortex mostly (Amaral & Lavenex, 2007). The entorhinal cortex receives around two-thirds of its input from the perirhinal and the parahippocampal cortex (Squire, 1992). Highly analyzed sensory data from the neocortex are transferred via the entorhinal cortex to the hippocampal formation. Its output is transferred to the entorhinal cortex again and delivered to the neocortex (Squire, 1992). From the point of view extending the role of the hippocampal complex to the generation of the general cognitive map, structures of processed sensory inputs are abstracted from the hippocampal complex and its reciprocal connections to the neocortex reinforce and update the context and contents of saved memory in the neocortex (Aronov, Nevers, & Tank, 2017; Behrens, et al., 2018; Constantinescu, O'Reilly, & Behrens, 2016; Stachenfeld, Botvinick, & Gershman, 2017). The construction of the internal world is affiliated to the representation of the experienced world equipped with reinforced and updated memory.

As previously mentioned, the active brain regions for the episodic memory retrieval task and the DMN are overlapped (Hassabis & Maguire, 2007; Spreng, Mar, & Kim, 2008). Back to the model of two memory systems in the cortex suggested by Ranganath and Ritchey (2012), the DMN of the posterior medial system processes contexts of memory. If only the posterior medial system is related to the construction of the internal world represented in the DMN, why does not the anterior temporal system contribute to it? The difference between the contents and contexts needs to be concerned to answer this question. Contents are parallel information that is grouped and abstracted from various experiences. They deliver commonality of episodes and objects. On the

contrary, context is determined by discriminating an object or an episode against the others in a row. Regarding one of the mental states described with the construction of the internal world, the consecutive flow of episodes is a dominant phenomenon. That may explain why cortical regions of the posterior medial system most dominantly have been found from fMRI studies of the construction of the internal world.

4.2 Functions of Brain regions in Default Mode Network

The DMN consists of six brain regions: the mPFC, the PCC, the PRC, the RSC, and the AG. In this chapter, I will summary their function.

4.2.1 Posterior Cingulate Cortex

The PCC, the PRC, and the RSC are in the posterior part of the medial line of the cerebral cortex. The three brain regions are prominently active in a resting state and an episodic memory retrieval state. The PCC (BA23, 31) is located between the PRC (BA7) and the RSC (BA 29,30) vertically (Vogt & Laureys, 2005). These three regions are located very close to each other and have reciprocal connections, but their cytoarchitecture and functional roles are differentiated (Cavanna & Trimble, 2006; Vogt & Laureys, 2005). Vogt and Laureys (2005) proposed that a function of the PCC and the PRC is related to the feeling of the present, which is the feeling of the present that is decided with the state of synchronization between the internal world and the external environment. Likewise, Leech and Sharp (2014) suggested the dorsal PCC possibly correlated with the regulation of deployment of attention by mediating the information exchanges between brain regions as a functional hub (Leech & Sharp, 2014). Supporting this point of view, Garrison and colleagues (2013) showed that the activity of the PCC reduced when people meditate without distraction (Garrison, et al., 2013). Altogether, the PCC seems to be a tuner of the internal representation. Following the connectionist model, the internal world is constructed while the various types of information connect or interact with each other. The PCC is one of the main functional hubs of the brain networks where various brain regions are connected (De Pasquale, et al., 2012; van den Heuvel & Sporns, 2013). The balance between brain activities and their efficient connections should be maintained to form a stable system when the internal world is constructed in a brain network. This may be processed via the PCC for the case of the DMN. As a result, one experiences the emergence of a balanced internal world and can recognize the external environment with the feeling of the present.

4.2.2 Precuneus

The PRC is located anterior to the PCC and the RSC. It has a multifunctional role that originated from its wide cortico-cortical and cortico-subcortical connection (Cavanna & Trimble, 2006). Margulies and colleagues (2009) measured functional connectivity of sub-region of the PRC using seed to voxel functional connectivity analysis (Margulies, et al., 2009). They reported that the medial part of PRC could be subdivided concerning its cytoarchitecture. Additionally, they delineated the functional role of each subdivision after analysis of their functional connectivity. The subdivided regions are the sensorimotor, cognitive, visual, and limbic regions. Among the four sub-regions, functional connectivity of the cognitive and the limbic regions overlapped with the DMN. The cognitive region of the PRC showed functional connectivity with the supramarginal gyrus, the angular gyrus, and the dorsolateral prefrontal cortex which are known for the center of

cognitive processes including language, working memory (Levy & Goldman-Rakic, 2000; Stoeckel, Gough, Watkins, & Devlin, 2009). The limbic region showed a particularly large overlap with the DMN including the mPFC, the angular gyrus, and the PHC (Margulies, et al., 2009). Utevsky and colleagues (2014) proposed a similar idea in their study on the task and resting state fMRI functional connectivity analysis (Utevsky, Smith, & Huettel, 2014). In their paper, they reported that the left frontoparietal network, known as a task-positive network, and the DMN both showed strong activity in the PRC. However, the activities of the sub-regions in the PRC were different. The ventral PRC was active in the resting state, and the dorsal PRC was active in task performance states (Utevsky, Smith, & Huettel, 2014). As one can guess from its functional connectivity pattern associated with the DMN, it also has a great association with memory retrieval (Fletcher, et al., 1995; Gilbo, Winocur, Grady, Hevenor, Moscovitch, 2004; Tulving, et al., 1994), self-perspective relevant tasks (Ruby & Decety, 2001; Vogeley, et al., 2001), and motor and visual imagery (Ghaem, et al., 1997; Knauff, Fangmeier, Ruff, & Johnson-Laird, 2003; Malouin, Richards, Jackson, Dumas, & Doyon, 2003). Cavana and Trimble (2006) reviewed the multi-functionality of the PRC and suggested that all these functions are linked to the processing of self-consciousness (Cavanna & Trimble, 2006). In this paper, they reported that the PRC takes its inputs from high cortex areas. Following their argument, the PRC processes information from functionally high cortex areas to construct the internal world. Similarly, Hassabis and Maguire (2007) showed in their fMRI study that the PRC was active for different types of retrieval or mental reconstruction tasks they performed (Hassabis & Maguire, 2007). In their study, the active brain regions for real and imaginary events, and in first- and third-person perspectives were identified. They found out that the PRC was active in all cases. Based on this result, they proposed that a fundamental role of the PRC is to construct scenes internally. In short, the functional role of the PRC for the construction of the internal world is summarized as constructing scenes by combining inputs from functionally higher cortical areas.

4.2.3 Restrospleinal Cortex and Parahippocampal Cortex

The RSC is located at the caudal end of the corpus callosum and ventral to the PCC. It has anatomical connections to the hippocampal formation, the PHC, and the anterior thalamus besides its connection to other cortical areas (Greicius, Supekar, Menon, & Dougherty, 2009; Kobayashi & Amaral, 2003). Its high activity in spatial navigation tasks has caught the attention of researchers. The dominant speculation on the functional role of the RSC is that it translates the perspective from allocentric to egocentric and vice versa (Vann, Aggleton, & Maguire, 2009). Burgess (2006) proposed that the role of the RSC in spatial navigation is to define one's relative location in an environment covering a large spatial area so that one can orient its direction (Burgess, 2006). By translating from allocentric to egocentric views and vice versa, one can define the progress in the environment. At the same time, the local scene should offer proper local information of each scene or place, and it is processed in the PHC. The proposal about the role of the RSC and the PHC in spatial navigation by Burguess (2006) can be extended to a more general function called 'contextual association' (Aminoff, Kveraga, & Bar, 2013). Aminoff and colleagues (2013) proposed that the RSC processes a large and abstract context of information. They speculated that this can be done by translating the contextual information from the egocentric reference of an object or a fact to allocentric reference and vice versa. From lesion studies of the hippocampal complex and the RSC, it has been reported that PHC is more sensitive to the local topography of each scene than the RSC (Burgess, 2006). Following this study, patients having lesions in the PHC could not recognize the place where they were by looking around the scene

they encountered. However, these patients could direct themselves once they recognized landmarks of the place. In the case of the RSC lesion patients, they could not direct themselves even if they were able to recognize the local scene (Burgess, 2006). Furthermore, Aminoff and colleagues (2013) pointed out that the PHC could be functionally subdivided into the anterior and posterior parts. They showed that the anterior PHC is functionally connected more to the RSC and active to the non-spatial stimuli. On the other hand, the posterior PHC is more active for spatial and visual stimuli (Aminoff, Kveraga, & Bar, 2013). This might explain how PHC joins both spatial and non-spatial contextual association tasks. To test the connectivity between the occipital cortex (OCC), the RSC, the PHC, and the PFC, Kveraga and colleagues (2011) performed an experiment using MEG (Kveraga, et al., 2011). They found out when objects presented as visual stimuli with strong contextual association (like an oven, a pot, a sink), the synchrony happened between PHC and OCC first, then PHC and RSC, and RSC and OCC, lastly RSC and mPFC. This result supports the proposal of Aminoff and colleagues (2013) that the PHC processes the associations and abstraction within a context. This may be closely related to the episodic memory system. Episodic memory is composed of episodes in a sequence. The sequential association between episodes and context within an episode is processed to encode and retrieve episodic memory. Considering these pieces of evidence, one could guess that the RSC processes the sequential association between episodic memory and the PHC process the local context within an episode.

4.2.4 Angular Gyrus

It is understood that the inferior parietal lobule including the AG (BA39) has multiple functional roles including processing convergence of sensory-motor inputs, language, number, and memory(Jäncke, Kleinschmidt, Mirzazade, Shah, & Freund, 2001; Rivera, Reiss, Eckert, & Menon, 2005; Simon, Mangin, Cohen, Le Bihan, & Dehaene, 2002). Especially, the AG is known to be a member of the DMN. Anatomically, it is divided into two sub-regions and their functional roles are discriminated (Seghier, 2013; Uddin, et al., 2010). The anterior and the posterior part of the AG are delineated into PGa and are PGp respectively, based on the cytoarchitectonic maps (Caspers, et al., 2006; Eickhoff, et al., 2005). Uddin and colleagues (2010) applied this anatomical subdivision of the AG to fMRI resting state connectivity study and DTI (Uddin, et al., 2010). They found that PGa is connected to the basal ganglia, the ventral premotor areas, and the ventrolateral prefrontal cortex. These regions are known to be correlated to working memory and language processing (Gruber & Goschke, 2004; O'Reilly & Frank, 2006). In contrast, PGp showed high connectivity with the DMN including the PCC, PRC, mPFC, and hippocampal complex, specifically with the PHC.

Recent studies of semantic memory proposed that retrieval of semantic memory is associated with the inferior frontal lobe, the ventrolateral temporal lobe, and the inferior parietal lobule (Binder, 2011; Bookheimer, 2002; Martin & Chao, 2001). These studies suggested semantic memory is embodied by the convergence of distributed features of memory contents, like the memory contents of piano including the image of piano, the sound of piano, etc., in the ventrolateral temporal lobe and inferior parietal lobule via a meta-analysis of fMRI studies. Besides, Cabeza and colleagues (2008) suggested the extended dorsal and ventral attention stream to the memory system, called the attention to memory model (AtoM model) (Cabeza, Ciaramelli, Olson, & Moscovitch, 2008). Their model combines functional roles of the inferior parietal lobule including the angular gyrus and supramarginal gyrus (BA40) to the entire episodic memory system. They

highlighted that two subdivisions of the lateral parietal cortex, the dorsal parietal cortex (the superior parietal lobule (BA7)) and ventral parietal cortex (inferior parietal lobule), are comparable to the two attention systems suggested by Corbetta and Shulman (Corbetta & Shulman, 2002). Following the AtoM model by Cabeza and colleagues, the ventral parietal cortex is sensitive to the bottom-up inputs of sensory stimuli arrived via sensory-motor cortices. Thus, the vividness of retrieved memory is closely correlated with the ventral parietal cortex. They also suggested that the dorsal parietal cortex is closely correlated with the prefrontal cortex. Goal-directed top-down attention is delivered from the prefrontal cortex to the dorsal parietal cortex and the attention is allocated to the memory system to recruit relevant information to the goal. In their model, the medial temporal cortex including the hippocampal complex combines the two memory systems through the top-down connection from the dorsal parietal cortex and the bottom-up connection from the ventral parietal cortex. The goal of memory retrieval directs the ventral parietal cortex where the convergence of distributed information is processed. The dorsal and ventral parietal cortex have reciprocal connections to monitor the relevance of retrieved memory (Cabeza, Ciaramelli, Olson, & Moscovitch, 2008). In short, the AtoM model suggested a memory model of how structure and features are combined in the brain via the parietal cortex. To sum up, the role of the AG in the construction of the internal world could be considered as follows. It offers vividness in the internal world by combining the sensory-motor memory of external stimuli.

4.2.5 Medial Prefrontal Cortex

The medial part of the prefrontal cortex is one of the components of the DMN that is spatially most remote from other components. Anatomically it is connected to the limbic system and medial temporal lobe (Miller & Cohen, 2001). The mPFC is a large compartment including BA 12, BA 25, BA 24, BA 32, and BA 33 (Murray, Wise, & Graham, 2017). As a result, researchers studying the DMN have named their region of interest the dorsal mPFC, anterior mPFC, and ventral mPFC depending on their research interests. It is yet unclear whether these sub-regions of the mPFC share functional roles or not. The putative functional roles of the mPFC are emotional control and decision making (Bechara, Tranel, & Damasio, 2000; Rahman, Sahakian, Hodges, Rogers, & Robbins, 1999). Recently, Preston and Eichenbaum (2013) reported that the critical role of the mPFC in memory encoding and retrieval concerning its connection to the hippocampal complex (Preston & Eichenbaum, 2013). In a meta-analysis of fMRI studies done by Andrews-Hanna and colleagues (2014), the functional role of the dorsal, anterior, and ventral mPFC was categorized (Andrews-Hanna, Smallwood, & Spreng, 2014). Their study delineated the DMN into sub-functional networks. They proposed three mPFC areas connected to three subdivisions of the DMN. The anterior mPFC and the PCC form the core system of the DMN connecting two other subsystems called the dorsal medial subsystem and the medial temporal subsystem. Surprisingly, the medial temporal subsystem is well-matched by the posterior medial system suggested in the two memory systems by Ranganath and Ritchey (2012). The spatial and functional clarification of the mPFC is abstract and broad in functional connectivity studies despite its importance in the DMN. Hence, further studies about the specified role of sub-regions in the mPFC are necessary.

4.3 Autobiographical Episodic Memory

Autobiographical episodic memory (AEM) is described as self-experienced episodic memory (Summerfield, Hassabis, Maguire, 2009). Therefore, it is the very elemental realization of the

construction of the internal world. Here I will review two interesting studies on episodic memory systems which could envisage the essence of autobiographical episodic memory.

The most predominant attribute of autobiographical episodic memory is that it requires the ability to travel in the subject timeline through one's past, present, and future while being self-aware (Tulving, 2002). Tulving and colleagues (1997; 2002) proposed the concept of 'autonoetic consciousness (self-knowing)' and 'autonoetic awareness' to explain independence of episodic memory from other higher cognitive functions (Wheeler, Stuss, Tulving, 1997) (Tulving, 2002). Autonoetic consciousness makes it possible to be aware of self through subjective time, i.e., to place oneself in a continuum of the past, the present, and the future. In their model, the autonoetic consciousness is the highest level of cognitive function processed in the prefrontal cortex. Apart from autonoetic consciousness, they defined autonoetic awareness which indicates the action or operation of autonoetic consciousness. From the prefrontal cortex lesion studies and the psychological development of infants, they specified the ability of episodic memory formation and retrieval was closely related to autonoetic awareness. Following their view, episodic memory retrieval is one of the cognitive functions which is defined with autonoetic awareness by traveling to the past of subjective time and re-experiencing it. By their definition of episodic memory, autobiographical episodic memory is a type of episodic memory operating on autobiographical contents (Wheeler, Stuss, Tulving, 1997) (Tulving, 2002).

Another episodic memory system is the self-memory system (SMS) suggested by Conway and colleagues (2000) SMS is composed of 'working-self' and 'autobiographical knowledge base' (Conway & Pleydell-Pearce, 2000). SMS is an emergent phenomenon by the reciprocal connections between working-self and autobiographical knowledge base. In this paper, they described that working-self is the functional aspect of the human brain setting goals and adjusting behaviors to attain goals. The autobiographical knowledge base is a collection of memory that are episodes in one's specific period of life, general memory without life timeline, and event-specific knowledge. This autobiographical knowledge base forms a hierarchy that life period memory cues the activation of general memory, then the activated general memory cues event-specific memory. Conway and colleagues (2000) suggested the mechanism of the SMS as follows. A cue is elaborated in respect of the current goals of the working self. Then specific memory is activated from the autobiographical knowledge base and verified by the working self. This reciprocal process is repeated till the goals of the working self are attained. Additionally, they suggested that the working self is in the left frontal lobe, and the autobiographical knowledge base is located in bilateral posterior (parietal and occipital) lobes from their reviews on EEG and PET studies (Conway & Pleydell-Pearce, 2000). The SMS is comparable to the AtoM model for its two subdivisions of the memory system that one is for the execution, and another is for the base of the content. It also can be compared to the model of episodic memory by Tulving and colleagues (1997; 2002). Especially the concept of working-self and autonoetic consciousness shares their supervisory role in their memory systems. Also, both models suggested that memory retrieval is an emergent phenomenon.

Following these two models, 'self' (working-self and autonoetic consciousness) should act to encode and retrieve autobiographical episodic memory. By the act of self, one constructs episodic memory realizing subjective experiences. Thus, one can say that the construction of the internal world including self-projection and scene construction is consistently found from these two models of autobiographical episodic memory.

4.4 Dynamical Two Memory Systems

As already mentioned, a resting state and an episodic memory retrieval state share the fundamental attribute of their mental state (self-projection and scene construction). Also, the spatial activity pattern of the brain when it is in those mental states is the same, the DMN. Nonetheless, they have many differences too when a close look is taken. Being in a resting state, or doing mind-wandering, does not need any structure or causality in the constructed internal world. In comparison, episodic memory retains its structure, especially the causality between episodes, and its correctness can be told (Tulving, 1972). Considering the commonality in spatial activity maps and differences of the mental states, it sounds reasonable to assume that the differences between two mental states are in the temporal domain. From the previous section, I proposed a scheme for the dynamical evolution of the episodic memory system as a self-organizing system. The two inversely coupled subsystems process contents (episodes) and contexts (time tags) maintaining the stability of the entire episodic memory system. To gauge the stability of the system, I used the term balance. The balance of the entire system is the sum of the balances of two subsystems, and to keep it constant is the law governing the episodic memory system. When this proposal is combined with the two memory systems in the cortex proposed by Ranganath and Ritchey (2012), the balance of the episodic memory system is computed in the hippocampal complex where the anterior temporal system and the posterior medial system connect to. I will call this model the dynamical two memory systems in the cortex.

If the DMN is a subsystem of the dynamical two memory systems in the cortex, changes in the subsystem induce changes in the entire system through their inverse coupling to the other system. At the same time, the small world network of the brain would spread changes from a subsystem to other connected brain regions via the functional hubs. If it is the case, one could expect to see different dynamical features of functional subsystems of the brain in different mental states. Even if its trajectory of time evolution could be stochastic due to the innate complexity of the brain, one could determine the measurable regularity of subsystems at the macroscopic scale, like the case of the self-organizing system described with many balls on an inclined wall (Ashby, 2007). At this point, one question is following naturally; is it possible to see such differences in the dynamical features of a resting state and an episodic memory retrieval state? If it is, is it achievable by analyzing the dynamic functional connectivity (DFC) of the DMN? What is the proper variable to take to define them? To answer these questions, I will introduce a new analysis method called one-ROI-centered DFC analysis to describe dynamical features of the DMN using fMRI data collected from an AEMR task state and a resting state, in the next chapter.

Before concluding this chapter, I will briefly discuss the limits of the assumptions proposed previously. One might argue that the differences in dynamical features of a resting and an episodic memory retrieval state depend on whether it is goal specific or goal-free (Spreng, Stevens, Chamberlain, Gilmore, & Schacter, 2010). Not only this, but the activity of the hippocampal complex could also count differences in the two mental states while the activity of the DMN maintains the same dynamics for both states. Thus, the extent of this study should include the reciprocal connection between the DMN and the other brain networks. It is an interesting direction to pursue over the scope of the current study to picture the construction of the internal world.

5. Material and Methods

5.1 Aim of the Experiment

Autobiographical episodic memory is the most common type of episodic memory that we experience. At the same time, it contains both the self-projection and scene construction perspective of the construction of the internal world. I compared the dynamical features of neuronal activity of three fMRI runs in the autobiographical episodic memory retrieval (AEMR) state. A new analysis method called one-ROI-centered DFC was proposed to define dynamical features of the mental state. By the comparison, the existence of deterministic dynamics in BOLD signals could be presented. Also, the abstracted dynamical features of three runs in the AEMR state was compared to that of in the resting state using the BOLD time series of the DMN to test whether these two mental states sharing the same spatial activity pattern can be discriminated by comparing their dynamical features abstracted by one-ROI-centered DFC analysis. A single case study and a group study were performed. First, a single case study was done with the data collected from a blind single subject. Following the experiment, an experiment with 7 non-blind subjects was performed.

5.2 Single Case Experiment

5.2.1 Subject

A single female subject aged 78 participated in this experiment. She lost her vision in the middle of her twenties and had no known brain damage or neuronal diseases at the time she attended the experiment. The participant was named Blind Lady (B.L) in this experiment. She could envisage vividly the physical environment that she encountered and knew already. It makes her compensate for her handicap. She had a regular morning routine that she could retrieve easily in detail. Her extraordinary ability to envisage the external world in her internal world was what the experiment required. The Ethics Committee of the Medical Faculty at the University of Munich approved the behavioral and MRI experiments protocols.

5.2.2 Behavioral Experiment

First, she verbally described her morning routine and was asked to retrieve it again three times in detail without an oral statement. The sign of the beginning of the retrieval session was given by an experimenter, and she reported orally when she finished the retrieval task. The measured time duration of each retrieval session was equal, approximately 7 min 40 seconds. B.L reported that she retrieved the same memory, her morning routine, in each retrieval session.

5.2.3 MRI Data Acquisition

In total, four runs of fMRI data were collected. The fMRI data acquisition was done by the following. In the first fMRI run, B.L was asked to do mind-wandering or not focus on any specific ideas for the fMRI run. After the resting state run, she repeated the retrieval of her morning routine three times so that three AEMR runs were collected in the same MRI session. The subject had brief pauses (less than one minute) between runs. The participant learned the beginning and the end

of each fMRI run through a speaker in the MRI room. All four runs were 7 minutes 40 seconds. The image scanning was done with a 3T MRI machine (Philips healthcare, Ingenia) in the University Hospital LMU Munich. A foam cushion was used to minimize the effect of head movement. T1-weighted structural image was acquired with magnetization-prepared rapid gradient-echo sequence (MPRAGE) with the following arrangement: repetition time (TR) = 8.2 ms, echo time (TE) = 3.76 ms, flip angle (FA) = 8°, number of slices = 220, matrix = 256 x 256, slice spacing and slice thickness = 1 mm, in axial orientation. T2*-weighed functional images were acquired after the T1 session with echo-planar image (EPI) sequence with the following arrangement: repetition time (TR) = 2.5 ms, echo time (TE) = 30 ms, flip angle (FA) = 90°, number of slices = 48, number of volumes = 180, matrix = 144 x 144, slice spacing and slice thickness = 3 mm, ascending sequential acquisition in axial orientation.

5.2.4 Data Preprocessing

Acquired T1-weighted and T2*- weighted images were preprocessed by the default preprocessing pipeline of the CONN toolbox (www.nitrc.org/projects/conn, RRID:SCR_009550) which is a toolbox for SPM 12 (https://www.fil.ion.ucl.ac.uk/spm/software/spm12/). The first six T2*-weighted images were discarded, and 174 functional images were used for further analysis. The preprocessing pipeline includes the realignment and unwrap, slice timing correction, outlier detection using ART (http://web.mit.edu/swg/software.htm), direct segmentation, and normalization to MNI space, and functional smoothing. Realignment and unwrap were done to the first scan using b-spline interpolation. Slice timing correction was done to match the slice at each TR/2. Images showing their frame-wise displacement above 0.9mm due to head motion or the deviation of the global BOLD signal above 5 standard deviations were marked as outliers and scrubbed. Segmented functional and structural data were normalized to MNI space with 2 mm and 1 mm isotropic voxels respectively using 4th order spline interpolation. Functional smoothing was done with a Gaussian kernel of 6mm full width half maximum. To remove the slow physiological noises, the high pass filter with a 0.008 Hz threshold was applied.

5.2.5 ROI Marks

The region of interest (ROI) within the DMN network was defined with 5 brain regions of the posterior medial system: the angular gyrus (AG), the posterior cingulate cortex (PCC), the parahippocampal cortex (PHC), the precuneus (PRC) and the retrosplenial cortex (RSC). The mPFC was excluded due to its unclear functional and structural definition in the DMN in general. Various DMN studies reported the dorsal medial prefrontal cortex (mPFC), just mPFC, or ventral mPFC as a member of the DMN. The locations of their foci are slightly different, but it is unclear how clearly, they could be discriminated against in the normalized brain. At the same time, its functional role is not yet defined to the same degree as that of the other ROIs. The subtlety of the mPFC is an ongoing issue, and some studies have suggested that the mPFC should be delineated into at least two sub-regions respecting its functional connectivity within the DMN (Andrews-Hanna, Reidler, Sepulcre, Poulin, & Buckner, 2010; Raichle, 2015). On the other hand, the AG, the PCC, the PHC, the PRC, and the RSC have been well defined in isolated brain regions in functional and structural studies. Therefore, the present experiment used only these five brain regions for further analysis. The ROI marks of the DMN were produced by two methods, independent component analysis (ICA) and predefined brain atlases. Even if one could extract the ROI marks of the DMN of an individual using ICA, the predefined brain atlases have been widely used for various task-specific fMRI experiments. To compare analysis results of the ROI marks

of the DMN generated by brain atlases to that of by ICA from an individual participant would indicate which one is proper to the suggested analysis method below. The 6th-gen Montreal Neurological Institute (MNI) 152 space T1 templates (MNI space) based brain coordinate system was used to report the coordinate of the center of ROI marks (Janke, L., Budge, Pruessner, & Collins, 2006).

ICA

To define the common DMN of all four runs of B.L, group ICA was applied to the preprocessed data of four runs. The analysis was performed with CONN toolbox. The spatial independent components (number of components = 40, dimensionality reduction = 64) were calculated by fast ICA with G1 contrast function and GICA3 subject back projection (Calhoun V. D., Adali, Pearlson, & Pekar, 2001; Hyvärinen, 1999). Among the 40 independent components, one of them was chosen as the DMN by comparing spatial correlation and spatial overlap with the predefined DMN offered in the CONN toolbox. The predefined DMN was processed by ICA of the resting state data (n=497) of the Human Connectome Project (Nieto-Castanon, Conn in Pictures, 2020). However, the chosen independent component did not cover the entire PCC and neither did the mPFC. Even if the mPFC is excluded from the ROI of the present analysis, it is one of the DMN members that are always observed in the resting state fMRI data. Therefore, one more independent spatial component was chosen which is the PCC and the mPFC are dominant in the spatial independent component. In summary, the members of DMN were separated into two spatial independent components (Figure d). ROI marks based on chosen independent spatial components were generated following two methods; sphere ROI marks based on peak voxel coordinates of two independent spatial components, and direct extraction from them. Sphere-shaped ROIs centered at each peak of independent spatial components were generated as follows. Within one of the chosen independent spatial components (IC1) fitting mostly well on the predefined DMN, the coordinates of voxel ($8\ mm^3$) level peaks (one-sample t-test, P uncorrected < 0.001, z-score > 3) were chosen. 7 peaks in the IC1 were chosen and their anatomical labels were checked by the labeling of FSL Harvard-Oxford atlas (Matthew, 2021); bilateral AG, PHC, RSC were defined, and the PRC was located at the midline. The peak coordinate of PCC (t-test, P uncorrelated < 0.05, z-score > 3) was chosen from the other independent spatial component (IC2). Sphere-shaped ROI marks centered on them with a radius of 4mm for the bilateral regions and 6mm for the PCC and PRC were created by the MarsBar SPM toolbox (Brett, Anton, Valabregue, & Poline, 2002). On the other hand, the direct extraction of ROI marks from the independent spatial components was done by the CONN toolbox. From IC1, the bilateral AG, PHG, RSC, and the PRC were extracted. The IC2 containing the PCC and the mPFC was used to extract the ROI mark of the PCC (Table 1)

Figure d: Two independent spatial components of the DMN

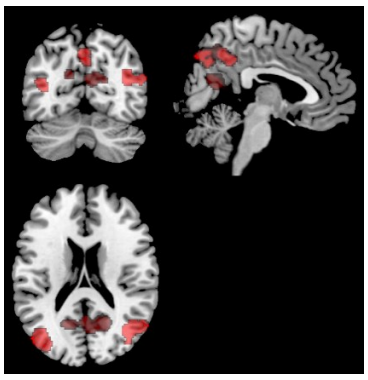

Independent spatial component 1 (IC1)

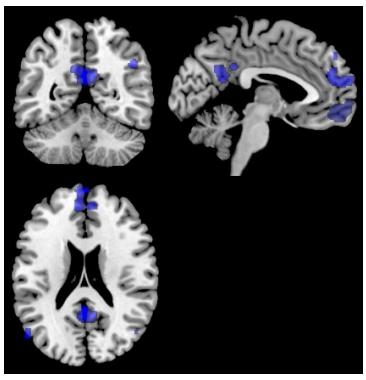

Independent spatial component 2 (IC2)

Brain Atlas

Predefined brain atlases based on structural and functional data were selected to define ROIs in the DMN. Dictionaries of Functional Mode (DiFuMo) is an atlas defined based on T2*-weighted functional images collected from 25 task studies and 2 resting state studies (n = 2192) (Dadi, et al., 2020). The atlas offers 64-, 128-, 256-, 512-, and 1024-dimensional resolutions defined by sparse dictionary learning with the stochastic online matrix factorization algorithm (Mensch, Mairal, Thirion, & Varoquaux, 2017). Sparse dictionary learning or sparse coding is an analysis method to decompose data into a set of patterns that can reconstruct the original signals by their sparse linear decomposition. The set of patterns is called the dictionary. It allows slight overlaps between brain regions so that they are described with gradients that are maximized at a central point decided by their analysis. The coordinates are registered to the MNI 152 space T1 templates. The labels of brain regions of DiFuMo with 1024 dimensions were used in the present study since it offers the finest spatial resolution. It includes 6 PCC regions, 17 PRC regions, 4 AG regions, 4 PHC regions, and 2 RSC regions. Based on the functional relevance for the current study (chapter 3.2.2), ROI marks of all 6 PCC regions, 2 pairs of PRC regions (left and right middle PRC and middle superior PRC), left and right posterior AG, left and right posterior PHC, RSC and RSC posterior were used for further analysis.

The FSL Harvard-Oxford atlas of cortical and subcortical areas is one of the most frequently used brain atlases, containing 132 cortical and subcortical brain regions (Matthew, 2021). It was generated based on T1-weighted structural images of 37 subjects (16 females, ages 15-80) and registered to the MNI 152 space T1 templates. The CONN toolbox offers it as the default atlas and its brain regions can be extracted separately. It does not have the RSC among its brain regions; therefore, I used the RSC marks offered from the DiFuMo 256-dimensional atlas (D RSC) and Brodmann area created by wfu_pickatlas (BM RSC) (Medicine & Maldjian, n.d.). Another popular structural image-based brain atlas is Automated Anatomical Labeling (AAL) (Tzourio-Mazoyer, et al., 2002). The AAL is based on T1-weighted images of a young man who was scanned 27 times with an MRI. Sulci limited bilateral 116 cortical and subcortical brain regions are labeled in the AAL brain atlas. The ROI marks were created by wfu_pickatlas which offers separated image files of each brain region in AAL. The coordinates of AAL have also been registered to the MNI 152 space T1 templates. It offers bilateral AG, PCC, PHC, PRC but does not include RSC. As in the previous case, I used D RSC and BM RSC.

Table 1: Coordinate of the center of ROIs

	Left	t	P_un	Right	t	P_un
AG	-54, -54,18	22.10	0.000	54, -56,16	11.77	0.001
PCC				0, -52,26	4.95	0.016
PHC	-30, -38, -16	12.07	0.001	18, -36, -14	13.62	0.001
PRC				2, -58,50	170.71	0.000
RSC	-12, -52,8	11.30	0.001	6, -44,12	12.30	0.001

Sphere shape ROI marks (IC1 & IC2): ROI marks centered at the peaks with 4mm radius were created. The PCC and PRC ROI mark has a 6 mm radius to include voxels in both hemispheres. One sample t test, d.o.f= 3

	Left		Right	
AG	-40, -75,22	n = 517	40, -71,26	n = 510
PCC			0, -53, 25	n = 420
PHC	-29, -38, -17	n = 86	22, -38, -16	n = 41
PRC			0, -60,42	n = 539
RSC			2, -60,16	n = 765

ICA based ROI marks:

PHC L/R ROI marks were imported from ICA1 with z-score > 2.5. AG L/R, PRC, RSC ROI marks were imported from ICA1 with z-score > 4. PCC ROI mark was imported from ICA2 with z-score > 3

FSL Harvard-Oxford Brain Atlas

	Left	Right
AG	-50, -56,30	52, -52,32
PCC	1, -37,30	
PHC	-22, -32, -17	23, -30, -17
PRC	1, -59,38	
D RSC	3, -40,3	
BM RSC	-11, -57,6	11, -56,6

AAL Brain Atlas

	Left	Right
AG	-44, -62,34	45, -61,37
PCC	-5, -44,23	7, -43,20
PHC	-21, -17, -22	25, -16, -22
PRC	-8, -57,47	10, -57,42
D RSC	3, -40,3	
BM RSC	-11, -57,6	11, -56,6

DiFuMo 1024-dimension atlas

	Left	Right
AG pst	-33, -72,45	60, -54,33
PCC	3, -48,27	
PCC ant	0, -36,33	
PCC ant-inf	0, -42,21	
PCC inf	9, -45,0	
PCC inf LH	-9, -54,15	
PCC pst inf	0, -57,18	
PHC pst	-27, -33, -6	24, -36, -3
PRC mid-sup	-6, -63,51	12, -63,57
PRC mid	-3, -57,42	9, -54,48
RSC	-3, -36,0	
RSC pst	3, -48,9	

5.3 Group study

5.3.1 Subjects

For the group study, seven nonblind healthy subjects (4 female, age 21 to 36 years) were recruited. A written consent form was given to subjects, and they were paid after the experiment. The Ethics Committee of the Medical Faculty at the University of Munich approved the protocol of the experiment.

5.3.2 Behavioral Experiment

Subjects were asked to practice retrieving their morning routine in advance of the experiment. The morning routine was defined from the moment they wake up and to the moment they start work. Subjects described verbally their morning routine and their description was recorded as audio files on the day of the experiment. The dictation of the verbal description of each participant was attached in Appendix B. After the verbal description and before an fMRI session, subjects retrieved their morning routine again in silence three times. The duration of the morning routine retrieval in silence was measured. Subjects informed the start and the end of each retrieval trial to an experimenter.

5.3.3 MRI data Acquisition

As a single case study, four runs of fMRI data were collected. In the first fMRI run, subjects were in a resting state closing their eyes. After the resting state run, subjects retrieved their morning routine three times (AEMR runs) and a total of four runs were done in an MRI session. Subjects had a brief pause between each run. The beginning and the end of each fMRI run were informed to the participant through a speaker in the MRI room. Each run was 7 minutes 50 seconds. The image scanning was done with a 3T MRI machine (Philips healthcare, Ingenia) in the University Hospital LMU Munich. A foam cushion was used to minimize the effect of head movement. Subjects wore earplugs with a hearing protection earmuff to cancel noises from the MRI machine. T1-weighted structural image was acquired with magnetization-prepared rapid gradient-echo sequence (MPRAGE) with the following arrangement: repetition time (TR) = 9.5 ms, echo time (TE) = 5.54 ms, flip angle (FA) = 8°, number of slices = 190, matrix = 256 x 256, slice spacing and slice thickness = 1 mm, in sagittal orientation. T2*-weighed functional images were acquired after the T1 session with echo-planar image (EPI) sequence with the following arrangement: repetition time (TR) = 2.5 ms, echo time (TE) = 30 ms, flip angle (FA) = 90°, number of slices = 49, number of volumes = 180, matrix = 144 x 144, slice spacing and slice thickness = 3 mm, ascending sequential acquisition in axial orientation.

5.3.4 Data Preprocessing

Data were preprocessed with the same procedure used for the single case study. Acquired T1-weighted and T2*- weighted images were preprocessed by the default preprocessing pipeline of the CONN toolbox (www.nitrc.org/projects/conn, RRID:SCR_009550) which is a toolbox for SPM 12 (https://www.fil.ion.ucl.ac.uk/spm/software/spm12/). Total 180 functional images were used for further analysis.

5.3.5 ROI Marks

The DMN of each subject was extracted by group ICA using CONN toolbox as the single case study. Independent components were abstracted from each subject independently without aggregating the data of all seven subjects together. The four runs of fMRI data were preprocessed and analyzed at the first and second levels within each subject to abstract independent components. The spatial independent components of each subject (number of components = 20, dimensionality reduction = 64) were calculated from four runs by fast ICA with G1 contrast function and GICA3 back projection (Calhoun V. D., Adali, Pearlson, & Pekar, 2001; Hyvärinen, 1999). In this group study, the DMN was well defined in all seven subjects when the number of independent components is 20. Among the 20 independent components, two of them for six subjects and three of them for a subject were chosen as the DMN by comparing its spatial correlation and spatial overlap with the predefined DMN offered in the CONN toolbox, and inspection with eyes. The number of voxels in each ROI mark was adjusted to be approximately balanced with other ROI marks within a subject. It was done by adjusting the threshold of independent components (one-sample t-test, d.o.f = 3, P uncorrected $\leq$ 0.001). The coordinates of ROI marks for each subject and the number of voxels were attached in Appendix C.

6. Analysis

6.1 Dynamic Functional Connectivity (DFC)

The present study aims to explore analytic methods to find a consistent dynamical feature of the AEMR state in different trials. At the same time, it might also be possible to see differences in the dynamical feature from two different mental states sharing their spatial domain. These two mental states belong to the same large functional category, the construction of the internal world. Consequently, the mental states are mainly executed in the DMN. However, they are not in the same mental state. An AEMR state requires contextual causality and orders whereas a resting state does not require any of them. On the contrary, a resting state requires being free from orders. Also, one can tell whether the contents of autobiographical episodic memory is true or false (Wheele, Stuss, Tulving, 1997) but it cannot be the case for the thoughts or ideas occurring in a resting state. If we assume that these two mental states truly share the spatial activity pattern, then their differences should be encoded in their dynamical feature. To abstract the dynamical feature of measured BOLD signals, I chose to find a proper way to approximate it to a deterministic dynamic system, because of its simplicity in calculation and interpretation.

The sliding window method with the window width of 10 consecutive images (=25 secs with TR=2.5 sec) was used to define dynamic functional connectivity between ROIs. The weight of the window is constant, i.e., the window has a rectangular shape. It slides an image per step, so the dynamic functional connectivity is described with 165 points of Pearson correlation coefficient between two brain regions for 174 preprocessed images. The Pearson correlation coefficients $r[A(t), B(t)]$ between a brain region $A(t)$ and $B(t)$ at time point t (t = 1, …,165) are

$$r[A(t), B(t)] = \frac{\sum_t^{t+9}(A(t) - \overline{A_t})(B(t) - \overline{B_t})}{\sqrt{\sum_t^{t+9}(A(t) - \overline{A_t})^2}\sqrt{\sum_t^{t+9}(B(t) - \overline{B_t})^2}}$$

The mean of BOLD signals for 10 consecutive images starting from time point t is $\overline{A_t}$ and $\overline{B_t}$. The dynamic functional connectivity map of the chosen ROIs shows the changes of functional correlation in BOLD signals between two brain regions (Figure e). The given dynamic functional connectivity between brain regions in the DMN is data in the form of a multivariable time series. The dimension of the data is the number of functional connectivity between the brain regions in question. In general, it is hard to analyze such multivariable time series data in its full dimension, and due to its high dimensionality, the system has high complexity. Therefore, to reduce the dimension of the data and to analyze its temporal characteristic in the reduced dimension is used to find macroscopic characteristics of the data. For that, a one-ROI-centered DFC map was used to reduce the number of correlations within the DMN, and the principal component analysis is applied to define the direction of its temporal variance.

Figure e: Functional connectivity maps (Blind Lady, Run1, ICA based ROI marks) at different time points. Values of $\mathrm{r}[\mathrm{A}(\mathrm{t}), \mathrm{B}(\mathrm{t})]$ are presented with a color map.

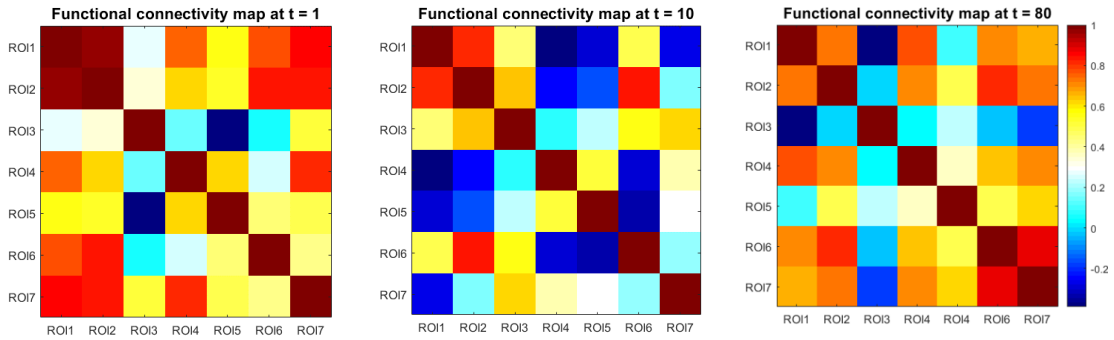

6.1.1 One-ROI-centered Analysis

To reduce the dimension of the DFC data, I suggested using one-ROI-centered dynamic functional connectivity (DFC) maps. A network of n nodes has $\frac{n(n-1)}{2}$ edges or connections between two components. When a node is chosen as a center, and only the edges (connection) between the center node and the other nodes (brain regions) are considered, then the one node centered network has $n-1$ edges (Figure f). As previously introduced, functional and structural hubs of the brain are centers of local clusters forming a small world network together (Achard, Salvador, Whitcher, Suckling, & Bullmore, 2006; Bassett & Bullmore, 2006; Sporns & Zwi, 2004). The nodes of a small world network are mostly connected to their local hubs and communicate with each other via the hubs. Hence, a local cluster or a subnetwork described with connections between its local hub and non-hub regions without connections between non-hub regions might carry enough information to define activities of the subnetwork. I call the DFC maps having reduced dimension by choosing an ROI as a center of the connection by neglecting the connections between non-center ROIs one-ROI-centered DFC maps. The DMN has 7 to 10 ROIs (nodes), then one-ROI-centered DFC map has 6 to 9 variables instead of 21 to 45. One-ROI-centered DFC map of each of the brain regions in the DMN was calculated in this thesis.

Figure f: Dimension reduction of one-ROI-centered DFC map

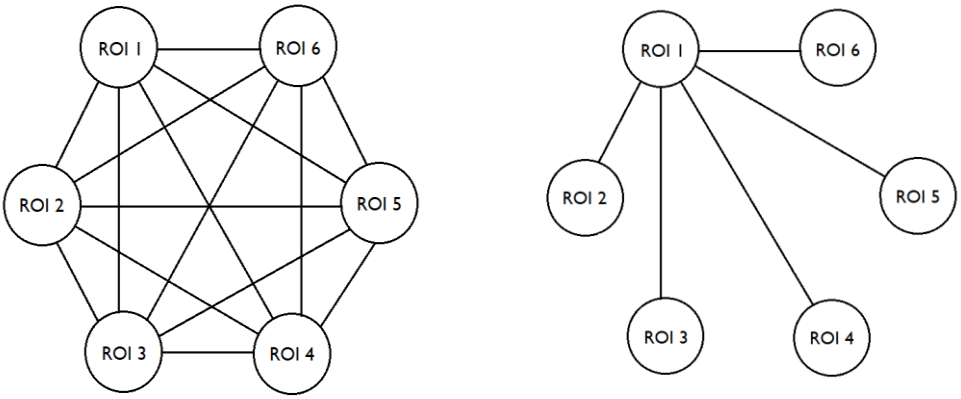

Full DFC of a brain network with 6 ROIs

ROI1 centered DFC map

6.1.2 Principal Component Analysis

Principal component analysis (PCA) is a type of analysis to show the distribution of multivariable data along with the orthogonal axes of the distribution. These orthogonal axes defined by principal component analysis are called principal components (Pearson, 1901; Wold, 1987). Orthogonality of principal components guarantees that the distribution of data along each axis is linearly independent, i.e., the variance of data along a principal component is explained independently from variances along the other axes. The variance along the first principal component explains the largest amount of the total variance of the given data, and that of the second principal component explains the next largest amount of the total variance and so on (Figure g). For the data with p variables for n time points, p principal components are defined by PCA.

There are a few methods to calculate principal components. One of the popular methods is singular value decomposition (SVD). Singular value decomposition decomposes a given data into vectors in an orthonormal space indicating the direction of data distribution and the amount of variance of the data to each direction in the orthonormal space. When a data set is organized as a matrix $\boldsymbol{X}$ which is an $n \times p$ matrix with n time points and p variables, it is decomposed as $\boldsymbol{X} = \boldsymbol{U\Gamma V^T}$ by SVD. $\boldsymbol{U}$ is a $n \times n$ left unitary matrix, $\boldsymbol{\Gamma}$ is a diagonalized $n \times p$ matrix with singular values in descending order, $\boldsymbol{V^T}$ is a $p \times p$ right unitary matrix. The left and right unitary matrices are collections of linearly independent unit vectors which give directional information, and their singular values are the amount of stretch along them. Columns of $\boldsymbol{V}$ are principal components, and each principal component could be written in terms of the components of the original space. When V_1 is the first principal component of $\boldsymbol{X}$, then its loadings L_{1i} for $i = 1, \dots, p$ shows the V_1 in the coordinate system of the original spaces, such that $V_1 = V_1(L_{11}, \dots, L_{1p})$. $\boldsymbol{U\Gamma}$ is the score of principal components, which means the amount of variance along with the principal components for n time points ($\boldsymbol{XV} = \boldsymbol{U\Gamma V^T V} = \boldsymbol{U\Gamma}$). Principal components were calculated with SVD in the present study.

Before applying PCA to one-ROI-centered DFC maps to define principal components, all data were aligned to have the zero mean. The first three principal components were chosen for further analysis because they explained 60 to 70 percent of the variance of one-ROI-centered DFC maps.

Figure g: Principal component analysis and angles between principal components

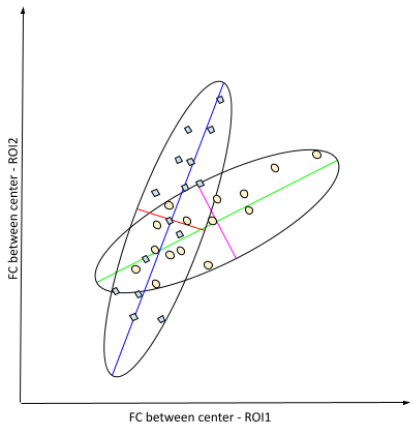

a) Diamond: DFC at a moment t of run1
Dot: DFC at a moment t of run2
Axes of ellipses: the first and second principal components of each run

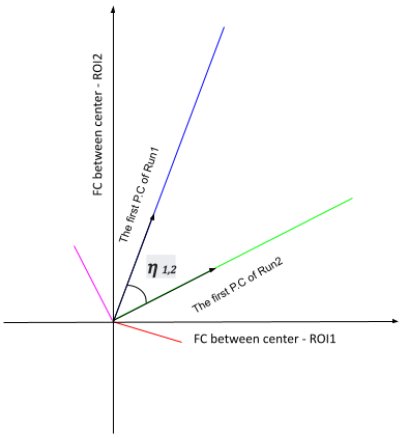

b) Arrows: unit vectors along each first principal component

6.1.3 One to One Principal Component Comparison

Since the evolution of a BOLD time series is determined by highly complex nonlinear mechanisms, to observe its abstracted variances is reasonable to find a hidden regularity instead of investigating their exact time evolution as mentioned in chapter 3. The directions of variances of DFC could be considered one of the methods of abstraction. The principal components of one-ROI-centered DFC maps of each fMRI run were chosen for that. For four data sets from three AEMR runs and one resting state run, the four different sets of principal components per each one-ROI-centered map were defined. If one of the chosen first three principal components from each run are similar, then one can say there is a common direction of variances for the one-ROI-centered DFC. When one-ROI-centered DFC map of three AEMR runs have similar principal components and that of the resting state shows less similarity to each of them, one could say it represents the different dynamical features of the one-ROI-centered DFC map of two different mental states (Figure h).

How can we compare the similarity between principal components from different runs? Using the loadings L of principal components, it is possible to compare the angle between principal components of a one-ROI-centered DFC map from each run in the original variable space. For example, the first principal component of a run $V_1 = V_1(L_{11}, \dots, L_{1p})$ with its loading vector L_{1i} for $i = 1, \dots, p$ means that the L_{11} amount of contribution from the variance of functional correlation between the center brain region and the first brain region, and likewise L_{1p} amount of contribution from the variance of functional correlation between the center brain region and $p\ th$ brain region. When L_1 is the loadings of the first principal component of run 1 and M_1 is that of run 2, the angle η $(0 \leq \eta_{1,2} \leq \frac{\pi}{2})$ between these principal components is calculated in the original variable space, such that $\eta_{1,2} = \cos^{-1}(L_1 \cdot M_1)$ when $L_1 \cdot M_1$ is the inner product of L_1 and M_1 and the norm of L_1 and M_1 is 1 (

Figure g, b). The angle $\eta_{1,2}$ tells how parallel or how similar the directions of the first principal components of run 1 and that of run 2 are in the original variable space. By repeating this one-to-one comparison for the chosen first three principal components of each four runs one could compare the main direction of variances of one-ROI-centered DFC map of a run to that of others.

The first principal component of multivariable data can explain that the largest amount of variance of the data. When it is applied to one-ROI-centered DFC maps, the largest amount of the variance of a one-ROI-centered DFC map is encoded in the direction of the first principal component, and the second-largest amount of the variance is encoded in the second principal components and so on. Therefore, if one of the first few principal components of a one-ROI-centered DFC map from a run is aligned parallel to that of other runs, one-ROI-centered DFC maps of these runs have a common direction to encode most of their variance. In other words, the variance of functional correlation of a brain region-centered brain network has a preferred direction to happen along with it, and it is decided by the mental state realized in the brain network.

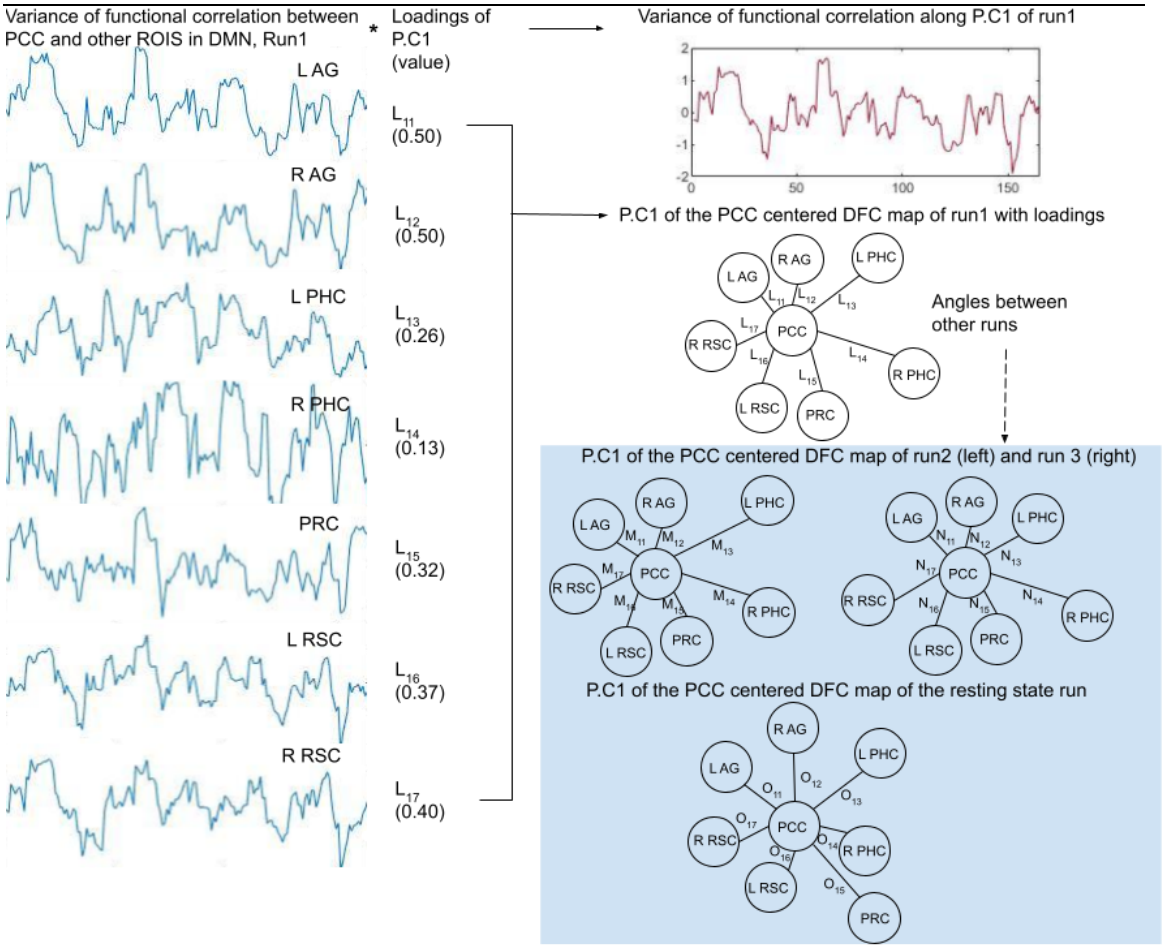

Figure h : First principal component of the PCC centered DFC map of subject 05 with loadings.

The score of the first principal component $V_1(L_{11}, L_{12}, L_{13}, L_{14}, L_{15}, L_{16}, L_{17})$ is visualized with loadings L_{1i} indicating the weight of the variance of functional correlation between the center ROI (PCC) and each of ROIs in the DMN to the variance (score) in the direction of the first principal component (P.C1). In the graph expression, the edge is inversely proportional to the value of loadings. In this example, the first principal components of each run were chosen to compare their similarity.

6.1.4 Principal Component Subspace Comparison

There are other ways to compare similarities between principal components of multivariable data of different data sets. The most relevant analysis of comparison of principal components from different multivariable data sets regarding similarity measured by the angle between principal components was chosen to compare principal components of one-ROI-centered DFC map from the AEMR runs. Kranzowski (1979) proposed to compare the similarity between subspaces of principal components of different data sets (Krzanowski, 1979). For the given data sets from three different groups (in our case, three different runs of a single participant), they have p original variables, with p principal components. To choose the first $k \leq p$ principal components of each data set, then one can compare similarity between the k dimension subspaces built from the chosen first k principal components. It is possible to define an eigenvector $\vec{b}$ of k dimensional subspaces of principal components, and the minimum angles between the eigenvector $\vec{b}$ and each k dimensional principal component subspaces tell the similarity between them. It is done by following processes. Let S_g be $p \times k$ matrices of group $g = 1, 2, 3$ such that they represent the k dimensional subspaces of principal components from each group. $\vec{b}$ is the eigenvector of the sum of

subspaces $H = \sum_{g=1}^{3} S_g S_g^T$, such that its k columns are the chosen principal components. To find $\vec{b}$ which is maximally close to all subspaces reveals the similarity between k dimensional subspaces with respect to $\vec{b}$ (Figure i). When the angle between a k dimensional subspace of group g and the eigenvector $\vec{b}$ is θ_g $(0 \leq \theta_g \leq \pi)$, the eigenvector $\vec{b}$ of the biggest eigenvalue λ_1 of H gives the maximally closest angle θ_g to all subspaces of groups. Therefore, $\vec{b}$ maximizes

$$\sum_{g=1}^{3} cos^2\theta_g = \sum_{g=1}^{3} \vec{b}^T S_g S_g^T \vec{b} = \vec{b}^T H \vec{b}$$

, since $\max_{||\vec{b}||=1} \vec{b}^T H \vec{b}$ is given by the biggest eigenvalue λ_1. The closest angle between group g and $\vec{b}$ is defined $\theta_g = \cos^{-1}\sqrt{\vec{b^T} S_g S_g^T \vec{b}}$. Such angle θ_g describes how subspaces of each group are close to $\vec{b}$ (Figure i). When it is applied to one-ROI-centered DFC maps of AEMR runs, $\vec{b}$ shows the preferred direction of variances that the most variances of one-ROI-centered DFC maps is encoded.

The previous one-to-one principal component comparison estimates how much the directions of the principal components are like each other. Most importantly, it compares a chosen principal component from each run one to one. So, it is possible to see the relative similarity of dynamics within AEMR runs and between AEMR runs and the resting state run. On the other hand, the comparison using subspace of principal components suggested by Kranzowski(1979) is a good method to know the similarity of subspaces generated by principal components of AEMR runs. However, it is not proper to compare the subspace of principal components of the resting state run to those of AEMR runs, since $\vec{b}$ is defined to find the maximally close angels of compared runs. To define $\vec{b}$ for all four runs including the resting state run shows the closeness of the four runs to the $\vec{b}$ but does not offer a comparison between runs from two different states. Therefore, the eigenvector $\vec{b}$ is used to see the similarity only between three AEMR runs.

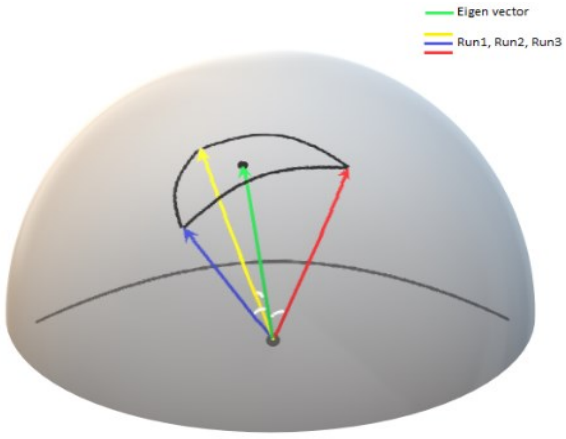

Figure i: Principal component subspace comparison.

The hemisphere is the span of normalized principal components in the original space, and the angles between principal components of three AEMR runs (blue, yellow, red) and their eigenvector (green) shows how the alignment of each principal component in the original space is like each other.

7. Results

7.1 Single Case Study

7.1.1 Behavior

B.L reported that she could retrieve the same morning routine in detail for all retrieval sessions, the verbal statement session, the retrieval session outside of the machine, and the fMRI session. The full transcript of her verbal statement is attached in Appendix B. Her statement of the morning routine was constructed with a sequence of episodes categorized by locations. She described each episode of her morning routine in detail involved mainly with objects, their location in the scene, and her movement within the scene of the episode. The changes of episodes are described with navigation to move to the next location from the current location.

For example, a scene in her sleeping room is as follow.

> *"I imagined lying in bed having just woken up. I then put my feet to the left, as usual; Out of the bed; Got the shoes, that were right there; Get up; Making my way around the bed; then there is the door; Through the door into the corridor; To the right and immediately to the left again, there is the toilet, something one needs in the morning."*

She reported that the last episode she had been retrieving was the same at the end of each fMRI run, that she is waiting for her husband sitting at the breakfast table in the living room. This behavioral result that she could construct a series of consecutive episodes in her internal world repeatedly showed that a regular mechanism is demanded to retrieve the same episodic memory repeatedly. Also, it took a similar time to retrieve the same episodic memory in each trial. Hence, such a mechanism should have certain regularity in its dynamics. Consequently, I speculated that her mental state that is realized in the DMN during AEMR was consistent for three runs. Not only this but also the difference in two mental states, the resting state, and the AEMR state sharing the same spatial activity pattern of the DMN, can be speculated based on the behavioral result. Even though both mental states belong to the same category called the construction of the internal world, the AEMR state retrieves a consistent memory that can be repeatedly performed. In contrast, the resting state allows the internal world freely to drift from one imagery to another one and does not allow the repetition of it.

7.1.2 fMRI Data

The first three principal components of each one-ROI-centered DFC map with ROI marks generated by ICA and brain atlases explained over 60 % of the total variance on average. They were selected to compare the similarity of principal components of each run. The probability distribution of angles between principal components was compared with the normal distribution of the same number of samples, the mean, and the standard deviation (Figure I). The chance of angles to be smaller than $45°$ was less than 0.07 on average. The probability distribution of angles from ICA based ROI marks and from DiFuMo1024-dim atlas differed from the normal distribution particularly. Both probability distributions had thick tails and sharp peak near the mean compared with the normal distribution. Therefore, one could expect to see clear independency between principal components for these two ROI marks cases.

To define absolute closeness between two principal components is not reasonable to explain the similarity within a one-ROI-centered DFC of three AEMR runs and between that and the resting state run. Therefore, how to interpret the similarity should rely on the data on the hand (Krzanowski, 1979). To define meaningfully similar or different principal components from AEMR runs and the resting state run for the one-to-one principal component comparison of one-ROI-centered DFC maps, three steps were made.

1. The choice of principal components among the first three principal components of each run for the one-to-one comparison was made by following. The angle between AEMR runs ($\eta_{i,j}, i \neq j,\ i,j = 1,2,3$) is calculated among the first three principal components of each run, $Run_1(P.C), Run_2(P.C)$ and $Run_3(P.C)$.

$$\eta_{i,j} = Angle\left[Run_i(P.C), Run_j(P.C)\right]$$

   The smallest $\eta_{i,j}$ is chosen as the parameter showing the similarity between runs. In the one-ROI-centered DFC map, their principal components show the directions of variance in functional correlation. The smallest angle tells the maximum similarity between the direction of variance in the functional correlation of each run. The principal component of the resting state run $Run_R(P.C)$ was chosen to have the smallest angle between AEMR runs.

$$\eta_{i,R} = \min\ Angle[Run_i(P.C), Run_R(P.C)]$$

2. To test the difference between chosen principal components of AEMR runs and the chosen principal component of the resting state run, the ratio of the mean angles of $\eta_{i,j}$ to the mean angle of $\eta_{i,j} + \eta_{i,R}$ was calculated. When the mean of angles between the chosen principal components from each AEMR run ($\bar{\eta} = \frac{\eta_{1,2}+\eta_{1,3}+\eta_{2,3}}{3}$) is smaller than the mean angle between all four runs ($\bar{\eta}_{all} = \frac{\eta_{1,2}+\eta_{1,3}+\eta_{2,3}+\eta_{1,R}+\eta_{2,R}+\eta_{3,R}}{6}$), the ratio $\bar{\eta}$ to $\bar{\eta}_{all}$ is smaller than 1. The brain region having the minimum ratio of its ROI-centered DFC means that the brain region-centered ROI DFC has the maximum difference between the AEMR state and the resting state.

$$\min\ {}^{\bar{\eta}}/_{\bar{\eta}_{all}} \leq 1$$

3. $\eta_{i,j}$ the angles between the chosen principal components of AEMR runs are smaller than $\eta_{i,R}$ the angles between AEMR runs and the resting state run.

$$\gamma_{i,R} = \frac{\eta_{i,R}}{\sum_{\substack{j=1 \\ j\neq i}}^{3} \eta_{i,j} + \eta_{i,R}} > \frac{\eta_{i,j}}{\sum_{\substack{j=1 \\ j\neq i}}^{3} \eta_{i,j} + \eta_{i,R}}$$

   This step tells us that the most different principal component from the chosen principal component of an AEMR run is always the principal component of the resting state. The second step only shows the difference in the mean angles without the resting run and with the resting run. If one-ROI-centered DFC maps of the resting run have less coherent principal components compared to the AEMR runs, the angles between AEMR runs and the resting state run, $\eta_{i,R}$ should be the biggest angle among $(\eta_{i,j}, \eta_{i,k}, \eta_{i,R})$.

Figure j : Probability distributions of angels between principal components of one-ROI-centered DFC maps from each ROI marks

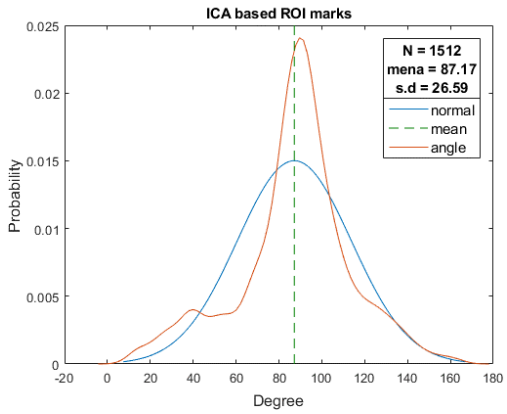

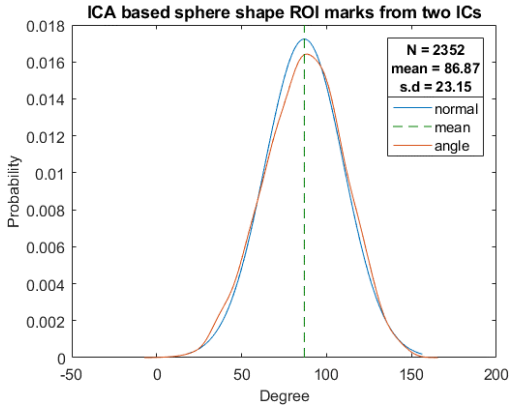

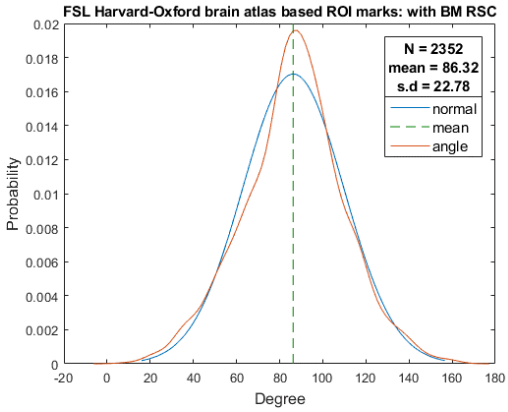

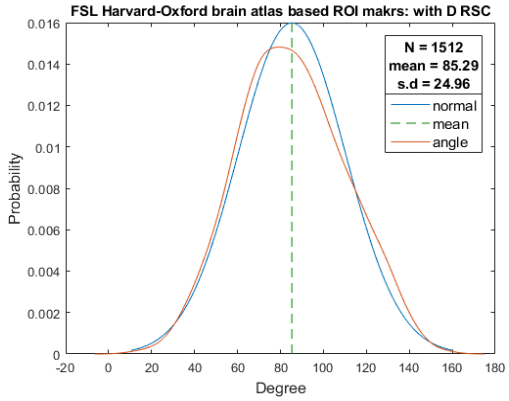

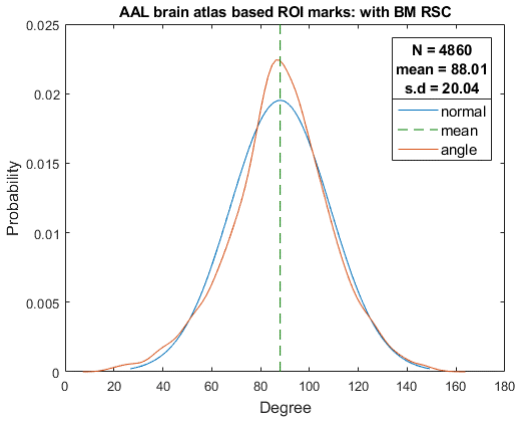

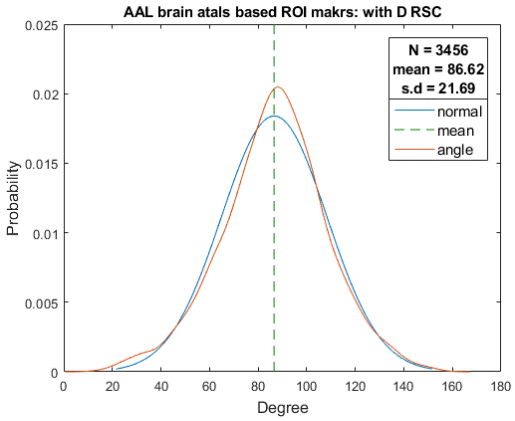

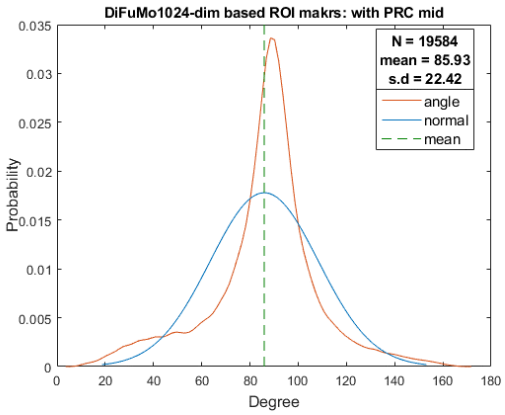

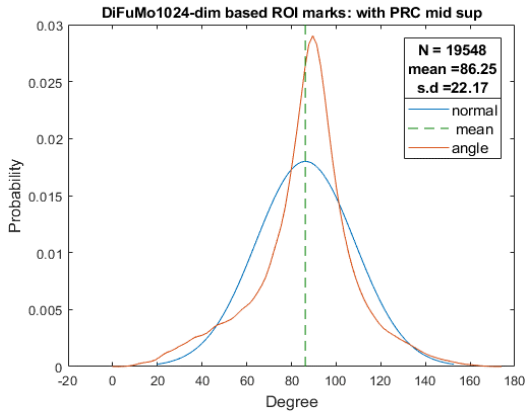

7.1.3 ICA based ROI Marks

The results fitted well with suggested conditions in the three steps were found the PCC centered DFC map and the R PHC centered DFC map of ICA based ROI marks (Table 2, Table5). Also, to show how similar the chosen principal components of three AEMR runs are, angles to their eigenvector in 1 dimension were calculated (Table4, Table7) (Krzanowski, 1979).

Table 2: PCC centered DFC analysis result from the ICA based ROI marks

Angle(°)	**Run1(P.C1)**	**Run2(P.C1)**	**Run3(P.C1)**	**Rest (P.C1)**	
Run1(P.C1)	0	8.93	13.54	21.09	
Run2(P.C1)	8.93	0	16.67	21.21	
Run3(P.C1)	13.54	16.67	0	33.03	
Mean		$\bar{\eta}$ =13.05		$\bar{\eta}_{all}$ = 19.08	$\frac{\bar{\eta}}{\bar{\eta}_{all}}$ = 0.68

a) Angle between chosen principal components from each run.

Ratio$(\gamma_{i,j})$	**Run1(P.C1)**	**Run2(P.C1)**	**Run3(P.C1)**	**Rest (P.C1)**
Run1(P.C1)	0	0.205013	0.310855	0.484132
Run2(P.C1)	0.190822	0	0.356109	0.453069
Run3(P.C1)	0.214133	0.263549	0	0.522318

b) Ratio of angles of $\eta_{i,j}$, $\eta_{i,k}$ and $\eta_{i,R}$. For example, the second row is the ratio of the angle between Run1(P.C1), i=1 and the others j=2, k=3, and R (rest).

Table 3: Value of components of eigenvector from the chosen principal components of AEMR and Rest(P.C1) run, PCC centered DFC

	Eigen V	**Rest(P.C1)**
L AG	0.520103	0.378994
R Ag	0.444821	0.285128
L PHC	0.316477	0.498003
R PHC	0.192268	0.496298
PRC	0.461888	0.380779
RSC	0.425631	0.368449

Table 4: Angle between the chosen principal components of AEMR runs and their eigenvector V, PCC centered DFC

Run \ **Eigen V**	**Angle(°)**
Run1(P.C1)	5.23
Run2(P.C1)	7.67
Run3(P.C1)	9.71

Table 5: R PHC centered DFC analysis result from the ICA based ROI marks

Angle(°)	**Run1(P.C1)**	**Run2(P.C1)**	**Run3(P.C1)**	**Rest (P.C1)**	
Run1(P.C1)	0	16.39	15.07	17.79	
Run2(P.C1)	16.39	0	13.77	32.54	
Run3(P.C1)	15.07	13.77	0	31.35	
Mean		$\bar{\eta}$ = 15.08		$\bar{\eta}_{all}$ = 21.15	$\frac{\bar{\eta}}{\bar{\eta}_{all}}$ = 0.71

a) Angle between chosen principal components from each run.

Ratio$(\gamma_{i,j})$	**Run1(P.C1)**	**Run2(P.C1)**	**Run3(P.C1)**	**Rest (P.C1)**
Run1(P.C1)	0	0.332824	0.30599	0.361185
Run2(P.C1)	0.261439	0	0.219634	0.518927
Run3(P.C1)	0.250382	0.228791	0	0.520826

b) Ratio of angles of $\eta_{i,j}$, $\eta_{i,k}$ and $\eta_{i,R}$.

Table 6: Value of components of eigenvector from the chosen principal components of AEMR and Rest(P.C1) run, R PHC centered DFC

	Eigen V	**Rest(P.C1)**
L AG	0.483674	0.459798
R Ag	0.511793	0.475027
PCC	-0.05415	0.390424
L PHC	0.188943	0.231172
PRC	0.522115	0.496129
RSC	0.439194	0.333047

Table 7: Angle between the chosen principal components of AEMR runs and their eigenvector V, R PHC centered DFC

Eigen V / **Run**	**Angle(°)**
Run1(P.C1)	9.46
Run2(P.C1)	8.76
Run3(P.C1)	7.92

Table 8: Mean angles between three AEMR runs and their eigenvector in one ROI-centered DFC map

Angle(°)	**L AG**	**R AG**	**PCC**	**L PHC**	**R PHC**	**PRC**	**RSC**
Mean	13.48	21.25	7.54	12.71	8.71	16.03	20.82

For the PCC centered DFC map and the R PHC centered ROI map, the angles between the chosen principal component of AEMR runs and their eigenvector was smaller than other ROI centered maps. It means that the dynamical feature of the PCC and the R PHC centered maps have more similarity between three runs than other brain region centered DFC maps do (Table8).

Figure k: PCC centered DFC map of ICA based ROI marks.

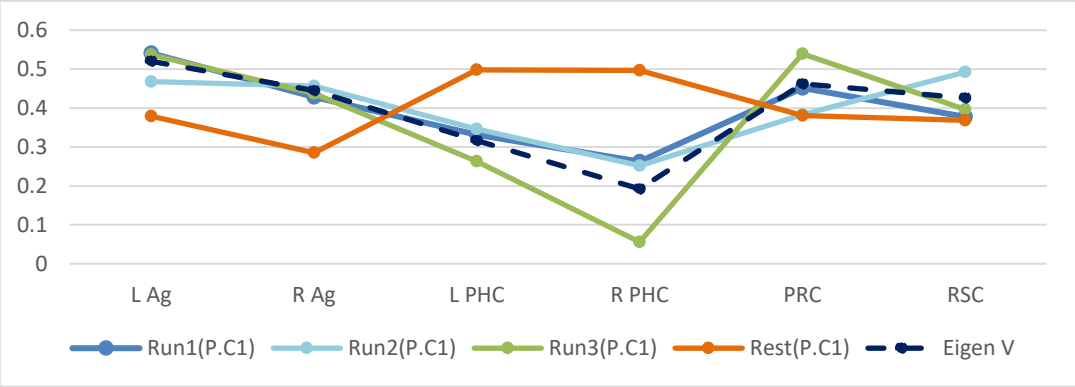

Figure l: R PHC centered DFC map of ICA based ROI marks.

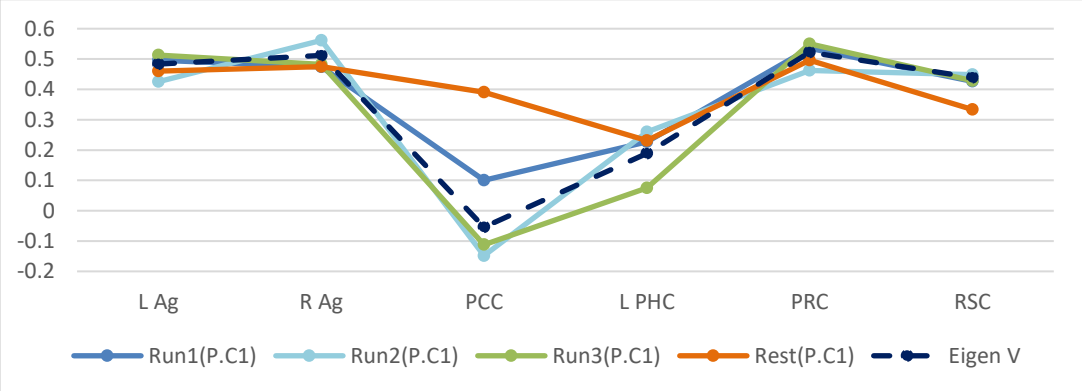

7.1.4 DiFuMo1024-dim Brain Atlas based ROI Marks

DiFuMO1024-dim brain atlas contains small sub-regions of the PRC and PCC. The chosen 6 PCC sub-regions and 2 PRC sub-regions give 12 different combinations of the DMN. The left middle PRC centered DFC map of the inferior PCC (PCC inf) and the middle PRC (PRC mid) combined DMN of DiFuMo1024-dim brain atlas had the result satisfying conditions suggested by three steps of analysis (Table9). However, the DMN defined with the inferior PCC has covered very partially the medial posterior parietal lobe. The inferior PCC is located in the inferior part of PCC, which is close to the BA29, 30 (the RSC). It was a restricted definition of the PCC compared with other ROI marks from ICA and other two brain atlases (Figure m). Therefore, the interpretation of the result should be limited to avoid overfitting it.

Table 9: DiFuMo1024-dim, the left middle PRC (L PRC middle) centered DFC analysis

Angle(°)	**Run1(P.C1)**	**Run2(P.C1)**	**Run3(P.C1)**	**Rest(P.C1)**	
Run1(P.C1)	0	18.71	11.29	27.19	
Run2(P.C1)	18.71	0	20.35	33.31	
Run3(P.C1)	11.29	20.35	0	26.20	
Mean		$\bar{\eta}$ =16.78		$\bar{\eta}_{all}$=22.84	$\frac{\bar{\eta}}{\bar{\eta}_{all}}$=0.73

a) Angle between chosen principal components from each run

Ratio($r_{i,j}$)	Run1(P.C1)	Run2(P.C1)	Run3(P.C1)	Rest(P.C1)	Total
Run1(P.C1)	0	0.327179	0.197379	0.475442	1
Run2(P.C1)	0.258558		0.281173	0.460269	1
Run3(P.C1)	0.195172	0.351817		0.453011	1

b) Ratio of angles of $\eta_{i,j}$, $\eta_{i,k}$ and $\eta_{i,R}$.

Table 10 :Value of components of eigenvector from the chosen principal components of AEMR and Rest(P.C1) run, L PRC mid centered DFC.

	Eigen V	Rest (P.C1)
L AG pst	-0.08188	0.134791
R AG pst	-0.21329	0.17767
PCC inf	0.486891	0.558208
L PHC pst	0.344874	0.287898
R PHC pst	0.301275	0.394647
R PRC mid	-0.00062	-0.00199
RSC	0.497741	0.41289
RSC pst	0.503278	0.479119

Table 11: Angle between the chosen principal components of AEMR runs and their eigenvector V, L PRC mid centered DFC.

Run \ Eigen V	Angle (°)
Run1(P.C1)	7.71
Run2(P.C1)	12.56
Run3(P.C1)	8.98

Figure m: PRC mid L centered DFC map of DiFuMo1024-dim brain atlas-based ROI marks

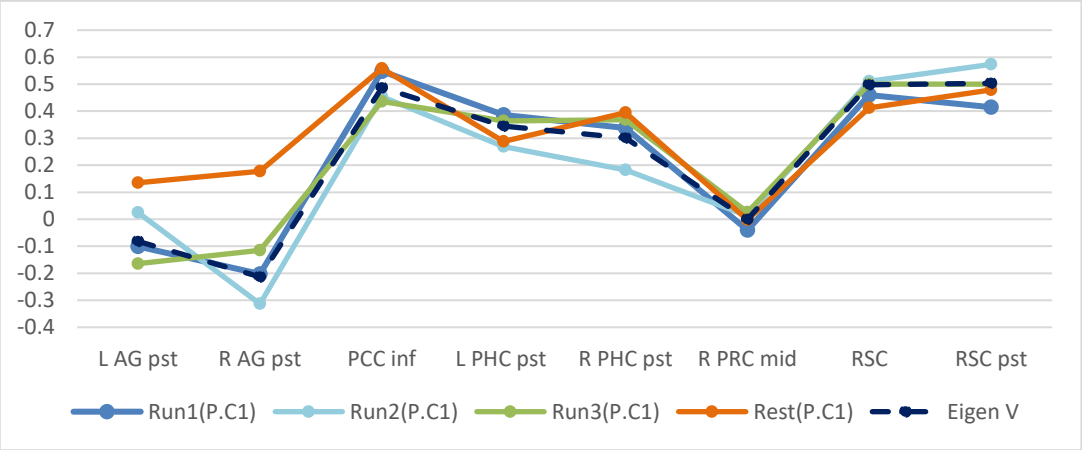

Figure n: DMN from each ROI marks

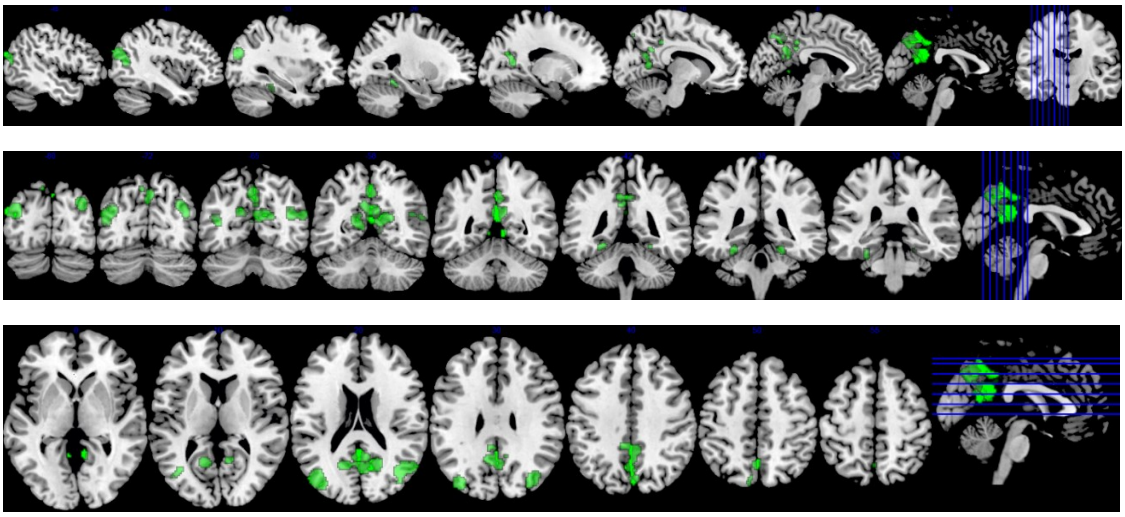

Green: The DMN defined with ROI marks by ICA

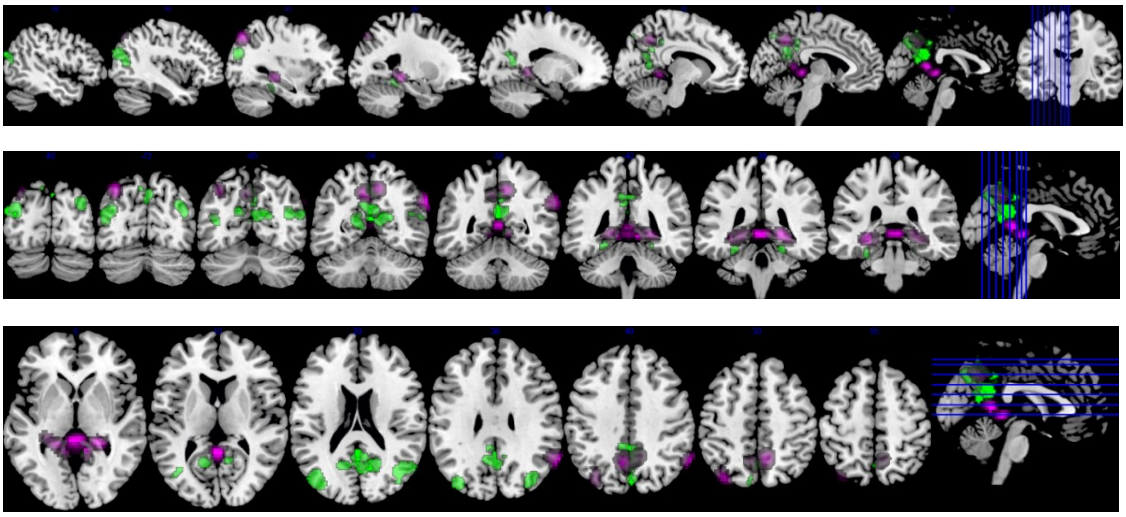

Pink: The DMN defined with DiFuMo1024-dim ROI marks

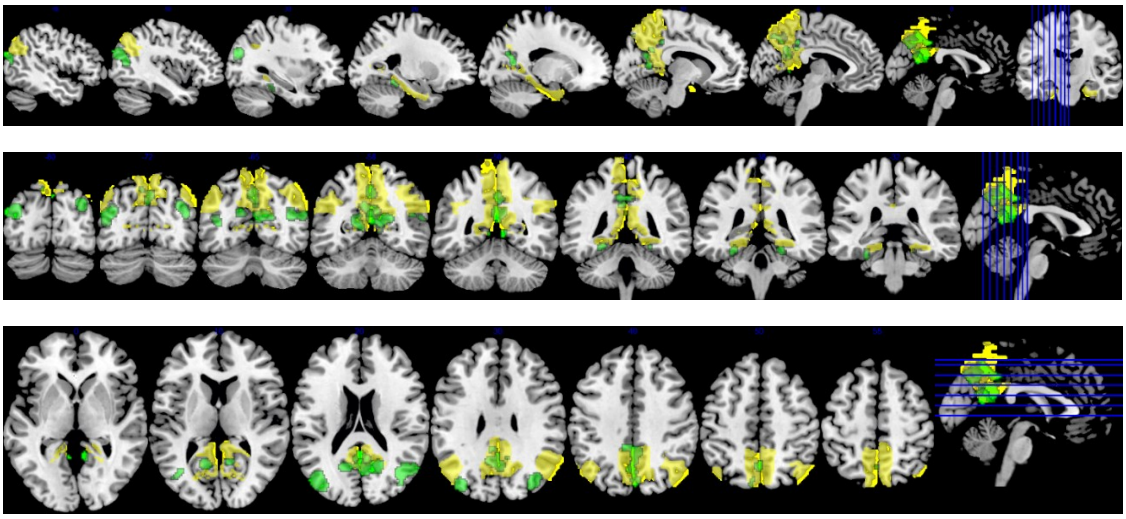

Yellow: The DMN defined with AAL brain atlas ROI marks (with Brodmann RSC)

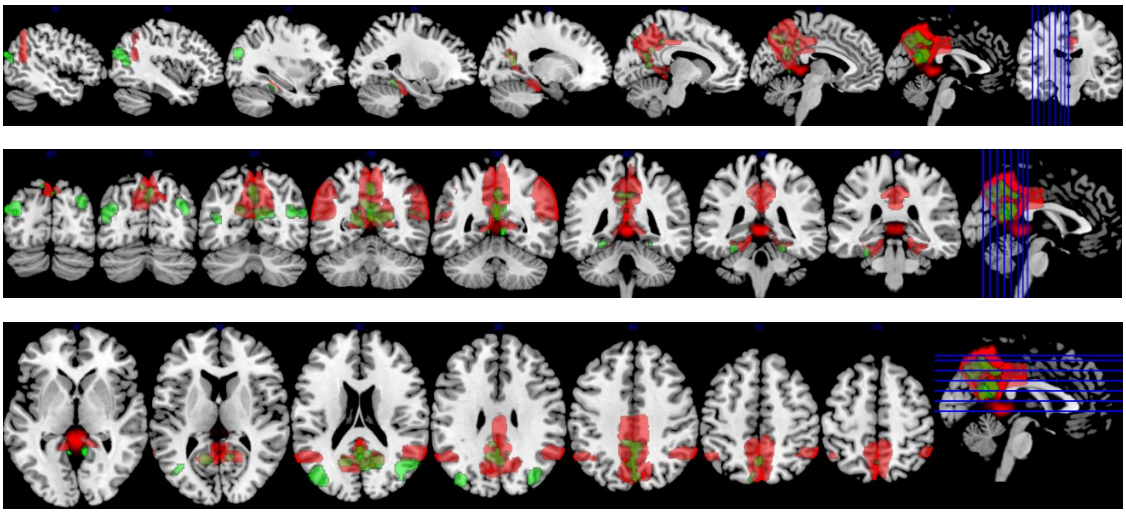

Red: The DMN defined with FSL Harvard-Oxford brain atlas ROI marks (with DiFuMo256-dim RSC)

According to the current results, I would like to suggest that individual ICA-based ROI marks are the most relevant choice for the DMN to perform a one-ROI-centered DFC analysis on it. fMRI data has a high spatial resolution (1 to 2 mm) so that different ROI marks give different BOLD time series of the ROIs. The one-ROI-centered DFC analysis detects the changes of the functional correlation for the given time course without taking its average over the entire time. When analysis of the BOLD time series is done by taking the average over the entire time, only the consistently and highly active brain voxels for the time are chosen for analysis. However, the DFC detects the temporal variance of functional correlation between brain regions. Therefore, it assumes to be performed explicitly on the functionally correlated brain regions, or the brain network. If ROI marks do not present the real brain network but contain other brain regions having small or no functional correlation with the centered ROI of the brain network, the result of one-ROI-centered DFC analysis cannot be well valid. The difference of the DMN from ICA-based ROI marks and other ROI marks was presented in Figure n. The two structure-based brain atlases, AAL and FSL Harvard-Oxford brain atlases offer good reference of ROI marks for many fMRI studies, but not for one-ROI-centered DFC analysis which requires exact ROI marks of individuals. The probability distributions of angles from the AAL and FSL Harvard-Oxford brain atlas were closely fit to the normal distribution except the very end of their tails (Figure j). This is well contrasted with those of ICA-based ROI marks and DiFuMo1024-dim brain atlas-based ROI marks.

The amount of explained variance by the first three principal components of the one-ROI-centered DFC map varied depending on the types of ROI marks also (Table12). The principal components of the one-ROI-centered DFC map of the ICA-based ROI marks explained a distinctively high amount of variance by the first principal component only. Hence, it is optimal for the one-ROI-centered DFC analysis when the chosen principal components of AEMR runs are the first principal components. I call the preferred direction described by the chosen principal components as the preferred dynamical feature of the DMN. The current analysis result of the single case study showed that the PCC centered DFC map and the R PHC centered DFC map defined based on the DMN extracted using ICA have consistent dynamical features in the AEMR state (Table). Also, it was shown that the dynamical feature in the AEMR state is distinguished from that of the resting state.

Table 12: Amount of variance explained by each principal component

(%)	Run1	Run2	Run3	Rest
P.C1	70.08	69.68	57.40	68.60
P.C2	14.16	13.91	16.40	13.96
P.C3	7.89	6.73	10.14	6.62
P.C4	3.40	5.20	8.85	4.93
P.C5	2.96	2.88	4.09	3.63
P.C6	1.51	1.60	3.12	2.25

a) PCC centered ROI map: ICA based ROI marks

(%)	Run1	Run2	Run3	Rest
P.C1	22.74	34.40	26.54	27.27
P.C2	21.57	20.75	21.22	19.24
P.C3	17.33	14.13	15.97	17.32
P.C4	14.32	11.42	13.17	11.56
P.C5	11.37	8.77	11.61	10.63
P.C6	8.81	7.85	6.24	8.69
P.C7	3.85	2.67	5.25	5.30

b) PCC centered ROI map: ICA based sphere shaped ROI marks

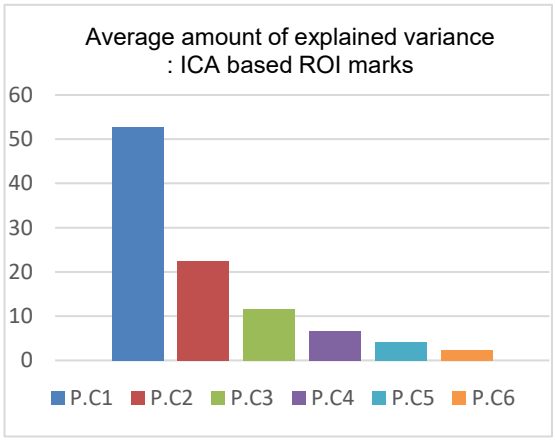

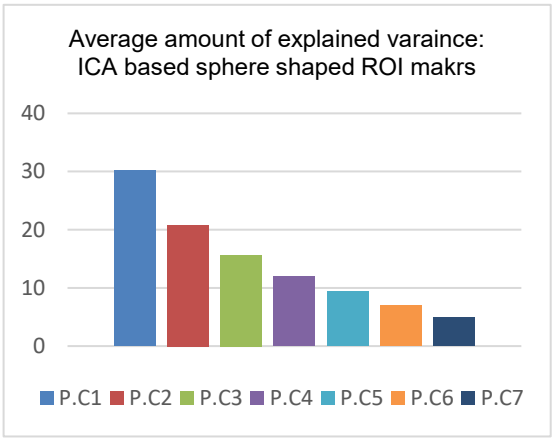

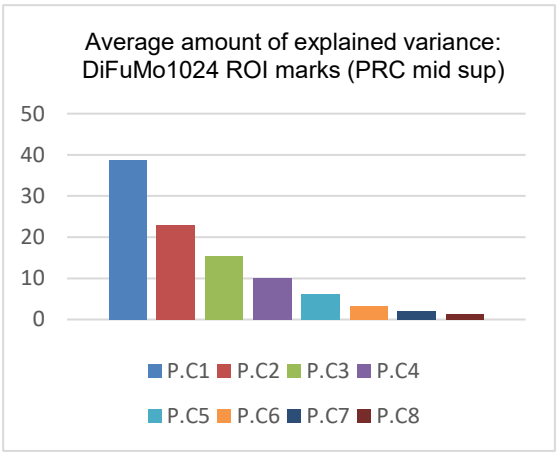

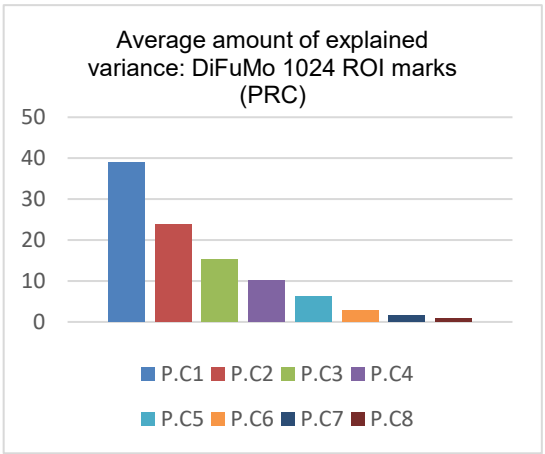

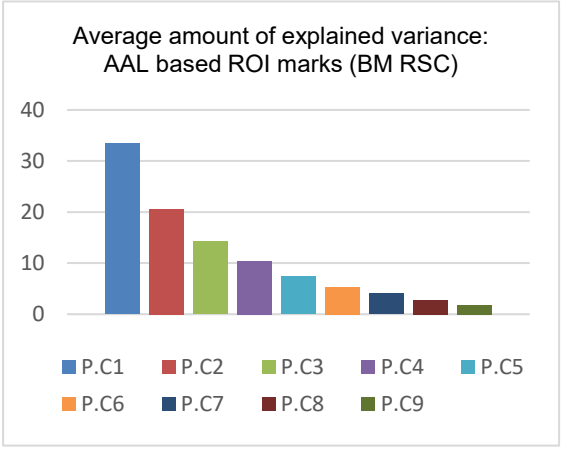

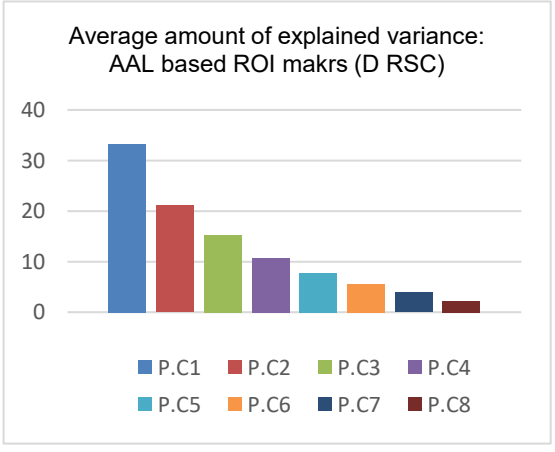

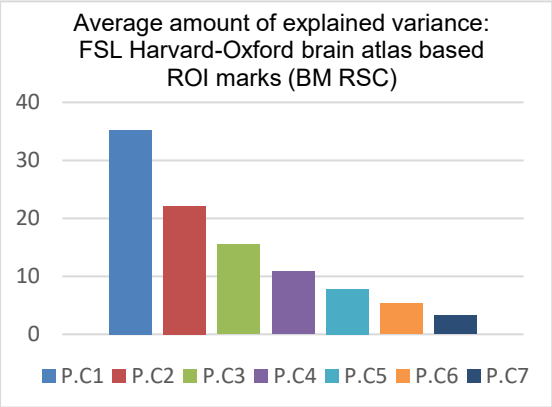

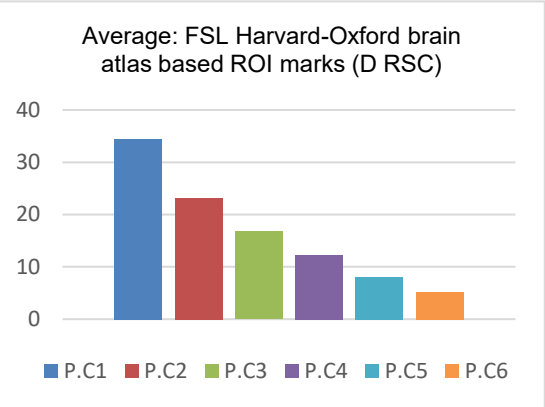

Lastly, the distribution of angles and the distribution of the amount of explained variance by the first three principal components of one-ROI-centered DFC maps from ICA-based sphere-shaped ROI marks were contrasted to the result from ICA-based ROI marks (Table 13, Figure o). Even the sphere-shaped ROI marks were created at the peak voxels of ICA-based ROI regions, they only contained the information from a small part of the entire DMN. It means that the dynamical feature of a one-ROI-centered brain network can be defined consistently only in the whole entity of brain regions which are functionally meaningful units.

Table 13: PCC centered DFC analysis result of the DMN from ICA based sphere shaped ROI marks

Angle(°)	**Run1(P.C1)**	**Run2(P.C1)**	**Run3(P.C1)**	**Rest(P.C1)**	
Run1(P.C1)		44.68	59.42	58.46	
Run2(P.C1)	44.68		29.95	33.37	
Run3(P.C1)	59.42	29.95		37.16	
Mean		$\bar{\eta} = 44.68$		$\bar{\eta}_{all} = 43.84$	$\frac{\bar{\eta}}{\bar{\eta}_{all}} = 1.02$

a) Angle between chosen principal components from each run

Ratio $(r_{i,R})$	**Run1(P.C1)**	**Run2(P.C1)**	**Run3(P.C1)**	**Rest(P.C1)**	**Total**
Run1(P.C1)		0.274837	0.365509	0.359654	1
Run2(P.C1)	0.41367		0.277345	0.308985	1
Run3(P.C1)	0.469573	0.236727		0.2937	1

b) Ratio of angles of $\boldsymbol{\eta_{i,j}}$, $\boldsymbol{\eta_{i,k}}$ *and* $\boldsymbol{\eta_{i,R}}$

Table 14: Value of components of eigenvector from the chosen principal components of AEMR and Rest (P.C1) run, PCC centered DFC map, ICA based sphere shaped ROI

	Eigen V	Rest (P.C1)
L AG	0.520103	0.19498
R Ag	0.019295	0.644911
L PHC	0.351014	0.479691
R PHC	0.351508	0.452907
PRC	0.582043	0.326825
L RSC	0.400983	0.054477
R RSC	0.453509	-0.03259

Table 15: Angle between the chosen principal components of AEMR runs and their eigenvector V, PCC centered DFC map, ICA based sphere shaped ROI

Run \ Eigen V	Angle (°)
Run1(P.C1)	35.34
Run2(P.C1)	14.71
Run3(P.C1)	26.56

Figure o: PCC centered DFC map of ICA based sphere shaped ROI marks

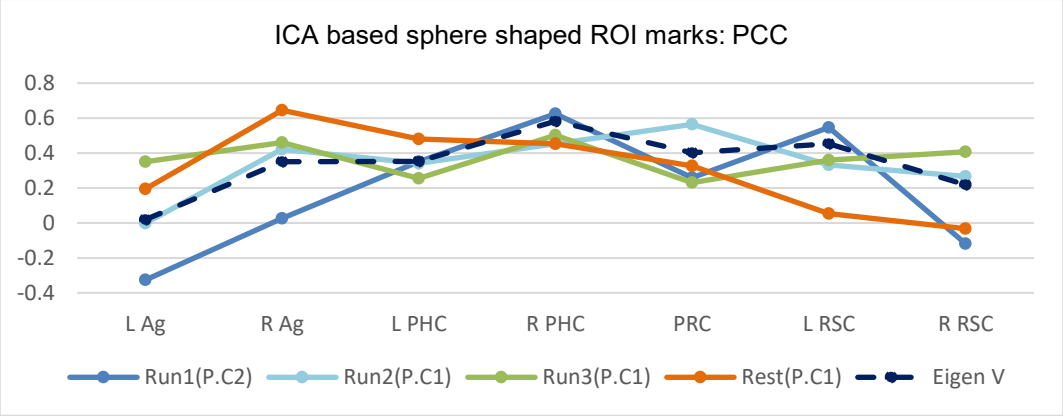

7.2 Group Study

7.2.1 Behavior

The verbal statements of the morning routine of seven subjects are attached in Appendix B. Subjects described that they had encountered more details of their morning routine by repeatedly retrieving it in the three times retrieval trials in silence. According to the recorded time per trial, a tendency was observed that the time of retrieval is increased for the later trials (Table17). However, subjects could retrieve their morning routine with consistency in time. The mean time and the standard deviation of each subject are reported in Table 17. In the case of subject 05, she/he stated that the second and third trials were comparable at the level of detail of the morning routine, but the first trial was done more abstractly. In a verbal statement session, subjects described their behaviors with involved objects within a location. The successive sequences could be categorized by location as it was in the case of the Blind Lady. The difference from the single case was that subjects could describe more episodes within a short time, which is around 5 minutes on average.

When subjects described more details in a verbal statement session, they spent more time retrieving their morning routine in silence. It could be connected to the level of the vividness of the reconstructed internal world. The more details in an episode require the longer inspection time of an episode when it is assumed that the amount of memory that one can retrieve for a given time is even between subjects. The vividness of the reconstructed internal world would be higher when there are more details of an episode. Consequently, one could tell that the subjects who could describe more details of their morning routine experienced their internal world more vividly. Table 16 is an example of verbal statements from two subjects. How detailed their memory was, for the time from when a subject wakes up and leaves from a bedroom, compared based on the verbal statements (Table 16). Subject 06 described her/his morning routine without circumstances. On the other hand, subject 07 described her/his morning routine with circumstances, the type of alarm, and motivations of behaviors. The mean time of the retrieval in the silence of subject 06 is 3 minutes 42 seconds, and of subject 07 is 6 minutes 10 seconds.

Table 16: Examples of verbal statements of subjects

Subject 06	**Subject 07**
When I wake up, first I check I close my alarm. And then I check my phone if there is a message from someone. And then I stretch my legs. Then I woke up, I wake up and wear my slippers and I wear my sweatshirt. And then I go to the bathroom.	*So, my morning starts with an alarm clock which is actually wristband which goes off because I don't want to wake up my daughter and girlfriend at 5:45. Then I tried to, I tried to get up and grab my clothes and sneak out of the room without waking up the two girls. And before I leave the room, I have to switch on the camera of the baby phone above my daughter's bed so that I can hear her when she wakes up then get out. And then I go to the living room.*

Table 17: Three trials of the morning routine retrieval in silence

Subject	**1st**	**2nd**	**3rd**	**Mean**	**S. D**
01	4 min 02 sec	4 min 01 sec	4 min 10 sec	4 min 4 sec	2 sec
02	7 min 03 sec	8 min 48 sec	7 min 28 sec	7 min 46 sec	25 sec
03	4 min 51 sec	5 min 58 sec	6 min 18 sec	5 min 42 sec	21 sec
04	3 min 11 sec	3 min 13 sec	3 min 44 sec	3 min 27 sec	9 sec
05	4 min 47 sec	9 min 09 sec	9 min 33 sec	7 min 50 sec	1 min 14 sec
06	3 min 03 sec	3 min 19 sec	4 min 44 sec	3 min 42 sec	25 sec
07	6 min 16 sec	6 min 06 sec	6 min 08 sec	6 min 10 sec	2 sec

7.2.2 fMRI Data

The data of seven subjects were analyzed with the same three steps suggested in the single case study. In most cases, the first principal component of each one-ROI-centered DFC map was chosen as the principal components fulfilling the conditions suggested in the three steps of analysis (Table 18).

Table 18: Chosen principal component and percent of variance that it explains, i-th component (%)

PCC	**Sub01**	**Sub02**	**Sub03**	**Sub04**	**Sub05**	**Sub06**	**Sub07**
Run1	1(68.83)	1(74.79)	2(25.38)	1(64.40)	1(63.13)	1(36.39)	1(65.54)
Run2	1(59.82)	1(79.19)	1(40.27)	1(68.46)	1(69.18)	1(53.90)	1(63.37)
Run3	1(49.43)	1(62.90)	1(38.91)	1(61.65)	1(58.45)	1(53.82)	1(58.22)

L AG							
Run1	3(22.33)	1(40.74)	1(36.03)	1(48.71)	2(25.77)	1(45.99)	1(45.27)
Run2	1(50.88)	1(42.83)	1(45.47)	1(49.12)	1(46.64)	1(54.35)	1(35.08)
Run3	1(37.77)	1(41.03)	1(49.24)	1(41.97)	2(28.14)	1(62.71)	1(38.61)
R AG							
Run1	1(37.21)	2(32.59)	1(40.06)	1(50.46)	2(23.23)	1(47.20)	1(56.76)
Run2	1(50.98)	1(41.29)	1(43.74)	1(47.26)	1(51.23)	1(54.80)	1(40.03)
Run3	2(28.07)	1(46.78)	1(53.65)	1(45.39)	1(40.66)	1(54.34)	1(31.00)
L PHC							
Run1	1(57.53)	1(42.86)	2(27.74)	1(48.99)	1(39.34)	1(48.49)	1(44.99)
Run2	1(64.75)	1(47.47)	1(41.48)	1(46.83)	1(55.44)	1(38.92)	1(63.99)
Run3	1(50.32)	1(44.55)	1(40.10)	2(23.91)	1(46.78)	1(57.21)	1(51.50)
R PHC							
Run1	1(53.23)	1(59.03)	2(26.15)	1(61.45)	1(61.79)	1(42.80)	1(50.25)
Run2	1(54.78)	1(63.92)	1(40.28)	1(62.55)	1(64.94)	1(40.96)	1(56.13)
Run3	1(56.54)	1(67.47)	1(42.30)	1(63.98)	1(51.50)	1(54.57)	1(57.11)
PRC							
Run1	1(37.59)	1(45.75)	1(40.28)	1(66.15)	1(48.37)	1(42.82)	2(30.11)
Run2	1(45.57)	1(49.75)	1(51.72)	1(70.57)	1(45.52)	2(20.83)	1(41.00)
Run3	2(25.34)	1(62.94)	1(43.27)	1(69.70)	2(29.56)	2(29.76)	1(35.83)
L RSC							
Run1	1(44.09)	1(37.98)	1(39.22)	1(45.59)	1(48.79)	1(47.83)	1(38.33)
Run2	1(45.71)	1(49.47)	1(47.68)	1(52.01)	1(53.20)	1(45.27)	1(36.84)
Run3	1(39.21)	2(24.43)	1(42.23)	1(44.55)	1(37.31)	1(56.29)	2(29.30)
R RSC							
Run1	1(44.20)	2(31.50)	1(33.92)	1(46.11)	1(38.57)	1(45.98)	1(41.58)
Run2	1(45.00)	2(21.48)	1(56.15)	1(53.50)	1(45.23)	1(48.18)	1(39.36)
Run3	1(40.50)	2(21.50)	1(44.93)	1(48.39)	1(51.46)	1(59.10)	2(23.27)

The ratio between two mean angles without and with the angles between the resting state and the AEMR runs, $\frac{\bar{\eta}}{\bar{\eta}_{all_n}}$ (n = 1, …,7) were calculated for individual subjects. When the mean of $\frac{\bar{\eta}}{\bar{\eta}_{all_n}}$ in each one-ROI-centered DFC map of seven subjects was calculated, the minimum among different one-ROI-centered DFC maps was found in the PCC-centered DFC map (Table 19). The mean of $\frac{\bar{\eta}}{\bar{\eta}_{all_n}}$ in R PHC-centered DFC maps and in the L RSC-centered DFC maps also were close to the mean of the PCC-centered DFC maps. In the case of the R PHC-centered DFC map, it was affected largely by the $\frac{\bar{\eta}}{\bar{\eta}_{all_4}}$, the ratio from the subject 04. The mean of $\frac{\bar{\eta}}{\bar{\eta}_{all_n}}$ without the smallest value is 0.87 for the PCC-centered DFC maps, 0.88 for the L RSC-centered DFC maps, and 0.89 for the R PHC-centered DFC maps. Even though the effect from the outlier is considered, still a dynamical feature of the PCC-, the L RSC- and the R PHC-centered DFC maps showed a relatively large difference in two different mental states.

Table 19: Ratio of the mean angles of AEMR runs to that of AEMR runs and resting state run

Ratio ($\frac{\bar{\eta}}{\bar{\eta}_{all_n}}$)	Sub01	Sub02	Sub03	Sub04	Sub05	Sub06	Sub07	Mean
L AG	1.18	1.01	0.91	0.8	1.01	0.8	1.05	0.96
R AG	1.13	0.73	1.14	0.89	1.13	0.81	1.01	0.98
PCC	1.04	0.72	0.73	1.08	0.72	0.93	0.53	0.82
L PHC	0.7	1.06	0.75	1.03	1.11	1.06	0.84	0.94
R PHC	1.1	0.64	0.84	0.49	0.85	1.05	0.88	0.83
PRC	1.16	1.05	0.82	0.88	1.09	1.05	0.68	0.96
L RSC	1.21	1.05	0.73	0.49	0.65	0.99	0.67	0.83
R RSC	1.2	0.9	0.74	0.85	1.03	0.88	0.94	0.93

The parahippocampal cortex and the retrosplenial cortex have an anatomical connection between them and are closely related to the function of spatial navigation and the contextual association (Aminoff, Kveraga, & Bar, 2013; Burgess, 2006; Epstein, 2008). Thus, the result is well matched to the known functions of these two areas; however, it is needed to explain why the difference in a dynamical feature was not observed in the bilateral parahippocampal cortex and the retrosplenial cortex but observed only one side of each cortex. One of the known functions of the right parahippocampal cortex is related to spatial memory. It was studied that patients with lesions in the right parahippocampal cortex were impaired on spatial memory tasks (Aguirre, Detre, Alsop, & D'Esposito, 1966; Bohbot, et al., 1998; Habib & Sirigu, 1987; Ploner, et al., 2000). In the case of the left retrosplenial cortex, researchers have suggested that it may process general episodic memory rather than spatial memory (Maguire, 2001; Mitchell, Czajkowski, Zhang, Jeffery, & Nelson, 2018). Lesion studies with humans showed that patients having damages in the left retrosplenial cortex were specifically impaired on verbal memory tasks (Kim, et al., 2007; McDonald, Crosson, Valenstein, & Bowers, 2001). However, it is hard to say that the number of studies of the isolated unilateral parahippocampal cortex and the retrosplenial cortex is enough to conclude their functions yet.

Despite the lack of understanding of exact functions of the unilateral parahippocampal cortex and retrosplenial cortex, their known functions of bilateral cortices are deeply related to episodic memory retrieval (Aminoff, Kveraga, & Bar, 2013). The verbal statements of the morning routine proved that indeed subjects should have used an internal image of a location where episodes happen. Also, it is important to know the order of episodes to successfully retrieve the morning routine and in general episodic memory. Consequently, the coherence of the dynamical feature from the R PHC centered and the L RSC centered DFC map between three AEMR runs and their inconsistency to the resting state run is what one could expect. It proves that one-ROI-centered DFC analysis is an effective analysis method to see changes in a brain network depending on the mental state.

In the case of the PCC-centered DFC map, its correlation to the behavioral result was found. Subjects having relatively small $\frac{\bar{\eta}}{\bar{\eta}_{all_n}}$ (n = 2,3,5,7, sub02, sub03, sub05, sub07) in the PCC-centered DFC map also spent a relatively long time (> 5 minutes) to retrieve their morning routine in silence (Table 17, Table 19). The posterior cingulate cortex is the representative brain region of the DMN. Its role as a functional and structural hub to connect brain regions fast and effectively is well known (De Pasquale, et al., 2012; Leech & Sharp, 2014; van den Heuvel & Sporns, 2013). When it is assumed that different mental states are realized with different configurations in the connectivity of a brain network, it should occur via the hubs. The current result of the PCC-cen-

tered DFC map fits well with this expectation. At the same time, the correlation between the behavioral result and the analysis on the PCC-centered DFC map implies that the vividness of the reconstructed internal world could bring changes in its dynamical feature (Table 16). Subjects were asked not to focus on any specific idea or thoughts, but to take rests for the resting state run. On the other hand, subjects should have focused on the reconstructed memory in their internal world for the three runs of AEMR states. Consequently, the clear experience of the internal world might have caused the changes in the dynamical feature of functional connectivity between the posterior cingulate cortex and other brain regions in the DMN.

The angles of the chosen principal components of three AEMR runs to their eigenvector were calculated to see how much the three runs are parallel (Krzanowski, 1979) (Figure p). In the case of the PCC-centered DFC maps and the R PHC-centered DFC maps, chosen principal components of three runs were aligned in parallel mostly (Table 20). For the case of the L RSC-centered DFC map, the three runs of AEMR are less parallel than them. It implies that the spatial memory and the clear experience in the internal world have the most consistent dynamical feature in the three runs of an AEMR state. The directions of variance of functional correlations of the left retrosplenial cortex to other brain regions from three AEMR runs were not coherent as much as the case of the posterior cingulate cortex and the right parahippocampal cortex, but their discrepancy to the resting state one was large as much as other two brain regions.

Table 20: Mean angles of three AEMR runs to their eigenvector in one ROI-centered DFC map (Group)

	PCC	L AG	R AG	L PHC	R PHC	PRC	L RSC	R RSC
Angle (°)	10.29	16.48	17.39	14.39	10.00	16.45	15.86	17.17

Figure p: Angles of chosen principal components of AEMR runs to their eigenvector

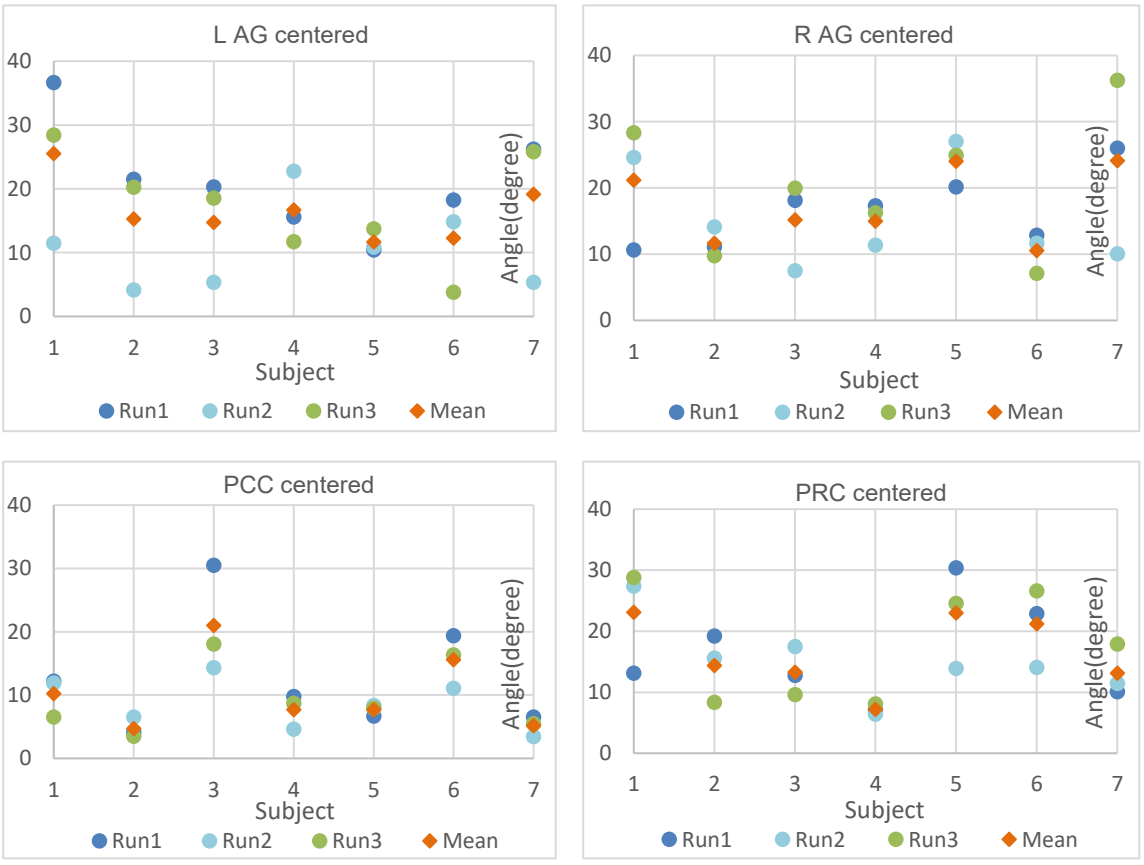

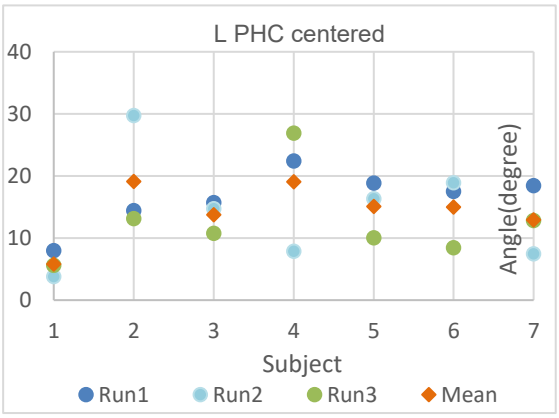
L PHC centered
40
30
20
10
0
1
2
3
4
5
6
7
Subject
Angle(degree)
Run1
Run2
Run3
Mean

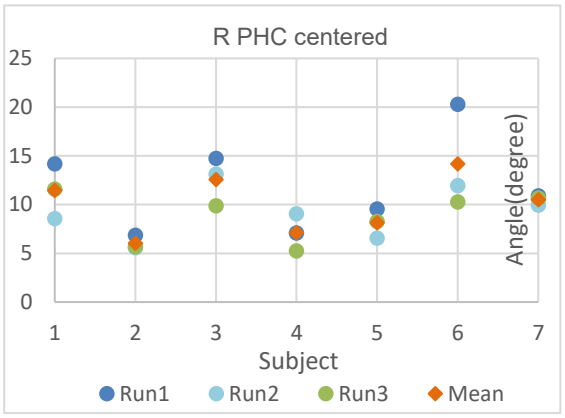
R PHC centered
25
20
15
10
5
0
1
2
3
4
5
6
7
Subject
Angle(degree)
Run1
Run2
Run3
Mean

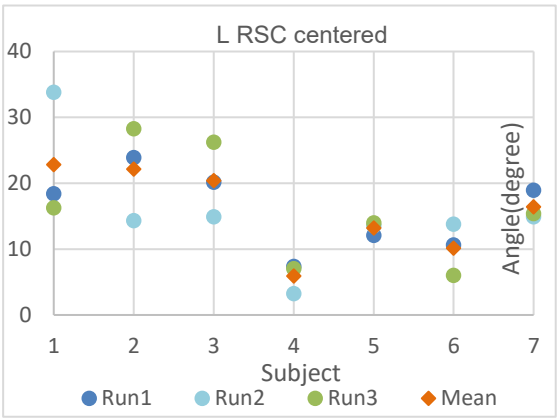
L RSC centered
40
30
20
10
0
1
2
3
4
5
6
7
Subject
Angle(degree)
Run1
Run2
Run3
Mean

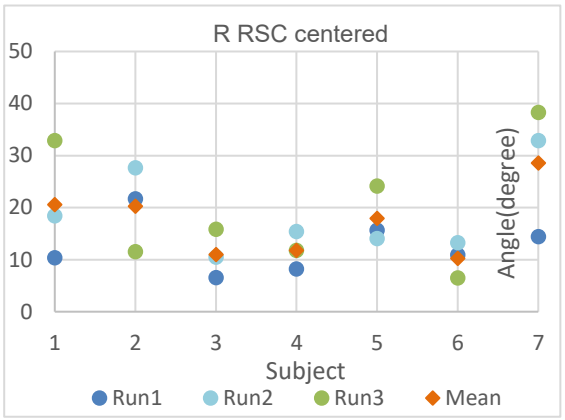
R RSC centered
50
40
30
20
10
0
1
2
3
4
5
6
7
Subject
Angle(degree)
Run1
Run2
Run3
Mean

8. Discussion

The current study aimed to compare temporal characteristics of two different mental states, the AEMR state and the resting state sharing the same spatial activity pattern called the DMN. Temporal characteristics of BOLD signals collected by fMRI have a highly nonlinear and complex correlation to its neuronal substrate (Logothetis & Wandell, 2004; Ogawa, Lee, Nayak, & Glynn, 1990). Due to the complexity, their temporal characteristics are close to stochastic dynamics. Therefore, to find the explicit dynamics of mental states realized in the DMN and to compare them is barely possible. However, by taking a point of view of the self-organizing system, a chaotic complex system could be explained as an approximately deterministic dynamic system (Ashby, 2017). Hence, the new analysis method to approximate the stochastic dynamics of BOLD signals to a deterministic dynamic system was suggested, called the one-ROI-centered DFC analysis. It describes how to approximate the functionally correlated brain regions to a deterministic dynamic system, in the sense that consistent dynamical features are observed for the same mental state. The complexity gets reduced by setting one ROI as a center of the DFC map. After this step, the dynamical feature of variance in functional connectivity between the centered ROI and other brain regions is defined. As a result, the temporal variance of a one-ROI-centered DFC map how the dynamic functional connectivity of the center ROI changes in different mental states. Then, by applying PCA to one-ROI-centered DFC maps, their multidimensional variance is represented with principal components. The first three principal components explain around 70 to 80 percent of the variance of one-ROI-centered DFC maps on average, so one could say the most variance of a one-ROI-centered DFC map is encoded in those first three principal components. The similarity between principal components from three AEMR runs, and the resting state run was calculated by measuring angles between them using their loadings. Small angles mean the direction of variance of functional connectivity in a one-ROI-centered map from different runs aligned nearly parallel. It means that the center brain region has a preferred configuration of functional connectivity represented with the loadings in the brain network to encode variances. In other words, dynamical features of one-ROI-centered maps from different runs are consistent if their major principal components are similar. Following the three steps of analysis to find meaningfully similar principal components between three AEMR runs and the resting state run, it was shown that the PCC, the R PHC, and the L RSC centered DFC map of the DMN have consistent dynamical features in the same mental state. Not only that, but they also have different dynamical features in different mental states. In addition, the most appropriate method to define the DMN for an individual was examined in the single case study. The outcome tells independent spatial component-based ROI marks are recommendable to catch the individual's DMN than predefined brain atlases-based ROI marks.

The parahippocampal cortex and the retrosplenial cortex are brain regions responsible for the contextual association, including spatial navigation and episodic memory (Aguirre, Detre, Alsop, & D'Esposito, 1966; Aminoff, Kveraga, & Bar, 2013; Bohbot, et al., 1998; Maguire, 2001). The verbal statements of subjects showed that they retrieved their morning routine as a sequence of episodes. Each episode happened in a specific spatial background, and the movement following the changes of a spatial background connected two episodes. To perform it, the spatial navigation by recognizing the topography of a space may be processed by the right parahippocampal cortex and the global connection between episodes may be processed by the left retrosplenial cortex. Due to the lack of understanding of the exact delineation of the functions of unilateral parahippocampal cortex and retrosplenial cortex, it is limited to be a speculation. Regardless of the expla-

nation about their exact function, the difference between the memory retrieval state and the resting state is related to the existence of causality in mental imagery (Eichenbaum, 2001; Tulving, 2002). The inconsistency between the two mental states, which was found from their one-ROI-centered DFC analysis, tells the following. It is indeed possible to detect the changes of a brain network in different mental states via one-ROI-centered DFC analysis.

The common function of the DMN is to construct the internal world (Buckner & Carroll, 2007; Hassabis & Maguire, 2007). The coherence between the behavioral result and the PCC-centered DFC analysis result implies that clear experience of the internal world could decide the dynamical feature of functional connectivity between the posterior cingulate cortex and other brain regions in the DMN. At the same time, the posterior cingulate cortex is a well-known functional and structural hub (De Pasquale, et al., 2012; Leech & Sharp, 2014; van den Heuvel & Sporns, 2013). Research on brain networks have proposed that the role of functional hubs is mainly related to the enhancement of the efficiency of connection between brain regions by forming small world networks (Bassett & Bullmore, 2006; Latora & Marchiori, 2001). Following the result of the current study, it was possible to observe the changes in dynamical features of the DMN. This observation might be expanded to the general mechanism of brain networks and functions of hubs. The dynamic functional connectivity of a hub has a particular configuration depending on the mental state when the non-hub brain regions share their locally processed information via the hub to form high-level perception and cognition. Cole and colleagues (2013) tested a similar idea that the configuration of the functional connectivity could change with the different mental states with a task fMRI experiment (Cole, et al., 2013). The frontoparietal network has been known for its contribution to cognitive control or executive function (Niendam, et al., 2012). Cole et al. reported that the functional connectivity between the hubs of the frontoparietal network and 264 functional nodes in the entire brain changed according to given tasks.

In the case of AEMR and resting state, there are no observable tasks from outside designed for analysis of the collected BOLD signals. These mental states purely leave the DFC analysis to depend on the measured BOLD signals having the innate stochastic property. Briefly, there is no complexity reduction at the experimental level offered by an experimental design. Therefore, one needs to find out how to reduce its complexity at the analysis level to approximate the BOLD signals to a deterministic dynamic system. For that, one-ROI-centered DFC analysis reduces the dimension of data by reorganizing it as the variance of correlation of one brain region (the center ROI) and the other regions in the brain network. Then, the principal components were calculated to describe the direction of variance of functional correlations. One-ROI-centered DFC analysis could be applied to study neuronal substrates of the mental state without external intervention or control from experimenters. In everyday life, our mental state is freely flowing without explicit control from third parties most of the time. However, this natural mental state has acted as an obstacle to observing human brain function due to the lack of control over it to reduce its complexity. The suggested one-ROI-centered DFC analysis is not only about the complexity reduction of data coming from the biophysical structure of the BOLD signals, but also about how to analyze data collected from the mental states under the condition that is close to reality.

On the other hand, the limits of the current study should be considered carefully before concluding this thesis. First, the number of subjects used in the two experiments is not enough to generalize the current result. Therefore, the following group study with more subjects and the same experimental setup should be performed to conclude that one-ROI-centered DFC analysis shows the variation of mental states of the DMN. There is also a limit coming from the choice of ROIs. The medial prefrontal cortex was excluded from the region of interest, due to its diverse spatial and

functional range of definition in the DMN. Further study to confine its pertinent spatial and functional range is necessary to include it in the current study. Lastly, PCA only represents a linear structure of the data distribution. In the case of non-linearly distributed data, it does not reveal the true distribution pattern of the data. PCA has been mainly used to reduce the complexity of the data before further in-depth analysis. Consequently, to apply non-linear time series analysis on the one-ROI-centered DFC map and compare this result with that of the suggested one-ROI-centered DFC analysis would be interesting to understand the neuronal substrate of the construction of the internal world.

fMRI is a new technology to measure brain activity noninvasively. The functional activities of the human brain have been collected by fMRI with high spatial resolution. Now we know the functional roles of well-defined isolated brain regions and it helps to diagnose pathological development of neurodegenerative diseases and mental disorders. At the same time, the very fundamental questions about individual beings, who have their history and character are studied with fMRI studies too. Autobiographical episodic memory is the foundation of an individual's history and has a critical role to learn the running mechanism of the environment in which we belong. It is also the most abundant type of memory we have. The neuronal activities measured by fMRI data are implicit and phenomenological presentations of the neuronal substrate of the brain activity. Subsequently, what we find from the fMRI data does not explain explicitly how autobiographical episodic memory is formed or retrieved in the brain. The microscopic biochemical mechanism that connects each brain region according to its function should be studied and linked to the observed changes in dynamical features of the DMN. On the other hand, noninvasive methods are necessary to study human brain activity despite its limits. To look back at the history of physics would be a good analogy to contemplate the current development of neuroscience. Before modern physics, including quantum physics, special and general relativity, most knowledge of classical physics had been accumulated from phenomenological observations. Only after the beginning of the 20th century, the theoretical knowledge on the microscopic and extra macroscopic leave behind the phenomenological observations. Neuroscience is a very young science field; therefore, it needs to collect enough phenomenological observations to enlarge the general knowledge on the function of the brain to eventually reach the level of abstracting theoretical principles and mechanisms of its neuronal substrates. In this context, defining observable variables of brain networks associated with natural mental states and elaborating their observed results would help us to reach a fundamental understanding of the human brain.

References

Achard, S., Salvador, R., Whitcher, B., Suckling, J., & Bullmore, E. (2006). A resilient, low-frequency, small-world human brain functional network with highly connected association cortical hubs. *Journal of Neuroscience, 26*(1), 63-72.

Adams, R. A., Shipp, S., & Friston, K. J. (2013). Predictions not commands: active inference in the motor system. *Brain Structure and Function, 218*(3), 611-643.

Aguirre, G. K., Detre, J. A., Alsop, D. C., & D'Esposito, M. (1966). The parahippocampus subserves topographical learning in man. *Cerebral Cortex, 6*(6), 823-829.

Alexander, A. L., Lee, J. E., Lazar, M., & Field, A. S. (2007). Diffusion tensor imaging of the brain. *Neurotherapeutics, 4*(3), 316-329.

Allen, E. A., Damaraju, E., Plis, S. M., Erhardt, E. B., Eichele, T., & Calhoun, V. D. (2014). Tracking whole-brain connectivity dynamics in the resting state. *Cerebral Cortex, 24*(3), 663-676.

Allman, J. M. (1999). *Evolving brains.* New York: Scientific American Library.

Amaral, D., & Lavenex, P. (2007). Hippocampal Neuroanatomy. In P. Andersen, R. Morris, D. Amaral, T. Bliss, & J. O'Keefe, *The HIppocampus Book* (pp. 37-114). New York: Oxford.

Amaro Jr, E., & Barker, G. J. (2006). Study design in fMRI: basic principles. *Brain and Cognition, 60*(3), 220-232.

Aminoff, E. M., Kveraga, K., & Bar, M. (2013). The role of the parahippocampal cortex in cognition. *Trends in Cognitive Sciences, 17*(8), 379-390.

Andrews-Hanna, J. R., Reidler, J. S., Sepulcre, J., Poulin, R., & Buckner, R. L. (2010). Functional-anatomic fractionation of the brain's default network. *Neuron, 65*(4), 550-562.

Andrews-Hanna, J. R., Smallwood, J., & Spreng, R. N. (2014). The default network and self-generated thought: Component processes, dynamic control, and clinical relevance. *Annals of the New York Academy of Sciences, 1316*(1), 29-52.

Anticevic, A., Cole, M. W., Repovs, G., Murray, J. D., Brumbaugh, M. S., Winkler, A. M., . . . Glahn, D. C. (2014). Characterizing thalamo-cortical disturbances in schizophrenia and bipolar illness. *Cerebral Cortex, 24*(12), 3116-3130.

Aronov, D., Nevers, R., & Tank, D. W. (2017). Mapping of a non-spatial dimension by the hippocampal-entorhinal circuit. *Nature, 543*(7647), 719-722.

Ashburner, J., Barnes, G., Chen, C., Daunizeau, J., Flandin, G., Friston, K., . . . Zeidman, P. (2016). *SPM12 Manual.* London: Wellcome Trust Centre for Neuroimaging.

Ashby, W. R. (2017). Principles of the self-organizing system. In W. Buckley, *Systems Research for Behavioral Science: A Sourcebook* (pp. 108-118). New York: Routledge.

Averbeck, B. B., Latham, P. E., & Pouget, A. (2006). Neural correlations, population coding and computation. *Nature Reviews Neuroscience, 7*(5), 358-366.

Barrett, L. F., & Simmons, W. K. (2015). Interoceptive predictions in the brain. *Nature Reviews Neuroscience, 16*(7), 419-429.

Bassett, D. S., & Bullmore, E. (2006). Small-world brain networks. *The Neuroscientist, 12*(6), 512-523.

Bassett, D. S., Meyer-Lindenberg, A., Achard, S., Duke, T., & Bullmore, E. (2006). Adaptive reconfiguration of fractal small-world human brain functional networks. *Proceedings of the National Academy of Sciences, 103*(51), 19518-19523.

Bassett, D. S., Wymbs, N. F., Porter, M. A., Mucha, P. J., Carlson, J. M., & Grafton, S. T. (2011). Dynamic reconfiguration of human brain networks during learning. *Proceedings of the National Academy of Sciences, 108*(18), 7641-7646.

Bastos, A. M., Usrey, W. M., Adams, R. A., Mangun, G. R., Fries, P., & Friston, K. J. (2012). Canonical microcircuits for predictive coding. *Neuron, 76*(4), 695-711.

Baumann, N., & Stiller, S. (2005). Network Models. In U. Brandes, & T. Erlebach, *Network Analysis* (pp. 341-372). Berlin, Heidelberg: Springer.

Bechara, A., Tranel, D., & Damasio, H. (2000). Characterization of the decision-making deficit of patients with ventromedial prefrontal cortex lesions. *Brain, 123*(11), 2189-2202.

Behrens, T. E., Muller, T. H., Whittington, J. C., Mark, S., Baram, A. B., Stachenfeld, K. L., & Kurth-Nelson, Z. (2018). What is a cognitive map? Organizing knowledge for flexible behavior. *Neuron, 100*(2), 490-509.

Bell, A. J., & Sejnowski, T. J. (1995). An information-maximization approach to blind separation and blind deconvolution. *Neural Computation, 7*(6), 1129-1159.

Berger, H. (1929). Über das elektroenkephalogramm des menschen. *Archiv für Psychiatrie und Nervenkrankheiten, 87*(1), 527-570.

Binder, J. R., & Desai, R. H. (2011). The neurobiology of semantic memory. *Trends in Cognitive Sciences, 15*(11), 527-536.

Biswal, B. B., Mennes, M., Zuo, X.-N., Gohel, S., Kelly, C., Smith, S. M., . . . Milham, M. (2010). Toward discovery science of human brain function. *Proceedings of the National Academy of Sciences, 107*(10), 4734-4739.

Biswal, B., Zerrin Yetkin, F., Haughton, V. M., & Hyde, J. S. (1995). Functional connectivity in the motor cortex of resting human brain using echo-planar MRI. *Magnetic Resonance in Medicine, 34*(4), 537-541.

Boccaletti, S., Grebogi, C., Lai, Y.-C., Mancini, H., & Maza, D. (2000). The control of chaos: theory and applications. *Physics Reports, 329*(3), 103-197.

Boccaletti, S., Kurths, J., Osipov, G., Valladares, D., & Zhou, C. (2002). The synchronization of chaotic systems. *Physics Reports, 366*(1-2), 1-101.

Bohbot, V. D., Kalina, M., Stepankova, K., Spackova, N., Petrides, M., & Nadel, L. (1998). Spatial memory deficits in patients with lesions to the right hippocampus and to the right parahippocampal cortex. *Neuropsychologia, 36*(11), 1217-1238.

Bookheimer, S. (2002). Functional MRI of language: new approaches to understanding the cortical organization of semantic processing. *Annual Review of Neuroscience, 25*(1), 151-188.

Brandes, U., & Erlebach, T. (2005). Fundamentals. In U. Brandes, & T. Erlebach, *Network Analysis* (pp. 7-15). Berlin, Heidelberg: Springer.

Brett, M., Anton, J.-L., Valabregue, R., & Poline, J.-B. (2002). Region of interest analysis using an SPM toolbox [abstract]. *8th International Conference on Functional Mapping of the Human Brain*, *16*, p. 497. Sendai.

Brin, M., & Stuck, G. (2002). *Introduction to Dynamical Systems.* Cambridge,New York,Port Melbourne: Cambridge university press.

Buckner, R. L., & Carroll, D. C. (2007). Self-projection and the brain. *Trends in Cognitive Sciences, 11*(2), 49-57.

Buckner, R. L., Andrews-Hanna, J. R., & Schacter, D. L. (2008). The brain's default network anatomy, function, and relevance to disease. *Annals of the New York Academy ofSciences, 1124*, 1-38.

Buckner, R. L., Sepulcre, J., Talukdar, T., Krienen, F. M., Liu, H., Hedden, T., . . . Johnson, K. A. (2009). Cortical Hubs Revealed by Intrinsic Functional Connectivity: Mapping, Assessment of Stability, and Relation to Alzheimer's Disease. *Journal of Neuroscience, 29*(6), 1860-1873.

Bullmore, E., & Sporns, O. (2009). Complex brain networks: graph theoretical analysis of structural and functional systems. *Nature Reviews Neuroscience, 10*(3), 186-198.

Burgess, N. (2006). Spatial memory: how egocentric and allocentric combine. *Trends in Cognitive Sciences, 10*(12), 551-557.

Buzsáki, G., & Draguhn, A. (2004). Neuronal oscillations in cortical networks. *Science, 304*(5679), 1926-1929.

Buzsáki, G., Geisler, C., Henze, D. A., & Wang, X.-J. (2004). Interneuron diversity series: circuit complexity and axon wiring economy of cortical interneurons. *Trends in Neurosciences, 27*(4), 186-193.

Caballero-Gaudes, C., & Reynolds, R. C. (2017). Methods for cleaning the BOLD fMRI signal. *Neuroimage, 154*, 128-149.

Cabeza, R., Ciaramelli, E., Olson, I. R., & Moscovitch, M. (2008). The parietal cortex and episodic memory: An attentional account. *Nature Reviews Neuroscience, 9*(8), 613-625.

Calhoun, V. D., Adali, T., Pearlson, G. D., & Pekar, J. J. (2001). A method for making group inferences from functional MRI data using independent component analysis. *Human Brain Mapping, 14*(3), 140-151.

Calhoun, V. D., Adali, T., Pearlson, G., & Pekar, J. J. (2001). Spatial and temporal independent component analysis of functional MRI data containing a pair of task-related waveforms. *Human Brain Mapping, 13*(1), 43-53.

Caspers, S., Geyer, S., Schleicher, A., Mohlberg, H., Amunts, K., & Zilles, K. (2006). The human inferior parietal cortex: cytoarchitectonic parcellation and interindividual variability. *Neuroimage, 33*(2), 430-448.

Cavanna, A. E., & Trimble, M. R. (2006). The precuneus: A review of its functional anatomy and behavioural correlates. *Brain, 129*(3), 564-583.

Chang, C., & Glover, G. H. (2010). Time-frequency dynamics of resting-state brain connectivity measured with fMRI. *Neuroimage, 50*(1), 81-98.

Cole, M. W., Reynolds, J. R., Power, J. D., Repovs, G., Anticevic, A., & Braver, T. S. (2013). Multi-task connectivity reveals flexible hubs for adaptive task control. *Nature Neuroscience, 16*(9), 1348-1355.

Constantinescu, A. O., O'Reilly, J. X., & Behrens, T. E. (2016). Organizing conceptual knowledge in humans with a gridlike code. *Science, 352*(6292), 1464-1468.

Conway, M. A., & Pleydell-Pearce, C. W. (2000). The construction of autobiographical memories in the self-memory system and the developmental psychologist is focused on the nature. *Psychological Review, 107*(2), 261-288.

Corbetta, M., & Shulman, G. L. (2002). Control of goal-directed and stimulus-driven attention in the brain. *Nature Reviews Neuroscience, 3*(3), 201-215.

Cowan, N. (2008). What are the differences between long-term, short-term, and working memory? *Progress in Brain Research, 169*, 323-338.

Craik, F. I., & Lockhart, R. S. (1972). Levels of processing: A framework for memory research. *Journal of Verbal Learning and Verbal Behavior, 11*(6), 671-684.

Dadi, K., Varoquaux, G., Machlouzarides-Shalit, A., Gorgolewski, K. J., Wassermann, D., Thirion, B., & Mensch, A. (2020). Fine-grain atlases of functional modes for fMRI analysis. *NeuroImage, 221*, 117126.

Dale, A. M. (1999). Optimal experimental design for event-related fMRI. *Human Brain Mapping, 8*(2-3), 109-114.

Damaraju, E., Allen, E. A., Belger, A., Ford, J. M., McEwen, S., Mathalon, D., . . . V.D, C. (2014). Dynamic functional connectivity analysis reveals transient states of dysconnectivity in schizophrenia. *NeuroImage: Clinical, 5*, 298-308.

Dayan, P., Hinton, G. E., Neal, R. M., & Zemel, R. S. (1995). The helmholtz machine. *Neural Computation, 7*(5), 889-904.

De Pasquale, F., Della Penna, S., Snyder, A. Z., Marzetti, L., Pizzella, V., Romani, G. L., & Corbetta, M. (2012). A cortical core for dynamic integration of functional networks in the resting human brain. *Neuron, 74*(4), 753-764.

Deco, G., Kringelbach, M. L., Jirsa, V. K., & Ritter, P. (2017). The dynamics of resting fluctuations in the brain: metastability and its dynamical cortical core. *Scientific Reports, 7*(1), 1-14.

Desai, M., Kahn, I., Knoblich, U., Bernstein, J., Atallah, H., Yang, A., . . . Boyden, E. (2011). Mapping brain networks in awake mice using combined optical neural control and fMRI. *Journal of Neurophysiology, 105*(3), 1393-1405.

Desmond, J. E., & Glover, G. H. (2002). Estimating sample size in functional MRI (fMRI) neuroimaging studies: statistical power analyses. *Journal of Neuroscience Methods, 118*(2), 115-128.

Doeller, C. F., Barry, C., & Burgess, N. (2010). Evidence for grid cells in a human memory network. *Nature, 463*(7281), 657-661.

Douglas, R. J., & Martin, K. A. (2004). Neuronal circuits of the neocortex. *Annual Review of Neuroscience, 27*, 419--451.

Eguiluz, V. M., Chialvo, D. R., Cecchi, G. A., Baliki, M., & Apkarian, A. V. (2005). Scale-free brain functional networks. *Physical Review Letters, 94*(1), 018102.

Eichenbaum, H. (2001). The hippocampus and declarative memory: cognitive mechanisms and neural codes. *Behavioural Brain Research, 127*(1-2), 199-207.

Eickhoff, S. B., Stephan, K. E., Mohlberg, H., Grefkes, C., Fink, G. R., Amunts, K., & Zilles, K. (2005). A new SPM toolbox for combining probabilistic cytoarchitectonic maps and functional imaging data. *Neuroimage, 25*(4), 1325-1335.

Engel, A. K., Fries, P., & Singer, W. (2001). Dynamic predictions: oscillations and synchrony in top-down processing. *Nature Reviews Neuroscience, 2*(10), 704-716.

Epstein, R. A. (2008). Parahippocampal and retrosplenial contributions to human spatial navigation. *Trends in Cognitive Sciences, 12*(10), 388-396.

Fair, D. A., Dosenbach, N. U., Church, J. A., Cohen, A. L., Brahmbhatt, S., Miezin, F. M., . . . Schlaggar, B. L. (2007). Development of distinct control networks through segregation and integration. *Proceedings of the National Academy of Sciences, 104*(33), 13507-13512.

Feldman, J. A., & Ballard, D. H. (1982). Connectionist models and their properties. *Cognitive Science, 6*(3), 205-254.

Flandin, G., & Friston, K. J. (2008). Statistical parametric mapping. *Scholarpedia, 3*(4), 6232.

Fletcher, P. C., Frith, C. D., Baker, S. C., Shallice, T., Frackowiak, R. S., & Dolan, R. J. (1995). The mind's eye - precuneus activation in memory-related imagery. *Neuroimage, 2*(3), 195-200.

Fortunato, S. (2010). Community detection in graphs. *Physics Reports, 486*(3-5), 75-174.

Fox, M. D., & Raichle, M. E. (2007). Spontaneous fluctuations in brain activity observed with functional magnetic resonance imaging. *Nature Reviews Neuroscience, 8*(9), 700-711.

Fox, M. D., Snyder, A. Z., Vincent, J. L., Corbetta, M., Van Essen, D. C., & Raichle, M. E. (2005). The human brain is intrinsically organized into dynamic, anticorrelated functional networks. *Proceedings of the National Academy of Sciences, 102*(27), 9673-9678.

Fransson, P. (2006). How default is the default mode of brain function?: Further evidence from intrinsic BOLD signal fluctuations. *Neuropsychologia, 44*(14), 2836-2845.

Friston, K. (2010). The free-energy principle: a unified brain theory? *Nature Reviews Neuroscience, 11*(2), 127-138.

Friston, K. J., Holmes, A. P., Poline, J., Grasby, P., Williams, S., Frackowiak, R. S., & Turner, R. (1995). Analysis of fMRI time-series revisited. *Neuroimage, 2*(1), 45-53.

Friston, K. J., Holmes, A. P., Worsley, K. J., Poline, J.-P., Frith, C. D., & Frackowiak, R. S. (1994). Statistical parametric maps in functional imaging: a general linear approach. *Human Brain Mapping, 2*(4), 189-210.

Friston, K. J., Trujillo-Barreto, N., & Daunizeau, J. (2008). DEM: a variational treatment of dynamic systems. *Neuroimage, 41*(3), 849-885.

Friston, K., Frith, C., Liddle, P., & Frackowiak, R. (1993). Functional connectivity: The principal-component analysis of large (PET) data sets. *Journal of Cerebral Blood Flow and Metabolism, 13*(1), 5-14.

Friston, K., Kilner, J., & Harrison, L. (2006). A free energy principle for the brain. *Journal of Physiology-Paris, 100*(1-3), 70-87.

Garrison, K., Santoyo, J., Davis, J., Thornhill, T., Kerr, C., & Brewer, J. (2013). Effortless awareness: using real time neurofeedback to investigate correlates of posterior cingulate cortex activity in meditators' self-report. *Frontiers in Human Neuroscience, 7*, 440.

Gerstner, W., Kistler, W. M., Naud, R., & Paninski, L. (2014). 1.Introduction: neurons and mathematics. In W. Gerstner, W. M. Kistler, R. Naud, & L. Paninski, *Neuronal Dynamics: From Single Neurons to Networks and Models of Cognition* (pp. 3-25). Cambridge: Cambridge University Press.

Gerstner, W., Kistler, W. M., Naud, R., & Paninski, L. (2014). 17.3 Memory networks with spiking neurons. In W. Gerstner, W. M. Kistler, R. Naud, & L. Paninski, *Neuronal Dynamics: From Single Neurons to Networks and Models of Cognition* (pp. 442-466). Cambridge: Cambridge University Press.

Gerstner, W., Kistler, W. M., Naud, R., & Paninski, L. (2014). *Neuronal Dynamics: From Single Neurons to Networks and Models of Cognition.* Cambridge: Cambridge University Press.

Ghaem, O., Mellet, E., Crivello, F., Tzourio, N., Mazoyer, B., Berthoz, A., & Denis, M. (1997). Mental navigation along memorized routes activates the hippocampus, precuneus, and insula. *Neuroreport, 8*(3), 739-744.

Gilboa, A., Winocur, G., Grady, C. L., Hevenor, S. J., & Moscovitch, M. (2004). Remembering our past: functional neuroanatomy of recollection of recent and very remote personal events. *Cerebral Cortex, 14*(11), 1214-1225.

Gluck, M. A., & Rumelhart, D. E. (1990). *Neuroscience and Connectionist Theory (1st ed.).* New York: Psychology Press.

Goense, J. B., & Logothetis, N. K. (2008). Neurophysiology of the BOLD fMRI signal in awake monkeys. *Current Biology, 18*(9), 631-640.

Graf, P., & Schacter, D. L. (1985). Implicit and explicit memory for new associations in normal and amnesic subjects. *Journal of Experimental Psychology: Learning, Memory, and Cognition, 11*(3), 501-518.

Gray, C. M., König, P., Engel, A. K., & Singer, W. (1989). Oscillatory responses in cat visual cortex exhibit inter-columnar synchronization which reflects global stimulus properties. *Nature, 338*(6213), 334-337.

Greicius, M. D., Srivastava, G., Reiss, A. L., & Menon, V. (2004). Default-mode network activity distinguishes Alzheimer's disease from healthy aging: Evidence from functional MRI. *Proceedings of the National Academy of Sciences, 101*(13), 4637-4642.

Greicius, M. D., Supekar, K., Menon, V., & Dougherty, R. F. (2009). Resting-state functional connectivity reflects structural connectivity in the default mode network. *Cerebral Cortex, 19*(1), 72-78.

Gruber, O., & Goschke, T. (2004). Executive control emerging from dynamic interactions between brain systems mediating language, working memory and attentional processes. *Acta Psychologica, 115*(2-3), 105-121.

Gusnard, D. A., & Raichle, M. E. (2001). Searching for a baseline: functional imaging and the resting human brain. *Nature Reviews Neuroscience, 2*(10), 685-694.

Habib, M., & Sirigu, A. (1987). Pure topographical disorientation: a definition and anatomical basis. *Cortex, 23*(1), 73-85.

Hafting, T., Fyhn, M., Molden, S., Moser, M.-B., & Moser, E. I. (2005). Microstructure of a spatial map in the entorhinal cortex. *Nature, 436*(7052), 801-806.

Hagmann, P., Cammoun, L., Gigandet, X., Meuli, R., Honey, C. J., Wedeen, V. J., & Sporns, O. (2008). Mapping the structural core of human cerebral cortex. *PLoS biology, 6*(7), e159.

Halassa, M. M., & Haydon, P. G. (2010). Integrated brain circuits: astrocytic networks modulate neuronal activity and behavior. *Annual Review of Physiology, 72*, 335-355.

Hall, D. A., Haggard, M. P., Akeroyd, M. A., Palmer, A. R., Summerfield, A. Q., Elliott, M. R., . . . Bowtell, R. W. (1999). “Sparse” temporal sampling in auditory fMRI. *Human Brain Mapping, 3*, 213-223.

Hartigan, J. A., & Wong, M. A. (1979). Algorithm AS 136: A k-means clustering algorithm. *Journal of the Royal Statistical Society. Series C (applied statistics), 28*(1), 100-108.

Hassabis, D., & Maguire, E. A. (2007). Deconstructing episodic memory with construction. *Trends in Cognitive Sciences, 11*(7), 299-306.

Hebb, D. O. (2005). *The organization of behavior: A neuropsychological theory.* Mahwah: Psychology Press.

Heeger, D. J., & Ress, D. (2002). What does fMRI tell us about neuronal activity? *Nature Reviews Neuroscience, 3*(2), 142-151.

Herculano-Houzel, S. (2009). The human brain in numbers: a linearly scaled-up primate brain. *Frontiers in Human Neuroscience, 3*, 31.

Hilgetag, C.-C., Burns, G. A., O'Neill, M. A., Scannell, J. W., & Young, M. P. (2000). Anatomical connectivity defines the organization of clusters of cortical areas in the macaque and the cat. *Philosophical Transactions of the Royal Society of London. Series B: Biological Sciences, 355*(1393), 91-110.

Hill, T. L. (1986). *An Introduction to Statistical Thermodynamics.* New York: Dover Publications.

Hindriks, R., Adhikari, M. H., Murayama, Y., Ganzetti, M., Mantini, D., Logothetis, N. K., & Deco, G. (2016). Can sliding-window correlations reveal dynamic functional connectivity in resting-state fMRI? *Neuroimage, 127*, 242-256.

Hinton, G. E. (1990). Connectionist learning procedures. In Y. Kodratoff, & R. Michalski, *Machine learning An artificial intelligence approach Voume III* (pp. 555-610). San Mateo: Morgan Kaufmann.

Hochstein, S., & Ahissar, M. (2002). View from the top: Hierarchies and reverse hierarchies in the visual system. *Neuron, 36*(5), 791-804.

Honerkamp, J. (1993). *Stochastic dynamical systems: concepts, numerical methods, data analysis.* New York: John Wiley & Sons.

Honey, C. J., Kötter, R., Breakspear, M., & Sporns, O. (2007). Network structure of cerebral cortex shapes. *Proceedings of the National Academy of Sciences, 104*(24), 10240-10245.

Hopfield, J. J. (1982). Neural networks and physical systems with emergent collective computational abilities. *Proceedings of the National Academy of Sciences, 79*(8), 2554-2558.

Hopfield, J. J. (1984). Neurons with graded response have collective computational properties like those of two-state neurons. *Proceedings of the National Academy of Sciences, 81*(10), 3088-3092.

Hopfield, J. J. (2007). Hopfield network. *Scholarpedia, 2*(5), 1977.

Hopfield, J. J., & Tank, D. W. (1986). Computing with neural circuits: A model. *Science, 233*(4764), 625-633.

Hubel, D. H., & Wiesel, T. N. (1965). Receptive fields and functional architecture in two nonstriate visual areas (18 and 19) of the cat. *Journal of Neurophysiology, 28*(2), 229-289.

Hutchison, R. M., Womelsdorf, T., Allen, E. A., Bandettini, P. A., Calhoun, V. D., Corbetta, M., . . . Chang, C. (2013). Dynamic functional connectivity: promise, issues, and interpretations. *Neuroimage, 80*, 360-378.

Hyvärinen, A. (1999). Fast and robust fixed-point algorithms for independent component analysis. *IEEE Transactions on Neural Networks and Learning Systems, 10*(3), 626-634.

Hyvärinen, A., & Oja, E. (2000). Independent component analysis: algorithms and applications. *Neural Networks, 13*(4-5), 411-430.

Jaeger, H., & Haas, H. (2004). Harnessing nonlinearity: Predicting chaotic systems and saving energy in wireless communication. *Science, 304*(5667), 78-80.

Jäncke, L., Kleinschmidt, A., Mirzazade, S., Shah, N., & Freund, H.-J. (2001). The role of the inferior parietal cortex in linking the tactile perception and manual construction of object shapes. *Cerebral Cortex, 11*(2), 114-121.

Janke, G. G., L., A., Budge, M. M., Pruessner, D. S., & Collins, D. L. (2006). Symmetric atlasing and model based segmentation: an application to the hippocampus in older adults. *International Conference on Medical Image Computing and Computer-Assisted Intervention.* (pp. 58-66). Berlin, Heidelberg: Springer.

Josephs, O., & Henson, R. N. (1999). Event-related functional magnetic resonance imaging: modelling, inference and optimization. *Philosophical Transactions of the Royal Society of London. Series B: Biological Sciences, 354*(1387), 1215-1228.

Josephs, O., Turner, R., & Friston, K. (1997). Event-related fMRI. *Human Barain Mapping, 5*(4), 243-248.

Kanwisher, N., McDermott, J., & Chun, M. M. (1997). The fusiform face area: a module in human extrastriate cortex specialized for face perception. *Journal of Neuroscience, 17*(11), 4302-4311.

Kendall, M. G., & Stuart, A. (1973). *The Advanced Theory of Statistics, Volume 2: Inference and Relationship.* London: Griffin.

Kim, H.-Y. (2014). Analysis of variance (ANOVA) comparing means of more than two groups. *Restorative Dentistry & Endodontics, 39*(1), 74-77.

Kim, J. H., Park, K.-Y., Seo, S. W., Na, D. L., Chung, C.-S., Lee, K. H., & Kim, G.-M. (2007). Reversible Verbal and Visual Memory Deficits after Left Retrosplenial Infarction. *Journal of Clinical Neurology, 3*(1), 62-66.

Klein, S. B., Cosmides, L., Tooby, J., & Chance, S. (2002). Decisions and the evolution of memory: multiple systems, multiple functions. *Psychological Review, 109*(2), 306-329.

Knauff, M., Fangmeier, T., Ruff, C. C., & Johnson-Laird, P. N. (2003). Reasoning, models, and images: Behavioral measures and cortical activity. *Journal of Cognitive Neuroscience, 15*(4), 559-573.

Knierim, J. J. (2015). The hippocampus. *Current Biology, 25*(23), R1116-R1121.

Kobayashi, Y., & Amaral, D. G. (2003). Macaque monkey retrosplenial cortex: II. Cortical afferents. *Journal of Comparative Neurology, 466*(1), 48-79.

Kourtzi, Z., & Kanwisher, N. (2001). Representation of perceived object shape by the human lateral occipital complex. *Science, 293*(5534), 1506-1509.

Krzanowski, W. (1979). Between-groups comparison of principal components. *Journal of the American Statistical Association, 74*(367), 703-707.

Kucyi, A., & Davis, K. D. (2014). Dynamic functional connectivity of the default mode network tracks daydreaming. *Neuroimage, 100*, 471-480.

Kveraga, K., Ghuman, A. S., Kassam, K. S., Aminoff, E. A., Hämääinen, M. S., Chaumon, M., & Bar, M. (2011). Early onset of neural synchronization in the contextual associations network. *Proceedings of the National Academy of Sciences, 108*(8), 3389-3394.

Kwong, K. K., Belliveau, J. W., Chesler, D. A., Goldberg, I. E., Weisskoff, R. M., Poncelet, B. P., . . . Turner, R. (1992). Dynamic magnetic resonance imaging of human brain activity during primary sensory stimulation. *Proceedings of the National Academy of Sciences, 89*(12), 5675-5679.

Latora, V., & Marchiori, M. (2001). Efficient behavior of small-world networks. *Physical Review Letters, 87*(19), 198701.

Laumann, T. O., Snyder, A. Z., Mitra, A., Gordon, E. M., Gratton, C., Adeyemo, B., . . . Petersen, S. (2017). On the stability of BOLD fMRI correlations. *Cerebral Cortex, 27*(10), 4719-4732.

Lee, J. H., Durand, R., Gradinaru, V., Zhang, F., Goshen, I., Kim, D.-S., . . . Deisseroth, K. (2010). Global and local fMRI signals driven by neurons defined optogenetically by type and wiring. *Nature, 465*(7299), 788-792.

Leech, R., & Sharp, D. J. (2014). The role of the posterior cingulate cortex in cognition and disease. *Brain, 137*(1), 12-32.

Levy, R., & Goldman-Rakic, P. S. (2000). Segregation of working memory functions within the dorsolateral prefrontal cortex. *Experimental Brain Research, 133*(1), 23-32.

Lewis, C. M., Baldassarre, A., Committeri, G., Romani, G. L., & Corbetta, M. (2009). Learning sculpts the spontaneous activity of the resting human brain. *Proceedings of the National Academy of Sciences, 106*(41), 17558-17563.

Logothetis, N. K. (2008). What we can do and what we cannot do with fMRI. *Nature, 453*(7197), 869-878.

Logothetis, N. K., & Wandell, B. A. (2004). Interpreting the BOLD signal. *Annual Review of Physiology, 66*, 735-769.

Logothetis, N. K., Pauls, J., Augath, M., Trinath, T., & Oeltermann, A. (2001). Neurophysiological investigation of the basis of the fMRI signal. *Nature, 412*(6843), 150-157.

Maguire, E. (2001). The retrosplenial contribution to human navigation: a review of lesion and neuroimaging findings. *Scandinavian Journal of Psychology, 42*(3), 225-238.

Maguire, E. A., Gadian, D. G., Johnsrude, I. S., Good, C. D., Ashburner, J., Frackowiak, R. S., & Frith, C. D. (2000). Navigation-related structural change in the hippocampi of taxi drivers. *Proceedings of the National Academy of Sciences, 97*(8), 4398-4403.

Mainen, Z. F., & Sejnowski, T. J. (1995). Reliability of spike timing in neocortical neurons. *Science, 268*(5216), 1503-1506.

Malouin, F., Richards, C. L., Jackson, P. L., Dumas, F., & Doyon, J. (2003). Brain activations during motor imagery of locomotor-related tasks: A PET study. *Human Brain Mapping, 19*(1), 47-62.

Margulies, D. S., Vincent, J. L., Kelly, C., Lohmann, G., Uddin, L. Q., Biswal, B. B., . . . Petrides, M. (2009). Precuneus shares intrinsic functional architecture in humans and monkeys. *Proceedings of the National Academy of Sciences, 106*(47), 20069-20074.

Markram, H., Toledo-Rodriguez, M., Wang, Y., Gupta, A., Silberberg, G., & Wu, C. (2004). Interneurons of the neocortical inhibitory system. *Nature Reviews Neuroscience, 5*(10), 793-807.

Martin, A., & Chao, L. L. (2001). Semantic memory and the brain: structure and processes. *Current Opinion in Neurobiology, 11*(2), 194-201.

MatthewWebster. (2021, 04 27). *FSL: Atlases*. Retrieved from FSL (FMRIB Software Library): https://fsl.fmrib.ox.ac.uk/fsl/fslwiki/Atlases

McClelland, J. L., McNaughton, B. L., & O'Reilly, R. C. (1995). Why there are complementary learning systems in the hippocampus and neocortex: insights from the successes and failures of connectionist models of learning and memory. *Psychological Review, 102*(3), 419-457.

McClelland, J. L., Rumelhart, D. E., & PDP-Research-Group. (1986). *Parallel Distributed Processing* (Vol. 2). Cambridge: MIT press.

McDonald, C. R., Crosson, B., Valenstein, E., & Bowers, D. (2001). Verbal encoding deficits in a patient with a left retrosplenial lesion. *Neurocase, 7*(5), 407-417.

McKeown, M. J., Makeig, S., Brown, G. G., Jung, T.-P., Kindermann, S. S., Bell, A. J., & Sejnowski, T. J. (1998). Analysis of fMRI data by blind separation into independent spatial components. *Human Brain Mapping, 6*(3), 160-188.

Medicine, W. F., & Maldjian, J. A. (n.d.). *Software Development: Radiology Informatics and Image Processing Laboratory : Research and Faculty Labs : Wake Forest School of Medicine Research* . Retrieved from Wake Forest School of Medicine Web site: https://school.wakehealth.edu/Research/Labs/Radiology-Informatics-and-Image-Processing-Laboratory/

Meiss, J. (2007). Dynamical systems. *Scholarpedia, 2*(2), 1629.

Mensch, A., Mairal, J., Thirion, B., & Varoquaux, G. (2017). Stochastic subsampling for factorizing huge matrices. *IEEE Transactions on Signal Processing, 66*(1), 113-128.

Merzenich, M. M., Knight, P. L., & Roth, G. L. (1975). Representation of cochlea within primary auditory cortex in the cat. *Journal of Neurophysiology, 38*(2), 231-249.

Miller, E. K., & Cohen, J. D. (2001). An integrative theory of prefrontal cortex function. *Annual Review of Neuroscience, 24*(1), 167-202.

Mitchell, A. S., Czajkowski, R., Zhang, N., Jeffery, K., & Nelson, A. J. (2018). Retrosplenial cortex and its role in spatial cognition. *Brain and Neuroscience Advances, 2*, 2398212818757098.

Mori, S., & Zhang, J. (2006). Principles of diffusion tensor imaging and its applications to basic neuroscience research. *Neuron, 51*(5), 527-539.

Moscovitch, M., Rosenbaum, R. S., Gilboa, A., Addis, D. R., Westmacott, R., Grady, C., . . . Nadel, L. (2005). Functional neuroanatomy of remote episodic, semantic and spatial memory: a unified account based on multiple trace theory. *Journal of Anatomy, 207*(1), 35-66.

Moser, E. I., Kropff, E., & Moser, M.-B. (2008). Place cells, grid cells, and the brain's spatial representation system. *Annual Review of Neuroscience, 31*, 69-89.

Mumford, D. (1992). On the computational architecture of the neocortex II The role of cortico-cortical loops. *Biological Cybernetics, 66*(3), 241-251.

Murray, E. A., Wise, S. P., & Graham, K. S. (2017). Chapter 1: The History of Memory Systems. In E. A. Murray, S. P. Wise, & K. S. Graham, *the Evolution of Memory Systems: Ancestors, anatomy, and adaptations* (p. 24). Oxford: Oxford University Press.

Nadel, L., & Moscovitch, M. (1997). Memory consolidation, retrograde amnesia and the hippocampal complex. *Current Opinion in Neurobiology, 7*(2), 217-227.

Nadel, L., Samsonovich, A., Ryan, L., & Moscovitch, M. (2000). Multiple trace theory of human memory: computational, neuroimaging, and neuropsychological results. *Hippocampus, 10*(4), 352-368.

Ng, A. Y., & Jordan, M. I. (2001). On discriminative vs. generative classifiers: A comparison of logistic regression and naive bayes. *Conference on Neural Information Processing Systems* (pp. 841-848). Cambridge: MIT Press.

Niendam, T. A., Laird, A. R., Ray, K. L., Dean, Y. M., Glahn, D. C., & Carter, C. S. (2012). Meta-analytic evidence for a superordinate cognitive control network subserving diverse executive functions. *Cognitive, Afective, & Behavioral Neuroscience, 12*(2), 241-268.

Nieto-Castanon, A. (2020). *Conn in Pictures*. Retrieved from Conn toolbox: https://web.conn-toolbox.org/

Nieto-Castanon, A. (2020). *Handbook of functional connectivity Magnetic Resonance Imaging methods in CONN.* Hilbert Press.

Nir, Y., Fisch, L., Mukamel, R., Gelbard-Sagiv, H., Arieli, A., Fried, I., & Malach, R. (2007). Coupling between neuronal firing rate, gamma LFP, and BOLD fMRI is related to interneuronal correlations. *Current Biology, 17*(15), 1275-1285.

Nir, Y., Hasson, U., Levy, I., Yeshurun, Y., & Malach, R. (2006). Widespread functional connectivity and fMRI fluctuations in human visual cortex in the absence of visual stimulation. *Neuroimage, 17*(15), 1313-1324.

Ogawa, S., Lee, T.-M., Kay, A. R., & Tank, D. W. (1990). Brain magnetic resonance imaging with contrast dependent on blood oxygenation. *Proceedings of the National Academy of Sciences, 87*(24), 9868-9872.

Ogawa, S., Lee, T.-M., Nayak, A. S., & Glynn, P. (1990). Oxygenation-sensitive contrast in magnetic resonance image of rodent brain at high magnetic fields. *Magnetic Resonance in Medicine, 14*(1), 68-78.

Ogawa, S., Menon, R., Kim, S.-G., & Ugurbil, K. (1998). On the characteristics of functional magnetic resonance imaging of the brain. *Annual review of biophysics and biomolecular structure, 27*(1), 447-474.

Ogawa, S., Menon, R., Tank, D. W., Kim, S., Merkle, H., Ellermann, J., & Ugurbil, K. (1993). Functional brain mapping by blood oxygenation level-dependent contrast magnetic resonance imaging. A comparison of signal characteristics with a biophysical model. *Biophysical Journal, 64*(3), 803-812.

Ogawa, S., Tank, D. W., Menon, R., Ellermann, J. M., Kim, S. G., Merkle, H., & Ugurbil, K. (1992). Intrinsic signal changes accompanying sensory stimulation: functional brain mapping with magnetic resonance imaging. *Proceedings of the National Academy of Sciences, 89*(13), 5951-5955.

O'keefe, J., & Burgess, N. (2005). Dual phase and rate coding in hippocampal place cells: theoretical significance and relationship to entorhinal grid cells. *Hippocampus, 15*(7), 853-866.

O'Keefe, J., & Nadel, L. (1978). *The Hippocampus as a Cognitive Map.* Oxford: Clarendon Press.

Öngür, D., Lundy, M., Greenhouse, I., Shinn, A. K., Menon, V., Cohen, B. M., & Renshaw, P. F. (2010). Default mode network abnormalities in bipolar disorder and schizophrenia. *Psychiatry Research: Neuroimaging, 183*(1), 59-68.

O'Reilly, R., & Frank, M. (2006). Making Working Memory Work: A Computational Model of Learning in the Frontal Cortex and Basal Ganglia. *Neural Computation, 18*(2), 283-328.

Parent, A., & Hazrati, L.-N. (1995). Functional anatomy of the basal ganglia. I. The cortico-basal ganglia-thalamo-cortical loop. *Brain Research Reviews, 20*(1), 91-127.

Pauling, L., & Coryell, C. D. (1936). The magnetic properties and structure of hemoglobin, oxyhemoglobin and carbonmonoxyhemoglobin. *Proceedings of the National Academy of Sciences, 22*(4), 210-216.

Pavlopoulos, G. A., Secrier, M., Moschopoulos, C. N., Soldatos, T. G., Kossida, S., Aerts, J., . . . Bagos, P. G. (2011). Using graph theory to analyze biological networks. *BioData Mining, 4*(10).

Pearson, K. (1896). Mathematical Contributions to the Theory of Evolution. III. Regression, Heredity, and Panmixia. *Philosophical Transactions of the Royal Society A, containing papers of a mathematical or physical character*(187), 253-318.

Pearson, K. (1901). LIII. On lines and planes of closest fit to systems of points in space. *The London, Edinburgh, and Dublin Philosophical Magazine and Journal of Science, 2*(11), 559-572.

Pecora, L. M., & Carroll, T. L. (1990). Synchronization in chaotic systems. *Physical Review Letters, 64*(8), 821-824.

Ploner, C. J., Gaymard, B. M., Rivaud-Péchoux, S. a., Clémenceau, S., Samson, S., & Pierrot-Deseilligny, C. (2000). Lesions affecting the parahippocampal cortex yield spatial memory deficits in humans. *Cerebral Cortex, 10*(12), 1211-1216.

Poldrack, R. A. (2007). Region of interest analysis for fMRI. *Social Cognitive and Affective Neuroscience, 2*(1), 67-70.

Pöppel, E. (1997). A hierarchical model of temporal perception. *Trends in Cognitive Sciences, 1*(2), 56-61.

Preston, A. R., & Eichenbaum, H. (2013). Interplay of hippocampus and prefrontal cortex in memory. *Current Biology, 23*(17), R764-R773.

Preti, M. G., Bolton, T. A., & Van De Ville, D. (2017). The dynamic functional connectome: State-of-the-art and perspectives. *Neuroimage, 160*, 41-54.

Quigley, M., Cordes, D., Turski, P., Moritz, C., Haughton, V., Seth, R., & Meyerand, M. E. (2003). Role of the corpus callosum in functional connectivity. *American Journal of Neuroradiology, 24*(2), 208-212.

Rabinovich, M., & Abarbanel, H. (1998). The role of chaos in neural systems. *Neuroscience, 87*(1), 5-14.

Rahman, S., Sahakian, B. J., Hodges, J. R., Rogers, R. D., & Robbins, T. W. (1999). Specific cognitive deficits in mild frontal variant frontotemporal dementia. *Brain, 122*(8), 1469-1493.

Raichle, M. E. (2015). The Brain's Default Mode Network. *Annual Review of Neuroscience, 38*, 433-447.

Raichle, M. E., MacLeod, A. M., Snyder, A. Z., Powers, W. J., Gusnard, D. A., & Shulman, G. L. (2001). A default mode of brain function. *Proceedings of the National Academy of Sciences, 98*(2), 676-682.

Ranganath, C., & Ritchey, M. (2012). Two cortical systems for memory-guided behaviour. *Nature Reviews Neuroscience, 13*(10), 713-726.

Rao, R. P., & Ballard, D. H. (1999). Predictive coding in the visual cortex: a functional interpretation of some extra-classical receptive-field effects. *Nature Neuroscience, 2*(1), 79-87.

Rivera, S. M., Reiss, A., Eckert, M. A., & Menon, V. (2005). Developmental Changes in Mental Arithmetic: Evidence for Increased Functional Specialization in the Left Inferior Parietal Cortex. *Cerebral Cortex, 15*(11), 1779-1790.

Rosenberg, M. D., Finn, E. S., Scheinost, D., Papademetris, X., Shen, X., Constable, R. T., & Chun, M. M. (2016). A neuromarker of sustained attention from whole-brain functional connectivity. *Nature Neuroscience, 19*(1), 165-171.

Ruby, P., & Decety, J. (2001). Effect of subjective perspective taking during simulation of action: a PET investigation of agency. *Nature Neuroscience, 4*(5), 546-550.

Saggar, M., Sporns, O., Gonzalez-Castillo, J., Bandettini, P. A., Carlsson, G., Glover, G., & Reiss, A. L. (2018). Towards a new approach to reveal dynamical organization of the brain using topological data analysis. *Nature Communications, 9*(1), 1-14.

Salvador, R., Suckling, J., Coleman, M. R., Pickard, J. D., Menon, D., & Bullmore, E. (2005). Neurophysiological architecture of functional magnetic resonance images of human brain. *Cerebral Cortex, 15*(9), 1332-1342.

Schacter, D. L. (1987). Implicit memory: history and current status. *Journal of Experimental Psychology, 13*(3), 501-518.

Schapiro, A. C., Turk-Browne, N. B., Botvinick, M. M., & Norman, K. A. (2017). Complementary learning systems within the hippocampus: a neural network modelling approach to reconciling episodic memory with statistical learning. *Philosophical Transactions of the Royal Society B: Biological Sciences, 372*(1711), 20160049.

Schreiber, T. (2000). Measuring information transfer. *Physical review letters, 85*(2), 461-464.

Seghier, M. L. (2013). The angular gyrus: multiple functions and multiple subdivisions. *Neuroscientist, 19*(1), 43-61.

Seydel, R. (2009). *Practical bifurcation and stability analysis* (Vol. 5). New York, Dordrecht, Heidelberg, London: Springer Science & Business Media.

Sherry, D. F., & Schacter, D. L. (1987). The evolution of multiple memory systems. *Psychological Review, 94*(4), 439.

Shirer, W. R., Ryali, S., Rykhlevskaia, E., Menon, V., & Greicius, M. D. (2012). Decoding subject-driven cognitive states with whole-brain connectivity patterns. *Cerebral Cortex, 22*(1), 158-165.

Simon, O., Mangin, J.-F., Cohen, L., Le Bihan, D., & Dehaene, S. (2002). Topographical layout of hand, eye, calculation, and language-related areas in the human parietal lobe. *Neuron, 33*(3), 475-487.

Sizemore, A. E., Giusti, C., Kahn, A., Vettel, J. M., Betzel, R. F., & Bassett, D. S. (2018). Cliques and cavities in the human connectome. *Journal of Computational Neuroscience, 44*(1), 115-145.

Smith, S. M. (2004). Overview of fMRI analysis. *The British Journal of Radiology, 77*(suppl_2), S167-S175.

Softky, W. R., & Koch, C. (1993). The highly irregular firing of cortical cells is inconsistent with temporal integration of random EPSPs. *Journal of Neuroscience, 13*(1), 334-350.

Sporns, O., & Zwi, J. D. (2004). The small world of the cerebral cortex. *Neuroinformatics, 2*(2), 145-162.

Spreng, R. N., Mar, R. A., & Kim, A. S. (2008). The Common Neural Basis of Autobiographical Memory, Prospection, Navigation, Theory of Mind, and the Default Mode: A Quantitative Meta-analysis. *Journal of Cognitive Neuroscience, 21*(3), 489–510.

Spreng, R. N., Stevens, W. D., Chamberlain, J. P., Gilmore, A. W., & Schacter, D. L. (2010). Default network activity, coupled with the frontoparietal control network, supports goal-directed cognition. *Neuroimage, 53*(1), 303-317.

Squire, L. R. (1992). Memory and the hippocampus: a synthesis from findings with rats, monkeys, and humans. *Psychological Review, 99*(2), 195-231.

Squire, L. R., & Alvarez, P. (1995). Retrograde amnesia and memory consolidation: a neurobiological perspective. *Current Opinion in Neurobiology, 5*(2), 169-177.

Squire, L. R., & Zola-Morgan, S. (1991). The medial temporal lobe memory system. *Science, 253*(5026), 1380-1386.

Squire, L., & Zola, S. (1996). Structure and function of declarative and nondeclarative memory systems. *Proceedings of the National Academy of Sciences, 93*(24), 13515-13522.

St, L., & Wold, S. (1989). Analysis of variance (ANOVA). *Chemometrics and Intelligent Laboratory Systems, 6*(4), 259-272.

Stachenfeld, K. L., Botvinick, M. M., & Gershman, S. J. (2017). The hippocampus as a predictive map. *Nature Neuroscience, 20*(11), 1643-1653.

Stoeckel, C., Gough, P. M., Watkins, K. E., & Devlin, J. T. (2009). Supramarginal gyrus involvement in visual word recognition. *Cortex, 45*(9), 1091-1096.

Summerfield, J. J., Hassabis, D., & Maguire, E. A. (2009). Cortical midline involvement in autobiographical memory. *NeuroImage, 44*(3), 1188-1200.

Sweller, J. (2003). Evolution of human cognitive architecture. *Psychology of learning and motivation, 43*, 216-266.

Szentágothai, J. (1975). The ‘module-concept’ in cerebral cortex architecture. *Brain Research, 95*(2-9), 475-496.

Tau, G. Z., & Peterson, B. S. (2010). Normal development of brain circuits. *Neuropsychopharmacology, 35*(1), 147-168.

Tomasi, D., & Volkow, N. D. (2011). Association between functional connectivity hubs and brain networks. *Cerebral Cortex, 21*(9), 2003-2013.

Tulving, E. (1972). Episodic memory and semantic memory. In E. Tulving, *Organization of Memory* (pp. 381-430). New York: Academic Press, INC.

Tulving, E. (2002). Episodic memory: From mind to brain. *Annual Review of Psychology, 53*(1), 1-25.

Tulving, E., Kapur, S., Markowitsch, H. J., Craik, F., Habib, R., & Houle, S. (1994). Neuroanatomical correlates of retrieval in episodic memory: auditory sentence recognition. *Proceedings of the National Academy of Sciences, 91*(6), 2012-2015.

Turelli, M. (1997). Random environments and stochastic calculus. *Theoretical Population Biology, 12*(2), 140-178.

Tye, K. M., & Deisseroth, K. (2012). Optogenetic investigation of neural circuits underlying brain disease in animal models. *Nature Reviews Neuroscience, 13*(4), 251-266.

Tzourio-Mazoyer, N., Landeau, B., Papathanassiou, D., Crivello, F., Etard, O., Delcroix, N., . . . Joliot, M. (2002). Automated anatomical labeling of activations in SPM using a macroscopic anatomical parcellation of the MNI MRI single-subject brain. *Neuroimage, 15*(1), 273-289.

Uddin, L. Q., Supekar, K., Amin, H., Rykhlevskaia, E., Nguyen, D. A., Greicius, M. D., & Menon, V. (2010). Dissociable connectivity within human angular gyrus and intraparietal sulcus: evidence from functional and structural connectivity. *Cerebral Cortex, 20*(11), 2636-2646.

Utevsky, A. V., Smith, D. V., & Huettel, S. A. (2014). Precuneus is a functional core of the default-mode network. *Journal of Neuroscience, 34*(3), 932-940.

Van Den Heuvel, M. P., & Pol, H. E. (2010). Exploring the brain network: a review on resting-state fMRI functional connectivity. *European Neuropsychopharmacology, 20*(8), 519-534.

van den Heuvel, M. P., & Sporns, O. (2013). Network hubs in the human brain. *Trends in Cognitive Sciences, 17*(12), 683-696.

Van Essen, D. C., & Maunsell, J. H. (1983). Hierarchical organization and functional streams in the visual cortex. *Trends in Neurosciences, 6*(9), 370-375.

Vanhaudenhuyse, A., Noirhomme, Q., Tshibanda, L. J.-F., Bruno, M.-A., Boveroux, P., Schnakers, C., . . . Boly, M. (2010). Default network connectivity reflects the level of consciousness in non-communicative brain-damaged patients. *Brain, 133*(1), 161-171.

Vann, S. D., Aggleton, J. P., & Maguire, E. A. (2009). What does the retrosplenial cortex do? *Nature Reviews Neuroscience, 10*(11), 792-802.

Varela, F., Lachaux, J.-P., Rodriguez, E., & Martinerie, J. (2001). The brainweb: phase synchronization and large-scale integration. *Nature Reviews Neuroscience, 2*(4), 229-239.

Vargha-Khadem, F., Gadian, D. G., Watkins, K. E., Connelly, A., Van Paesschen, W., & Mishkin, M. (1997). Differential effects of early hippocampal pathology on episodic and semantic memory. *Science, 277*(5324), 376-380.

Vincent, J. L., Snyder, A. Z., Fox, M. D., Shannon, B. J., Andrews, J. R., Raichle, M. E., & Buckner, R. L. (2006). Coherent spontaneous activity identifies a hippocampal-parietal memory network. *Journal of Neurophysiology, 96*(6), 3517-3531.

Vogeley, K., Bussfeld, P., Newen, A., Herrmann, S., Happé, F., Falkai, P., . . . Zilles, K. (2001). Mind reading: neural mechanisms of theory of mind and self-perspective. *Neuroimage, 14*(1), 170-181.

Vogt, B. A., & Laureys, S. (2005). Posterior cingulate, precuneal and retrosplenial cortices: cytology and components of the neural network correlates of consciousness. *Progress in Brain Research, 150*, 205-217.

Von Helmholtz, H. (1925). *Treatise on physiological optics* (Vol. 3). (J. P. Southall, Ed.) Menasha: The Optical Society of America.

Watts, D. J., & Strogatz, S. H. (1998). Collective dynamics of ‘small-world’networks. *Nature, 393*(6684), 440-442.

Welvaert, M., & Rosseel, Y. (2013). On the definition of signal-to-noise ratio and contrast-to-noise ratio for fMRI data. *PloS One, 8*(11), e77089.

Wheeler, M. A., Stuss, D. T., & Tulving, E. (1997). Toward a theory of episodic memory: The frontal lobes and autonoetic consciousness. *Psychological Bulletin, 121*(3), 331-354.

Whitfield-Gabrieli, S., & Nieto-Castanon, A. (2012). Conn: a functional connectivity toolbox for correlated and anticorrelated brain networks. *Brain Connectivity, 2*(3), 125-141.

Wold, S., Esbensen, K., & Geladi, P. (1987). Principal component analysis. *Chemometrics and Intelligent Laboratory Systems, 2*(1-3), 37-52.

Woodward, N. D., Karbasforoushan, H., & Heckers, S. (2012). Thalamocortical dysconnectivity in schizophrenia. *American Journal of Psychiatry, 169*(10), 1092-1099.

Worsley, K. J., & Friston, K. J. (1995). Analysis of fMRI time-series revisited—again. *Neuroimage, 2*(3), 173-181.

Zohary, E., Shadlen, M. N., & Newsome, W. T. (1994). Correlated neuronal discharge rate and its implications for psychophysical performance. *Nature, 370*(6485), 140-143.

Appendix A

Pearson Correlation Coefficient

Pearson correlation coefficient calculated the linear dependency between two data sets. Let A and B a data set with n data points. Then the Pearson correlation coefficient of A and B is defined

$$r[A,B] = \frac{\sum_{i=1}^{n}(A_i - \bar{A})(B_i - \bar{B})}{\sqrt{\sum_{i=1}^{n}(A_i - \bar{A})^2}\sqrt{\sum_{i=1}^{n}(B_i - \bar{B})^2}}$$

when (A_i, B_i) is a pair of two data sets, $\bar{A}$ and $\bar{B}$ is the sample mean of each data set. By its definition, the range of Pearson correlation coefficient is $-1 \leq r[A,B] \leq 1$. When $r[A,B]$ is close or equal to $r[A,B]$ is close to 1, the two data sets are anti-correlated if it close or equal to -1. The two data set has no linear correlation, $r[A,B]$ is close to zero.

Independent Component Analysis

There are two types of independent component analysis (ICA), spatial and temporal ICA in fMRI studies (Calhoun, Adali, & Pekar, 2001). As Calhoun and colleagues (2001) showed, temporal ICA is not proper to use for data having a temporal dependency. In my study, I used group spatial ICA in the CONN toolbox (www.nitrc.org/projects/conn, RRID:SCR_009550) to define spatially independent brain regions which might have a temporal dependency in correlation changes. Details of the analysis are as follows (Calhoun, Adali, & Pekar, 2001; Nieto-Castanon, 2020). Since the number of voxels is around a million and the time points are over a hundred per fMRI run, it is required to reduce the dimension of the data. For that, principal component analysis was performed on the data of each run of a subject. The first 64 principal components were chosen from this step. Then the chosen principal components were concatenated, and principal component analysis was applied to the concatenated matrix. The first 40 or 20 components were chosen, and these components went through FastICA (Hyvärinen & Oja, 2000). FastICA calculated the mixing matrix and independent components by maximizing the negentropy of the probability distribution of independent components. The choice of the non-linear contrast function to calculate the negentropy could differ and I choose the G3 which is suggested by Hyvärinen & Oja (2000).

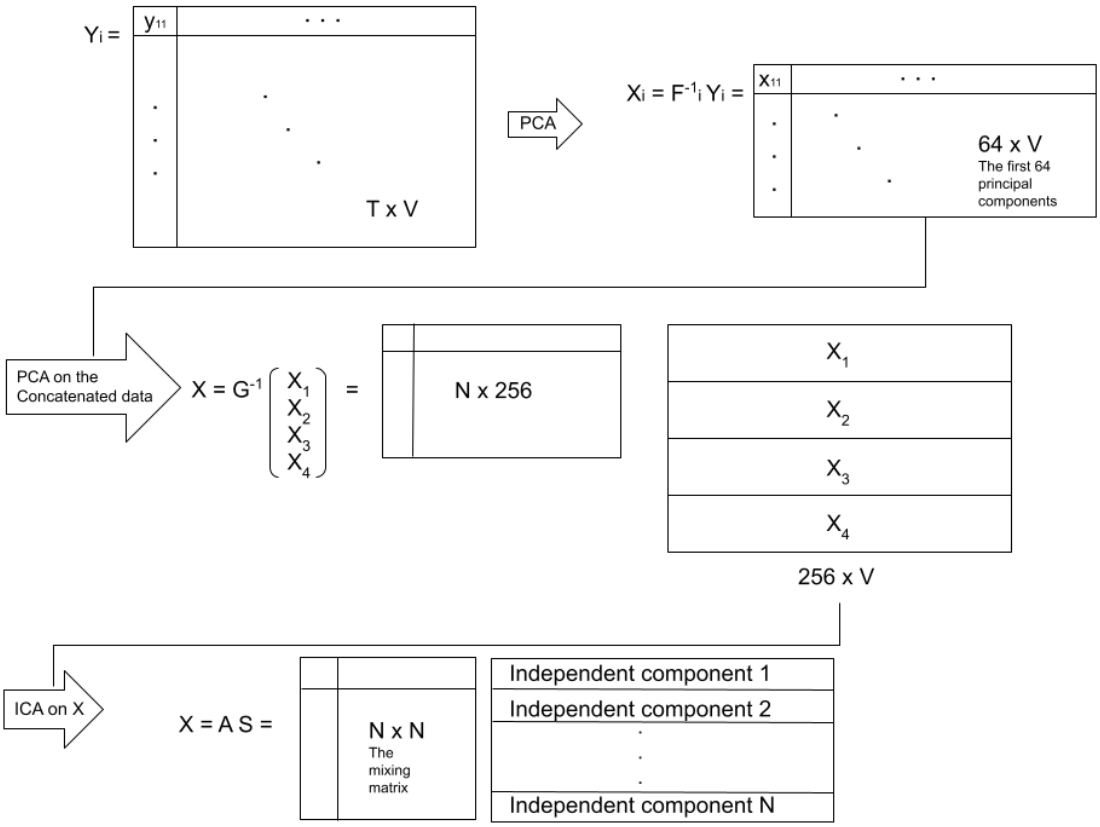

Figure A: Group spatial independent analysis

Y_i is the preprocessed data of a run (i=1,2,3,4). X_i is the reduced data after PCA on Y_i. F_i is the first 64 principal components of Y_i. X is the reduced data of all four runs after PCA on the concatenated data of X_i. G_i is the first N (the number of independent components) principal component of concatenated data of X_i. A is a mixing matrix, and each row of S is an independent component.

Appendix B: Transcript of Morning Routine Statement

Single case study

Ich habe mich hingelegt und erstmal in mir Ruhe gefunden. Dann gemacht, was Sie gerne gehabt haben. Ich fühlte mich im Bett liegend und aufgewacht; Habe dann meine Füße nach links getan, wie immer; Aus dem Bett heraus; Die Schuhe geholt, die auch da gleich standen; Aufstehen; Um das Bett herum, zack, zack, zack, noch ein Stück, noch ein Stück, dann ist die Türe; Türe in den Gang raus, gleich nach rechts hinein, gleich wieder links, da ist die Toilette, die braucht man in der Früh; Nach der Toilette aufstehen und wieder nach links gehen; und rechts ist das Waschbecken, wo man die Hände wäscht; Abtrocknen; Umdrehen; Wieder zur Türe hinaus, dann ist man wieder in dem Gang, und direkt gegenüber ist die Küchentüre; Durch die Türe durch, links ist der Ofen, neben dem Ofen das Wasser; Wasser gelassen in den ganz normalen Wassertopf, zack, und auf “drei” schalten, dann ist der Strom drin; Kanne drauf, zack; Wieder umdrehen; Bei der Türe raus und dann nach rechts, das ist das Wohnzimmer, dabei nehme ich gleich die Tischdecke mit; Und hab die Tischdecke dann auf den Tisch gebreitet; Schön alles andere weg, was man nicht braucht zum Frühstück; Tischdecke; Wieder umdrehen; Wieder zurück in die Türe raus, wieder nach links und dann Porzellan holen; Erst mal nur zwei Tellerchen; Umdrehen; Wieder ins Wohnzimmer; Die Teller auf den Tisch geben, schön hinstellen alles; Wieder umdrehen; Wieder raus zur Türe; Nach links; Noch einen Teller, wo man die Sachen hat, die man dann braucht; Dann habe ich den Kühlschrank aufgemacht; Das alles, was wir zum Futtern brauchen: Wurst, Käse, Aufstrich und sonst noch so Geschmacksverstärker und so was und, ja ja, und dann habe ich gleich das erste Mal die Früchte vergessen, die wir sonst immer essen, also Tomaten und alles, was wir halt essen; Wieder umdrehen; Raus; rüber wieder ins Wohnzimmer das tragen. Dann bin ich wieder zurückgegangen in die Küche; Hab in den Kaffeetopf den Kaffee rein, den muss ich natürlich zuerst vom Schrank wieder holen von der linken Seite, und da ist so eine große Tonne drin und die Tonne, die hat einen kleinen Schöpfer; Und da kommen drei große Schöpfkellen rein, zack; Und dann die ganze Kanne da wo sonst das Wasser steht; Dann höre ich, ob das Wasser schon kocht; Wenn es gekocht hat, dann kommt was rein, dann wird mit dem Löffel umgerührt; Noch mal rühren, noch mal rühren; Dann den Kaffee voll machen, das Wasser genügend rein, zack; Und zuvor natürlich das Kaffeepulver wieder aufräumen, den geriebenen Kaffee, der kommt wieder in den Schrank, zack; Und dann nochmal den Kaffee umrühren, schön, schön, mit dem großen Löffel; Dann kommt der Deckel drauf; Dann muss er derweil noch ein bisschen stehen; Und die anderen Sachen, die wir brauchen: Zucker und Salz und was man noch alles hat; Dann noch mal rüber gehen ins Wohnzimmer; Alles wieder schön hinstellen; Ach Gott - und dann, ist mir eingefallen, habe ich die kleinen Kaffeelöffel vergessen; Wieder raus; Wieder links rein; Wieder in den Schrank schauen, die Kaffeelöffel holen, die Richtigen, weil bei uns kriegt ja jeder seinen; Wieder raus; Alles wieder präsentieren im Wohnzimmer; Dann wieder zurück; Den Kaffee holen; wieder rüber ins Wohnzimmer; Da hinstellen, wo er immer steht; So: hmm, hmm; Und dann wieder raus; Und dann nicht nach links in die Küche, sondern nach rechts ins Schlafzimmer zu meinem Mann und sagen: “Hallo, Loewe, Das Frühstück ist fertig”. Dann zupfe ich immer noch ein bisschen am Blumeaux; Und drehe mich um; Und gehe wieder raus in den Gang; Wieder links rein ins Wohnzimmer und setze mich hin und warte bis der Loewe dann zum Frühstück kommt.

Group Study

Subject 01

Ich steh morgens so meistens um 5 oder 6 auf. Ich hab so einen Tageslichtwecker, der 15 Minuten vorher langsam hell wird und je nachdem wie müde ich bin, werde ich auch schon etwas eher wach oder sonst erst, wenn der Wecker klingelt. Dann steh ich erstmal kurz auf, ich nehm etwas Medizin. Je nachdem hab ich mir schon Wasser rausgestellt, hol mir etwas Wasser oder nehm sie einfach so. Und danach gehe ich auf Toilette falls ich schon muss. Danach lege ich mich meistens noch etwas hin - wenn ich müde bin - und lese ein bisschen. Und wenn ich dann irgendwann wach genug bin - so eine halbe Stunde bis Stunde später - stehe ich auf, such mir Waesche fuer den Tag raus und geh dann ins Bad. Als erstes putze ich mir immer die Zähne; mit einer elektrischen Zahnbürste und danach geh ich dann duschen. Dann wasche ich mir immer erst die Haare und dann dusch ich mich ab. Und danach trockne ich auch erst meine Haare ab und rolle sie in so einen Turban mit dem Handtuch ein und trockne mich danach ab. Da ich meistens etwas länger dusche und auch meistens ziemlich warm ist dann das Bad auch ziemlich bezogen. Ich mach dann immer die Lüftung an und wenn ich dann das Bad verlasse, lasse ich die Tuer ein bisschen auf Kipp stehen, damit das abzieht. Nach dem Duschen gehe ich eigentlich immer zurück wieder in mein Zimmer; verstaue die alte Waesche, haenge gegebenenfalls mein Handtuch auf und fange dann an mir ein Frühstück vorzubereiten. Je nachdem manchmal mache ich mir morgens Brot, dann belege ich es mit Käse. Wenn ich was vorbereitet habe, habe ich dann abends immer Obst aufgetaut und mache mir dann statt Brot, Obst mit Joghurt und Muesli. Je nachdem wie ich drauf bin, mach ich dann schon Kaffee, dazu nehme ich meinen Espressokocher; leere das alte Pulver aus, reinige ihn, fuelle ihn und stelle ihn auf den Herd. Und waehrend ich dann warte, bis der Kaffe fertig ist, setze ich mich schon mal ins Wohnzimmer und esse. Beim Frühstück lese ich meistens nebenbei oder guck ein bisschen fern, und trink dann - wenn er fertig ist - auch meinen Kaffee dazu. Nach dem Frühstück guck ich mir an, wie das Wetter für den Tag wird, und ueberlege, was ich anziehe und ziehe mich dann um fuer denTag. Wenn ich dann angezogen bin sind hoffentlich meine Haare schon ein bisschen getrocknet ueber den Morgen und dann foehne ich den Rest. Danach mach ich entweder einen Zopf, flechte ich sie zu einem Zopf oder roll sie einfach zusammen zu einem Dutt. Danach geh ich dann rueber ins Arbeits- bzw. Wohnzimmer und mach mich frisch fuer den Tag; trag noch ein bisschen Puder auf, ein bisschen Abdeckcreme und benutze dafuer den Spiegel im Flur. Wenn Ich dann fertig bin, falls ich mich vorher noch keinen Kaffee gemacht habe, fange ich jetzt erst an, setz ihn auf den Herd, damit er dann fertig ist, wenn ich anfange zu arbeiten. Wenn ich dann fertig bin, kann ich mich einfach an den Schreibtisch im Wohnzimmer setzen und fange an, zu arbeiten.

Subject 02

I wake up in the morning at 6 or something. And the first thing I do is listen to the radio. Because I have a radio alarm clock, so listen to the radio first. Then after couple of minutes, I check my phone; WhatsApp or maybe mails, maybe Instagram very quick. Then I get up and I slip into my shoes, house shoes. Then I go into the kitchen. And then in the kitchen I pick up a glass and a blender and I fill up the glass with water and also the blender with 600 ml of water and in the blender, I put 16 grams of essential amino acid, and I blend it. And then I take the glass of water and put my blender in the hallway and take my glass of water with me to my room. I put into the glass of water three gram of creatine monohydrate, and I take it together with other supplements. Then I get dressed with my gym clothes because the first thing in the morning that I do is going to a gym so I describe it with more details. In the gym, or first, I get dressed, put on my shoes. I don't have to pack my bag because it has been already done. But I put in the blender, my gym card, my mask and my keys. I lock the door behind me before I go. Then I walk to the gym. While walking to the gym I usually listen to pot cast episodes, something about politics or comedy. And when I arrive at the gym I change to music, into a rock music, because I like rock. And then I go upstairs and then I check in with my card. I do not warm up because I hate warming up. And then I do one of six different training slots that I have. So, I just will describe the one I did yesterday. Yesterday was push one, push one I start with bench press, a sport press. I went to a bar or the bench, I put on 6.25 kg each side, put on my towel on a bench, yeah, I start with the first set. This is the first exercise of this exercise or after two sets of exercise, I do the next exercise which is also sport press but with more weight and less repetition. As third exercise I do the chest flies at the machine, also two sets around 11 to 14 repetitions. And then after that I go to the bench again and no, I don't go to the bench, I go to barbells. I do the (a name of an exercise), with an around 5 kg four sets. Then I do pushups, three sets as many as possible. And then I do (a name of an exercise) again but bent over and with around 7 kg three sets, 11to 14 repetitions. During the work out, I drink my shake which I have put on the blender before the amino acid. And I walk home again. I put on the pot-cast episode again. I enter the house. This is usually by 8:45, 9 am something like that. And my roommate is usually already awake when I enter the house again, so I say good morning to her, and we chat a little bit. Then I quickly jump on the shower. I take a shower, when I get out, out of the shower in my bathing suite. I go back into the kitchen I clean my blender from the amino acid, and I put in 300ml of water and 30 grams of protein powder. I shake it blend it while preparing my breakfast which is usually porridge. I put in the water in the pot, boil it together with 60 g of oatmeal. I prepare porridge, I prepare also usually two slices of bread with some kind of topping. I take it with me on a plate into my room and I sit up my desk. I enjoy my protein drink and my breakfast. I switch on my computer. And then I check my mail, first my private mail, my university mail. And then I open my planner, and during taking my breakfast I just plan the day. Then I usually end my breakfast. I put plates and everything back into the kitchen, then I go back to my room. I get dressed then I start a day.

Subject 03

Today I woke up around 6 o'clock. I didn't get out immediately. I just played my mobile phone on the bed, read several paragraphs of a novel. And then I get up to go to the bathroom, brushed my teeth, washed my face with my face cleaning machine and the cleaner, then pet some toner and the moisturizer and uses some eye cream, day cream and some cream. I think it is very, women are always waste a lot of time for these procedures. And then I went to the kitchen to get something for my breakfast. I used the microwave-oven to heat a butter croissant which I bought yesterday from Odeonsplatz and the boil some hot water and make a cup of (a name of a tea) tea, and with sauces from Korean, and then cut the piece of cheese. This is a goat milk cheese. I love it very much. And then I bring all the things back to my room and draw back the curtains, open a window a little bit, because I wanted to exchange some air and looked outside little bit. It was really nice weather, the blue sky with no clouds at all. I ate my breakfast at the same time watched an episode of TV series, a Japanese TV series, which its name is the Chief. The Chief is also a famous detective, so because it tells about story of a chief in a French bistro. So, I think my butter croissant tastes even better when I see other people eats French cuisine in the tv series. Then I finished my breakfast, washed the plates and cups. Then I changed my clothes and go outside to go to Westpark for walk. I go across the neighborhood and passed the sky-over and entered the Westpark. There is a Chinese garden inside of the park. So, I see the garden at first. But the garden was closed. Tt was very strange. It is usually closed I don't know why. Then I see there is a Buddha sculpture next to the Chinese garden. And then there is the Japanese garden next to the Buddha sculpture but today it is also very strange that the Japanese garden is closed which is usually open to the public. Because there is a truck with a lot of equipment and stuffs are there. So, I think maybe they were taking some TV programs or something like that. And so, it is the first time in Germany I saw these activities. Then I walked a little bit around the lake, saw a lots of ducks, swans, and the wild gooses. I even saw a group of wild gooses like five or six ones flied directly through the surfaces of the lake. It was very interesting. Then I saw a rabbit. It is astonished when it saw me. It turned around immediately and run away. Then I continue a little bit walk and saw the rose garden. You know the autumn of Munich comes very, comes immediately. And last week all the trees were still green but this morning some of trees already changed into another color, in red or in yellow. But the rose garden still has a lot of roses of the color with the color of pink, red, yellow. Very beautiful. Then I come back, according to my previous path and go out of the Westpark and go across the sky-over and go into my neighborhood. And then lastly, I met a cat. It's a cat lives in our neighborhood. And when it saw me, it's immediately disappearing on a bush. And I also see some neighbors walk with their dogs, one of the dogs is a black one and very cute. And I came back to home, but I didn't enter my home immediately but at first, I go downstair, the laundry room to put away my clothes, bring all my clothes back to my home. And that moment my husband gives me call, a video call. He showed me his apartment in Bremen, is a very nice apartment with a very nice work room and I can see the outside there is a garden, so we chat a little bit. And then stopped the call to make myself a cup of coffee with milk in the kitchen. Then I drink the coffee and wash the cup and do other preparations and go out.

Subject 04

Usually, I set my alarm at 7am, and when it rings, I am having hard time actually to get up right away. So, I snooze it a couple of times may be two or three times. Also, actually I am having the urge to use the toilet, also in a fight happening. And then when the urge of going to the toilet is too much, I actually get up then I use the toilet. And then I immediately go to the kitchen I drink a glass of water. And then afterwards I am preparing coffee. So, I put in water into the water filter and it's dropping through. Then the water I am pouring it into the mocha. And then I am putting the coffee powder into the mocha, closing it, and hitting up the stove. In the meantime, I am getting the milk out of the fridge. And I am pouring it into the milk foam machine. I need to time advise. If I put it too early, then the foam is too thick to out of it to pour so I am waiting a little bit. And I am adding it in to the foam maker, then the coffee is ready. I take two cups and I put the coffee into those two cups, and add the foam on top, and sometimes I also trying to make the coffee out on top maybe hot or something. Then I am going to the bedroom to bring one coffee to my boyfriend, and I go back. I am also preparing breakfast. I usually cut some fruits whatever we have, maybe apples, maybe some pomegranates, or some berries on top. And I add some cereal, it is usually crunch cereal, maybe with some nuts, then I put yogurt on top. And then I have my breakfast so put all these in a bowl, sit down, eat my breakfast, maybe check my phone in the meantime, my emails, and slide messages or things like this, WhatsApp messages. After coffee and breakfast is done, I go to the bathroom, and I take a shower. So I go to the shower, close the shower curtain. I wash my hair and my body and use conditioner usually. And then I leave the shower put in, go into my towel, dry myself. I brush my teeth. I comb my hair with a hope that it dries quite fast that I don't need to use the hairdryer. And then I also wash my face. I first use soap with it and then I have this cleanser, and then put on a face cream. And then I go to the bedroom. And then I am putting on my clothes. And if it's a day I have to go to office I pack my suite case. So, I have to, my backpack, I have to put in my laptop, my phone, my wallet, maybe something to drink, something to eat. Then if the weather is nice, I usually walk to the office. Before I leave, I say goodbye to my boyfriend. And then I walk through English Garden, the first of Leopoldstrasse, then till English Garden. So, at Ohmstrasse I enter English Garden. Then I cross the bridge, walk through the garden. And there is the Chinse tower by next to my office, there is where I leave English Garden. And then if I reach my office, I have to open the door and sit down, then start.

Subject 05

I set an alarm. My alarm usually was off at 8 on weekdays, 9 on weekends, unless I have to go to Garching, then it's little bit earlier, but on average, it goes on 8. I get up, I snooze the alarm, and go back to sleep. And I do it for two or three times. And then eventually I start getting more and more awake, but I am still lying there, thinking of reasons why I should get up, and why I should not sleep more. And usually, it takes some more of convincing. Why I shouldn't get up unless my girlfriend is also still in bed, then she has to force me to get up to make coffee. But usually, I just keep lying down till that feel find a good enough reason to get up. Sometimes the reason is that I have been thinking about a problem, the previous night, that is a good enough motivation for me to get up. And if I have not been doing that, then I usually look at the news to find a good enough reason to get up. News and if that doesn't work, then I usually go to Instagram and then I finally find a good enough reason to get up. And after all that, when I am able to convince myself to get up, I usually get up and if there is no coffee then I make coffee. If there is already coffee, then I usually drink it while reading either a book or some kind of problem typically in mathematics. And then I think of sometimes probably, I do just puzzle, in the morning sometimes I play a card game anything to get my brain going fast because if that's not working then usually, I go back to sleep again soon enough. So, if I make coffee then I go through the process of making it. I make the coffee. I clean the mocha right afterwards. I take the coffee to the bedroom where my girlfriend is still asleep. I open the curtains. I try to wake her up. Then I try to give her good enough reasons to get up. But it's not usually hard to find because I just have to remind her that she has to go to work, then she is up really quickly. Right afterwards, I am usually going through whatever book I am reading. It might be some problems which I still have left over unsolved from the previous night, or I am reading a fiction. So usually, it's that I'm working on a problem because that's the easiest way I find to get up. And if I am doing that, then I try to really get into it. And then I have my laptop in front of me. I look into whatever things I've done, I've already known about the problem, and I keep doing that till sufficiently find myself into an idea I have not explored before. Then I ask to myself a question, not consciously, why am I doing this? Then I stop going round and round circles in my head because that's a good question to ask yourself why you are doing this. But if you keep on repeatedly asking yourself the same question, then you would not really have been doing anything, after all. This is the witch's cycle. I finally realized okay, that's been enough. I should probably get the breakfast. But by then, the breakfast is already there. Because it's all beaten at least thirty minutes. My girlfriend probably has made me a breakfast. I take the yogurt out. I add the yogurt to muesli and the fruits that she already cut. I start having my breakfast, then I realized that I also have some bodily functions to take care of. I go to the toilet then. Then since I've already finished my breakfast, I wear something to get me up and go through the routine of my day which is again looking at some other problems associated to the one I am looking at, which I am interested in.

Subject 06

When I wake up, first I check I close my [inaudible]. And then I check my phone if there is a message from someone. And then I stretch my legs. then I woke up, I wake up and wear my slippers and I wear my sweatshirt. And then I go to the bathroom. And I go to the toilet. Then I wash my hands, I wash my face. And yeah, then I brush my teeth. after I brush my teeth, I go to the kitchen I take a cup of water and after I drink it. I go to the living room, and I started to do my morning exercises. At first, I stretch my legs. I stretch my body then I do some pushups. After that I go to the bathroom, I take a shower. First, I wash my hand then heads. And then I wash my hair I wash my body. After that, I dried myself with towels then I dried my hair. Then I wear my clothes, daily looks, like Jean T shirt. Then I go to the kitchen to prepare my breakfast. I open the fridge. I take out 2 eggs, baby spinach, mushroom, tomato, and cheese and also lactose free low-fat milk. Then I put two eggs in a cup, and I put a little bit milk, I put a bit salt and pepper and start mix it. After I mixed it, I put this mixture into pan, and I start cooking. While my omelet is cooking, I start to prepare other things like, I start to cut tomato, mushroom in small pieces and also baby spinach and after my omelet is done, I put cheese, tomato, mushroom and baby spinach on top of it and then I start eating. And also, I prepare a tea, a black tea. While I'm eating and drinking, I also check Daily News from my phone. After my breakfast is done, I start preparing my lunch. I want breads, two small breads and I cut tomato and mozzarellas. And I put these mozzarellas, this already cut mozzarellas, tomato inside breads and covered the bread with aluminum foil. And I put these breads into my bag also put my laptop and cable charge and my notebook into my bag. And then I'm ready to go to work. Then I wear my shoes. I wear my jackets then I start walking to Ubahn. I go down to Ubahn and I get in U2 and after I arrive to Sendlinger Tor, I get out and get out from Ubahn and start walking to the institutes. By walking, at the right side on the way, there's a bakery. I go there, and I buy a Nussbreze. Then I continue walking to the institute. And in the door, in the institute door I opened the door with my transponder. I get in. I go to the office, and I put my bag next to my chair. I sit at my computer.

Subject 07

So, my morning starts with an alarm clock which is actually wristband which goes off because I don't want to wake up my daughter and girlfriend at 5:45. Then I tried to, I tried to get up and grab my clothes and sneak out of the room without waking up the two girls. And before I leave the room, I have to switch on the camera of the baby phone above my daughter's bed so that I can hear her when she wakes up then get out. And then I go to the living room. And get dressed there, in darkness usually. and after that I go to the kitchen and start with opening the water tap and let it run for half a minute or so. And then I drink a glass of water. And then I start making my coffee. So, I grind beans and I heat 300 ml of water. And then I do my coffee things. And then once the coffee is done and I cannot drink it because it has to cool down. So, I start with preparing breakfast for my daughter. So, I get, I get out a pot and fill it with water. And then I put some kind of cereals into it. And then I cook it. This comes quite quickly. And then once this is done, I wash some fruits and I cut the fruits into the pot. All the time I have to look at the baby phone to see if my daughter has woken up already. And yeah, and then once I'm done with that and usually this is the time when also my daughter wakes up or if not then 6:45 I have to wake up her. So, I get into bedroom, try to wake her as calmly and peacefully as possible. And I take her out of her bed and take her to the living room where I change her diapers. I am trying to fight her usually and to take care her that she doesn't fall off the cupboard. And then by the time I finish with that, usually my girlfriend already has also been gotten up. So, then I place my daughter and her chairs and put in such a thing around her neck that her clothes don't get dirty. And then my girlfriend takes it over and feeds her with the food while I am going to the kitchen and prepare my own breakfast. So, I just heat milk and some cereals and oats and yeah just takes couple of minutes longer. So, during that time I prepare clothes. So, I am dressed for going out. and I also prepare my daughter's stuffs which we need for her morning in the Kita. And then the oats are cooked by then, by that moment. And then I also cut some fruits into it. And then I eat my breakfast usually standing up while trying to finish the other two exercises, tasks and sometimes helping my girlfriend holding my daughter and stuff. And so, then this when I finish with the breakfast. I go to the bathroom, then I do the bathroom stuffs and brush my teeth. And then after that it's already time to leave so I put my daughter into my bag thing. Then I go down the stairs to the basement where we have a buggy. So, I place her buggy and put her stuffs and then we climb one staircase. And then we leave the house and just cross the street where we wait for the bus for a couple of minutes. And then we take the bus which is usually drives like 5 to 7 minutes. And then at our destination we get off or you get out. And then we still have to walk like 10 minutes where we go through a very calm park, a small park which is usually very empty because it's still very early. And then after that, we have to cross one more street. And then after a couple of 100 meters we arrive at the Kita. Then we greet to women there taking care of my daughter and I leave my daughter there. And I go out and then take the bike which is already parked outside in Kita and drive home for like 10 to 15 minutes. And then once I am home, I get up to our apartment then I tells my girlfriend about how everything went and what the person in the Kita told us, when we can pick up our daughter again. And then I just grab a cup of water, go into my office, the bedroom. And then my working day starts.

Appendix C: ROI Marks of Group Study

Subject 01

ROI	Threshold	Independent Component	Number of voxels
PHC L	TH 1	IC 1 (-22,-36,-13)	n=146
PHC R		IC 1 (21,-24,-16)	n=7
AG L	TH 4.5	IC 1 -39, -77,28)	n=347
AG R		IC 1 (40, -74,32)	n=218
RSC L	TH 4.5	IC 1 (-7, -50,9)	n=17
RSC R		IC 1 (8, -45,5)	n=7
PRC	TH 5.5	IC 1 (-1,-65,33)	n=171
PCC	TH 2.5	IC 2 (1,-48,28)	n=198

Subject02

ROI	Threshold	Independent Component	Number of Voxels
PHC L	TH3	IC 1 (-26,-44,-7)	n=67
PHC R		IC 1 (18,-36,-13)	n=9
AG L	TH4	IC 1(-30, -80,36)	n=410
AG R		IC 1 (38, -73,32)	n=489
RSC L	TH4	IC 1 (-12, -61,14)	n=157
RSC R		IC 1 (12, -59,15)	n=321
PRC	TH4.5	IC 1 (5,-55,53)	n=397
PCC	TH 3	IC 2 (5,-42,36)	n=222

Subject03

ROI	Threshold	Independent Component	Number of voxels
PHC L	TH 2	IC 1 (-23,-19,-22)	n=7
PHC R		IC 1 (23,-20,-17)	n=18
AG L	TH 2	IC 2 (-47,-60,39)	n=240
AG R		IC 2 (55,-54,34)	n=736
RSC L	TH 2.2	IC 1 (-18, -56,8)	n=14
RSC R	TH 2.5	IC 1 (12,-55,6)	n=20
PRC	TH 2.2	IC 1 (4,-57,51)	n=244
PCC	TH 2	IC 2 (2,-56,32)	n=538

Subject04

ROI	Threshold	Independent Component	Number of voxels
PHC L	TH 3	IC 1 (-29,-42,-10)	n=118
PHC R		IC 1 (23,-38,-13)	n=13
AG L	TH 3	IC 1 (-36,-78,31)	n=872
AG R		IC 1 (40,-74,34)	n=423
RSC L	TH 3	IC 1 (-10,-58,11)	n=332
RSC R		IC 1 (13,-51,11)	n=292
PRC	TH 5	IC 2 (3,-65,37)	n=733
PCC	TH 5	IC 2 (1,-26,27)	n=213

Subject05

ROI	Threshold	Independent Component	Number of voxels
PHC L	TH 2	IC 1 (-29,-41,-15)	n=82
PHC R		IC 1 (28,-39,-17)	n=92
AG L	TH 4.5	IC 1 (-27,-78,35)	n= 231
AG R		IC 1 (40,-75,28)	n= 230
RSC L	TH 3.8	IC 1 (-17,-59,18)	n=58
RSC R		IC 1 (17,-59,19)	n=146
PRC	TH 4.5	IC 1 (1,-62,56)	n=184
PCC	TH 3.5	IC 2 (-1,-53,35)	n=154

Subject06

ROI	Threshold	Independent Component	Number of voxles
PHC L	TH 2	IC 1(-30,-37,-17)	n=114
PHC R	TH1.9	IC 1(30,-37,-14)	n=9
AG L	TH 3	IC 2 (-52,-64,28)	n=433
AG R		IC 2 (51,-58,26)	n=434
RSC L	TH 3.9	IC 1 (-14,-56,13)	n=171
RSC R		IC 1(13,-51,17)	n=165
PRC	TH 4.5	IC 3 (2,-68,45)	n= 491
PCC	TH 3	IC 2 (-1,-56,30)	n= 498

Subject07

ROI	Threshold	Independent Component	Number of voxels
PHC L	TH 2	IC 1 (-30,-37,-15)	n=110
PHC R	TH1.5	IC 1 (30,-40,-13)	n=18
AG L	TH3	IC 2 (-53,-60,18)	n=253
AG R		IC 2 (50,-59,17)	n=126
RSC L	TH 4	IC 1 (-13,-54,9)	n=476
RSC R		IC 1 (14,-53,13)	n=300
PRC	TH 4	IC 1 (-1,-63,42)	n=651
PCC	TH 3	IC 2 (-4,-54,27)	n=646

Acknowledgements

I would like to express my profound gratitude to my supervisor, Prof. Ernst Pöppel. His sincere support for me was my biggest motivation to carry out research in ‘the cellar’. His passionate life as a scientist suggested to me the direction I would like to follow. I also would like to thank Isolde Zondler and Dr. Urs Zondler who provided me the funding for my study. It was such a special experience to meet them in Beuerberg. Their warm-hearted welcome always made me appreciate the opportunity they granted me. I would like to thank all members of the Institute of Medical Psychology of LMU. They offered their time and effort generously to help me. Especially, I appreciate Prof. Martha Merrow who kindly supported my research in IMP. I thank the pure friendship from my colleagues and friends in the cellar. It always cheered me up so I could feel confident. Juyeon Shim and Ruth Schulte read my thesis and reviewed it to make it in the right shape. The thesis would have looked much more miserable without their help. Lukas Eisemann, who also read part of my thesis, I thank him for showing me his love and support for staying closest to me. Also, I would like to send all my thanks to my family and friends in Korea. My mother, Sunhee Pak, and my sister, Boram Jeong, have always led my life to a better place. Minyoung Lee and Jiyeon Im, I thank them for being my friend and becoming a daughter and a sister for my family instead of me. My father, Sangjae Jeong, I feel that you are always with me. My lovely family cat Lalla, thank you for being my family and rest in peace with our father till the day we meet again.

Affidavit

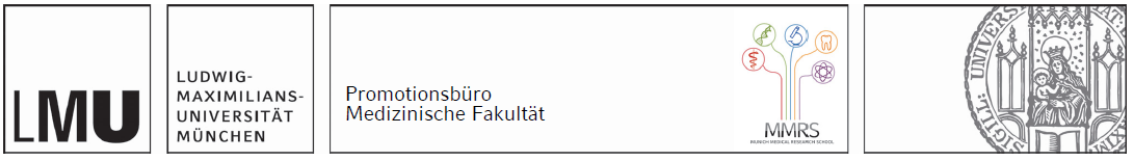

Affidavit

Jeong, Garam
Surname, first name

Street

Zip code, town, country

I hereby declare, that the submitted thesis entitled:

Changes in Dynamic Functional Connectivity of Default Mode Network in Two Different Mental States: Episodic Memory Retrieval and Resting State

……

is my own work. I have only used the sources indicated and have not made unauthorized use of services of a third party. Where the work of others has been quoted or reproduced, the source is always given.

I further declare that the submitted thesis or parts thereof have not been presented as part of an examination degree to any other university.

Munich, 15.12.2022
place, date

Garam Jeong
Signature doctoral candidate